UNIVERSIDADE ESTADUAL DE CAMPINAS
Faculdade de Engenharia Mecânica

FELIPE MIRANDA AZEVEDO

Bi-directional Evolutionary Acoustic Topology Optimization for Muffler Design

Otimização Topológica Bidirecional Evolucionária Acústica para o Projeto de Silenciadores

CAMPINAS
2017

FELIPE MIRANDA AZEVEDO

Bi-directional Evolutionary Acoustic Topology Optimization for Muffler Design

Otimização Topológica Bidirecional Evolucionária Acústica para o Projeto de Silenciadores

Thesis presented to the School of Mechanical Engineering of the University of Campinas in partial fulfillment of the requirements for the degree of Master in Mechanical Engineering in the area of Solid Mechanics and Mechanical Design.

Tese de Mestrado apresentada à Faculdade de Engenharia Mecânica da Universidade Estadual de Campinas como parte dos requisitos exigidos para obtenção do título de Mestre em Engenharia Mecânica na área de Mecânica dos Sólidos e Projeto Mecânico.

Orientador: Prof. Dr. Renato Pavanello

ESTE EXEMPLAR CORRESPONDE À VERSÃO FINAL DA DISSERTAÇÃO DEFENDIDA PELO ALUNO FELIPE MIRANDA AZEVEDO E ORIENTADO PELO PROF. DR. RENATO PAVANELLO.

....

ASSINATURA DO ORIENTADOR

CAMPINAS
2017

Agência(s) de fomento e nº(s) de processo(s): CAPES

Ficha catalográfica
Universidade Estadual de Campinas
Biblioteca da Área de Engenharia e Arquitetura
Luciana Pietrosanto Milla - CRB 8/8129

Az25b
Azevedo, Felipe Miranda, 1991-
Bi-directional evolutionary acoustic topology optimization for muffler design / Felipe Miranda Azevedo. – Campinas, SP : [s.n.], 2017.

Orientador: Renato Pavanello.
Dissertação (mestrado) – Universidade Estadual de Campinas, Faculdade de Engenharia Mecânica.

1. Otimização topológica. 2. Análise acústica. 3. Silenciadores. I. Pavanello, Renato,1959-. II. Universidade Estadual de Campinas. Faculdade de Engenharia Mecânica. III. Título.

Informações para Biblioteca Digital

Título em outro idioma: Otimização topológica bidirecional evolucionária acústica para o projeto de silenciadores
Palavras-chave em inglês:
Topology optimization
Acoustic analysis
Mufflers
Área de concentração: Mecânica dos Sólidos e Projeto Mecânico
Titulação: Mestre em Engenharia Mecânica
Banca examinadora:
Renato Pavanello [Orientador]
José Maria Campos dos Santos
Renato Barbieri
Data de defesa: 13-03-2017
Programa de Pós-Graduação: Engenharia Mecânica

UNIVERSIDADE ESTADUAL DE CAMPINAS
FACULDADE DE ENGENHARIA MECÂNICA
COMISSÃO DE PÓS-GRADUAÇÃO EM ENGENHARIA MECÂNICA
DEPARTAMENTO DE MECÂNICA COMPUTACIONAL

DISSERTAÇÃO DE MESTRADO ACADÊMICO

Bi-directional Evolutionary Acoustic Topology Optimization for Muffler Design

Otimização Topológica Bidirecional Evolucionária Acústica para o Projeto de Silenciadores

Autor: Felipe Miranda Azevedo
Orientador: Prof. Dr. Renato Pavanello

A Banca Examinadora composta pelos membros abaixo aprovou esta Dissertação:

Prof. Dr. Renato Pavanello
DMC/FEM/UNICAMP

Prof. Dr. José Maria Campos dos Santos
DMC/FEM/UNICAMP

Prof. Dr. Renato Barbieri
CCT/UDESC

A Ata da defesa com as respectivas assinaturas dos membros encontra-se no processo de vida acadêmica do aluno.

Campinas, 13 de Março de 2017.

Dedicatória

Aos meus queridos pais, Aldemir Azevedo e Larice Miranda, que estiveram comigo durante todos os momentos de minha jornada me apoiando e guiando. Agradeço-os por seu amor e carinho inabaláveis.

Agradecimentos

A Deus, meu salvador, agradeço pelas bençãos que me permitiram a conclusão deste trabalho e todas as outras que foram e são colocadas sob minha família.

A toda minha família, Aldemir, Larice e Camila por terem me apoiado e amado em todos os momentos, sem vocês esta conquista não faria sentido.

Ao meu orientador, Prof. Dr. Renato Pavanello, não apenas pelos ensinamentos e conselhos, mas também pelo grande exemplo de pessoa, professor e pesquisador, pela paciência e amizade durante esses incríveis 2 anos.

Ao meu professor e orientador de TCC, Prof. Dr. Elson, por ter me mostrado caminhos que eu nunca havia pensado seguir e por ser um grande amigo durante toda esta jornada.

Aos amigos e companheiros de laboratório, Sérgio, Jaime, Cláudia, Zulma, Tainan, Marcela, Vinicius, Daniel, Renato Jr. e de departamento, dos quais pretendo levar a amizade para toda a vida. Ir ao trabalho sempre foi fácil sabendo que estaria na presença de pessoas tão boas quanto vocês.

A meus amigos William M. V. e Renato P. S. pelo apoio e conhecimento transmitidos durante o mestrado, até mesmo á distância, que foi essencial para conclusão deste trabalho.

A minha tia, La Ires, e primos por terem me dado carinho, amor de família e apoio em São Paulo.

À Faculdade de Engenharia Mecânica da UNICAMP, em especial ao DMC, representada pelos professores e funcionários, pela oportunidade de realizar este trabalho.

A Coordenação de Aperfeiçoamento de Pessoal de Nível Superior - CAPES, ao E-Science UNICAMP e a FAPESP pelo suporte financeiro essencial para desenvolvimento deste trabalho.

Acknowledgements

To God, my savior, thanks for the blessings that allowed the conclusion of this work and all other that were placed in my family.

To my family, Aldemir, Larice and Camila for the support and love in through all moments, without you this victory would have no meaning.

To my advisor, Prof. Dr. Renato Pavanello, not only for the teaching and counselling, but also for the great example of person, professor and researcher, for the patience and friendship during this 2 years.

To professor and advisor of my graduation paper, Prof. Dr. Elson, for showing me new paths I had never thought of seeking and for being a great friend throughout this journey.

To my friends and laboratory partners, Sérgio, Jaime, Cláudia, Zulma, Tainan, Marcela, Vinicius, Daniel and Renato Jr. whose friendship I will treasure for my entire life. Going to work was always easy knowing I would be in the presence of good people such as you.

To my friends William M. V. and Renato P. S. for the support and knowledge transmitted during the masters, even at a distance.

To my aunt, La Ires, and cousins for caring, loving and supporting me in São Paulo.

To the Faculty of Mechanical Engineering of UNICAMP, especially to DMC, represented by its professors and staff, for the opportunity of doing this work.

To CAPES, E-Science UNICAMP and FAPESP for the financial support of this work.

He stretches out the north over the void and hangs the earth on nothing. He binds up the waters in his thick clouds, and the cloud is not split open under them. He covers the face of the full moon and spreads over it his cloud. He has inscribed a circle on the face of the waters at the boundary between light and darkness. The pillars of heaven tremble and are astounded at his rebuke.

Job 26:7-11

Resumo

AZEVEDO, Felipe Miranda. Otimização Topológica Bidirecional Evolucionária Acustica para o Projeto de Silenciadores. 2017. 120p. Dissertação (Mestrado). Faculdade de Engenharia Mecânica, Universidade Estadual de Campinas, Campinas, Brasil.

Este trabalho propõe um procedimento para projeto de silenciadores automotivos baseado em modelos acústicos por elementos finitos usando Otimização Acústica Evolucionária Bi-direcional. O objetivo principal é descobrir a melhor configuração de barreiras dentro do silenciador acústico usado na indústria automobilística que minimiza o nível de pressão sonoro na saída do silenciador. O meio acústico é governado pela equação de Helmholtz e condições de contorno de paredes rígidas são introduzidas para representar barreiras acústicas. O problema continuo é resolvido no domínio da frequência e é discretizado usando o método dos elementos finitos.

A função objetivo adotada é Perda de Transmissão (TL). A maximização da TL garante que o nível de pressão sonoro na saída do silenciador seja reduzido. Para encontrar a configuração de barreiras acústicas que maximiza a função TL do silenciador o método de Otimização Topológica Evolucionária Bi-direcional (BESO) é utilizado. O método de otimização BESO foi escolhido devido as suas características binárias e para evitar o uso de algoritmos de pós-processamento.

Usando o método BESO topologias simples em modelos 2D são encontradas, maximizando TL para diferentes frequências. As soluções 2D encontradas podem ser utilizadas como referência para a manufatura de silenciadores reais. Alguns exemplos são apresentados para mostrar a eficiência do método proposto.

Palavras-chave: Otimização Topológica; Análise acústica; Silenciadores.

Abstract

AZEVEDO, Felipe Miranda. Bi-directional Evolutionary Acoustic Topology Optimization for Muffler Design. 2017. 120p. Thesis (Mestrado). School of Mechanical Engineering, University of Campinas, Campinas, Brazil.

This work proposes an automotive acoustic muffler design procedure based on finite element acoustic models using a Bi-directional Evolutionary Acoustic Topology Optimization. The main goal is to find the best configuration of barriers inside acoustic mufflers used in the automotive industry that minimizes sound pressure level in the outlet of the muffler. The acoustic medium is governed by Helmholtz equation and rigid wall boundary conditions are introduced to represent acoustic barriers. The continuum problem is solved in the frequency domain and it is discretized using the finite element method.

The adopted objective function is Transmission Loss (TL). Maximizing TL guarantees that the sound pressure level at the outlet of the muffler is reduced. To find the configuration of acoustic barriers that maximizes the Transmission Loss function of the muffler a Bi-directional Evolutionary Structural Optimization (BESO) method is used. The optimization method (BESO) used was chosen because of its binary characteristics and to avoid using post-processing algorithms.

Using BESO method simple topologies in 2D models are reached, which maximizes the Transmission Loss function for different frequencies. The 2D solutions can be used as reference to manufacture 3D mufflers. A few examples are presented to show the efficiency of the proposed design procedure.

Keywords: Topology Optimization; Acoustic analysis; Mufflers.

List of Figures

List of Tables

Table of Contents

1 INTRODUCTION

This chapter's objective is to present the purpose and general scope of this work by introducing the main concepts of typical exhaust systems used in automotive industries. Initially, the motivations and context that instigated this work are exposed showing the current search for healthier environments in regards to sound pollution. Secondly, a brief bibliographic review is done on the main themes surrounding this work creating a background and overall understanding of the state of the art in regards to mufflers and optimization research. Following this work's thematic review general and specific goals of this research are listed. Thereon, a general description of this works content is made, providing an understanding of each chapter's layout.

1.1 Motivation and Context

Noise levels attributed to automobiles have been an important topic of study. Since the first appearance of combustion engines, noise-related health problems have been an issue not only for passengers but to pedestrians (GENUIT, 2004). The demand for power and speed in automobiles grew quickly throughout the years and to answer that demand the industry created lighter and more powerful engines. Noise generated inside and outside automobiles grew together with road traffic requiring better noise absorbing technology (Krebber *et al.*, 2002; García and Faus, 1991).

Noise created in urban centers was raised to a point that regulations had to be created to control the harmful effects of the noise pollution generated by the automobiles. Recently those have been updated to apply a more strict limit, the Environment Action Programme to 2020 adopted by the European Union proposed a significant decrease in noise pollution, almost reaching the recommended noise levels by the World Health Organization (JURAGA *et al.*, 2015). One of the pieces of equipment used to reduce noise in the circumstances mentioned above is the vehicles silencer or muffler.

Positioned at the end of an internal combustion engine exhaust system, mufflers are an engineering solution to control engine noise levels. Figure 1.1 presents an acoustic muffler model. The principal goal of the exhaust system is to minimize the automobile's engine radiated noise. The constant pressure made by international organizations to decrease noise levels, recently updating the Environmental Noise Directive (2002/49/EC), encouraged the development of new muffler schemes and other techniques for noise attenuation.

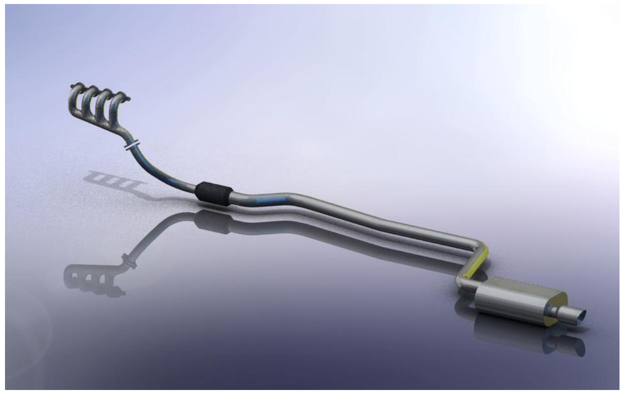

Figure 1.1: Acoustic muffler at the end of an exhaust system.

The modeling of a muffler and the evaluation of its effectiveness have been important study topics, Munjal (1987a) comprehensive work in this subject enabled new lines of research and had a big impact in the automotive industry. Since then, optimization methods together with the Finite Element Method have become popular tools for design in the most diverse research fields. Figure 1.2 presents a muffler model with perforated pipe.

Figure 1.2: Muffler model whit perforated pipe (YEDEG *et al.*, 2016a).

In the scenario described above, this work proposes the usage of an optimization technique in order to achieve a muffler internal topology with optimum characteristics. In this work, the parameter or characteristic that must be maximized is the acoustic filter transmission loss (TL). A bi-directional evolutionary structural optimization method (BESO) (HUANG AND XIE, 2010) was chosen. Using this method the design of muffler internal barriers can be performed considering different frequencies of operation and a certain amount of material.

1.2 Bibliographic Review

In this section, a succinct bibliographic review is presented. A development timeline for muffler acoustics, topology optimization, and acoustic optimization is created. The review starts with references about acoustic filters transmission loss. In the sequence, a brief review about evolution of structural optimization is presented. Finally acoustic topology optimization (ATO) area is reviewed.

1.2.1 Muffler Acoustics

Muffler and duct acoustics have been studied for a long time, but the first comprehensive experimental investigation of muffler analysis and design was done by Davis *et al.* (1954) (MUNJAL, 2013). The evolution of manufacturing techniques and the growing requirements for less noise encouraged new researches in muffler design, since Davis *et al.* (1954) work several authors studied the noise attenuation phenomena inside the muffler.

The acoustic filter theory first introduced by Davis *et al.* (1954) had wide acceptance, however, it still left phenomena unexplained, for instance, different behavior than expected when mufflers were subjected to higher frequencies and failure to describe muffler behavior for intricate muffler configurations. Evaluating transmission loss in complex expansion chambers was a difficult task. Until the decade of 1970, engineers would have to rely on approximations and numerical techniques like Finite Difference Method (FDM), but the application of those for complex geometries was difficult. Young and Crocker (1975) developed an easier way of characterizing the muffler noise attenuation property. The method proposed estimates TL using a finite element method (FEM) with the advantage of working well with arbitrary geometries opposed to FDM. Following the same trend, Craggs (1976) modeled acoustic muffler as damped acoustic systems using FEM.

In the subsequent years, some other aspects of muffler acoustics were introduced and studied. The porosity of the duct inside a resonator or muffler presented a big issue in higher frequencies. Sullivan and Crocker (1978) work created a mathematical model that accurately predicts the behavior of resonators solving the issue mentioned above to a certain extent. Peat (1982) work introduced flow into the analysis and four-pole parameters of ducts were evaluated using FEM.

In 1983 a considerable amount of muffler design studies had been reported but only a small percentage of those included theoretical models and experimental studies on real exhaust systems

(PRASAD AND CROCKER, 1983). Prasad and Crocker (1983) used a real eight-cylinder Ford engine for experimentation and validation of their proposed model, which revealed the source conditions importance to design and analysis of mufflers.

The main usage of low frequencies in order to take advantage of plane wave propagation in most works reached a problem when the presence of higher modes started being noticed at area discontinuities of mufflers with intricate geometries (MUNJAL, 1987b). Those non-accounted higher modes presented problems for the mufflers noise attenuation and diminished their performance. Munjal (1987b) work presented a low computational cost 3D analysis method that accounted for those problematic 3D higher modes facilitating muffler analysis.

Transmission Loss is an important characteristic of a muffler, its evaluation was mainly done through the four-pole transfer matrix approach, to some, this approach was indirect and time-consuming. Wu and Wan (1996) proposed a new method to effectively calculate TL, the Three-Pole Method (TPM). Opposed to the transfer matrix approach which needed 2 sets of boundary conditions resulting in 2 different systems to be solved, the TPM only needed 1 set of boundary conditions and 1 system to be solved for evaluating TL at a given frequency (WU AND WAN, 1996). Later on, Tao and Seybert (2003) reviewed the different methods of calculating TL, which included TPM, Two-Source Method and the Two-Load method both using the transfer matrix method. Bilawchuk and Fyfe (2003) compared TPM and the 4-pole transfer matrix methodology using FEM and Boundary Element Method (BEM) approaches showing that both methods reach similar results but the TPM with FEM approach was faster.

In the last decade, a lot of effort have been made towards finding muffler designs with higher performance. Oh and Cha (2000) and Gerges *et al.* (2005) works took a step towards finding more effective muffler designs using optimal design schemes and the transfer matrix method with experimentation respectively.

1.2.2 Structural topology optimization

Structural optimization in a simplistic way is the search for the best structure that can withstand a certain load. Three types of optimzation can be cited: sizing optimization, shape optimization and topology optimization. By rearranging the material (removing/adding) inside the structure using a sensitivity number as a guide, topology optimization can find the best topology for the proposed scenario. Prager and Rozvany (1977) work in modern optimal layout theories was a pioneer research in the field. Several methods of optimization were developed and improved since then.

Bendsøe and Kikuchi (1988) presented a work about homogenization theory of periodic media using porous materials as means to generate optimal topologies. One year later Bendsøe (1989) proposed a simplified material model named Solid Isotropic Material with Penalization (SIMP). The SIMP method became one of the most used methods in the optimization field being extremely used even nowadays. Its popularity and development can be attributed to Ole Sigmund works (Sigmund, 1994, 1995, 2001). Along with, SIMP, other optimization techniques were developed with the growing computational power and expansion of the field. Level-set method, homogenization methods, evolutionary methods among others are examples of optimization methods.

Level-set method has appeared more recently, Wang *et al.* (2003) and Allaire *et al.* (2004) first introduced and used the method. It consists in representing structural boundaries using a level set model. Level set methods can represent complex topologies and boundary shapes of the structure in a concise way. The flexibility of the method is one of its great advantages.

The BESO method presented in (QUERIN *et al.*, 1998), an evolutionary optimization method, was first introduced as the Evolutionary Structural Optimization (ESO) method in (Xie and Steven, 1993, 1997). The ESO method used a methodology of gradual removal or addition of elements with discrete design variable instead of continuum variables. With further research, the method changed to be more robust, becoming the Bi-directional Evolutionary Structural Optimization (BESO) method. In its work Zhou and Rozvany (2001) pointed some shortcomings the method had commenting on its validity. Zuo *et al.* (2010) and Huang and Xie (2007) works presented studied tools such as numeric filters in order to make the method more robust and general.

Since its creation, the BESO method was used in several optimization problems showcasing the versatility of the method. Vicente *et al.* (2016) did a multi-scale optimization to minimize frequency response. Picelli *et al.* (2015) used the method to maximize the natural frequencies considering acoustic-structure interaction. Vicente *et al.* (2015) optimized frequency response considering fluid-structure interaction.

1.2.3 Acoustic topology optimization

As mentioned before, topology optimization seeks to find the best structural design for a certain case. Acoustic topology optimization (ATO) tries to achieve topologies that are optimum in an acoustical point of view. Until 2006 only a few problems in acoustics had been worked with topology optimization (DÜHRING, 2006). One of the few works published was (BARBIERI AND BARBIERI, 2006). Barbieri and Barbieri (2006) used shape optimization in order to maximize muffler TL using Zoutendijk's Feasible Directions Method (FDM). The FDM optimized each of the design variables and a new analysis would be done until convergence criteria were met.

In regards to topology optimization, Dühring (2006) used SIMP method to control the acoustic properties in a room by changing the material distribution in the ceiling. The possibility of decreasing sound levels in a specific portion of a room is of great interest in the automotive industry, where the method could be applied to diminish sound levels where the passengers would be sited for instance. In this case, the application of the topology optimization could also be used for the design of soundproof materials or in the project of recording rooms.

Other applications of topology optimization with acoustic purposes were studied as well. Wadbro and Berggren (2006) used the Method of Moving Asymptotes (MMA) to optimize an acoustic horn trying to minimize the sound reflections that go back into the waveguide. Including material in the expanding area of the horn and changing its configurations through the optimization process created horns with more efficiency. Essentially the fact that better horns were designed for a specific span of frequency proved that a topology optimization process for elastic structures could also be applied in the acoustic field.

In further works, Dühring *et al.* (2008) showed that topology optimization can be used effectively to minimize sound pressure amplitude in a chosen area inside a room and to create barriers for noise attenuation purposes. Kim and Yoon (2015) proposed new shapes of sound barriers in an outside environment by distributing rigid and porous material with a topology optimization approach, the "T" shape barrier was shown to be one of the most efficient sound barriers. Once the applicability of the optimization approaches to this type of problem had been demonstrated several other acoustic problems were studied.

Optimization approaches started being used in order to achieve greater noise attenuation in mufflers . In Lee and Kim (2009) the muffler internal partitions were optimized using the MMA method to achieve maximum TL. Using FEM and a three-pole methodology Lee and Kim (2009) achieved a higher TL parameter introducing sound barriers inside the expansion chamber. Following the same trend, other authors have come to study the addition of partitions in expansion chambers.

Muffler TL maximization was done using different methods and different conditions and muffler models. Lee and Jang (2012) optimized the muffler partitions layout considering TL and flow characteristics. Yoon (2013) used a Delany-Bazley empirical model of a fibrous material in the optimization process in order to find the best configuration of a porous material inside the muffler. Other works presented acoustic-thermal coupling (LEE AND OH, 2014), flow-reversing chambers (JANG AND LEE, 2016) etc.

New muffler models are being created and/or adapted to represent more realistically the working conditions and characteristics of a muffler. Yedeg *et al.* (2016a) proposed and studied a muffler model with a perforated pipe implemented as a thin impedance layer inside the muffler and Yedeg *et al.* (2016b) researched a way of using a Nitsche-type method for acoustic problems with embedded permeable surfaces, this method cane be used as a modeling tool for muffler optimization.

While many works were done on ATO and more specifically on topology optimization of mufflers, only a few used experimental data to further observe its simulation results, in Lee (2015) work, acrylic mufflers were produced to validate Transmission Loss levels of two muffler optimized topologies, the experiments presented similar TL curves thus validating the optimization results. Most of the presented works in the field use 2D formulation to model the muffler, for the sake of simplicity or to avoid big computational costs. Others used different softwares to study design and definition of exhaust systems, Moura *et al.* (2008) used a commercial one-dimensional virtual simulation software.

1.3 Objectives and Contributions

This works main purpose is to adapt and implement an acoustical topology optimization algorithm using the BESO method for reactive muffler design. In order to optimized a reactive muffler one of its performance parameters (TL) was chose as objective function and strategies of how to evaluate this performance parameter and its sensitivities in the design domain are proposed. Finite element mesh influence in the optimum topologies reached is investigated. This works specific objectives are listed bellow:

- Acoustical analysis of the behavior of reactive mufflers to develop the transmission loss optimization problem.
- Propose and validate a strategy for transmission loss evaluation together with a finite element

approach.

- Implement an adapted BESO algorithm for the muffler acoustical problem.
- Evaluate the efficiency of the mufflers with the final topologies found using the proposed method.
- Analyze finite element mesh influence in the final topologies.

This works most important contribution is the first usage of the BESO method for the muffler optimization problem. Secondary investigations are done in order to observe the methods compatibility with the proposed optimization case. This work gives a general understanding of the muffler acoustical problem as well.

1.4 Work layout description

This dissertation is organized into five chapters. This chapter presents a general overview of acoustic mufflers including their functionality and importance in today's society health. A brief bibliographic review is done over the main themes of this dissertation, muffler acoustics, structural topology optimization and acoustic topology optimization. The motivations for this research are presented, general and specific objectives are listed and the contributions of this work are exposed.

Chapter 2 introduces the main study theme of this dissertation, expansion chamber mufflers. Functionality, types and performance parameters are presented in order to lay a solid foundation of the subject. The continuum formulation starting with the Helmholtz equation and boundary conditions is described. A discrete finite element formulation is developed for the acoustical muffler using a Weighted residual method. The method proposed for evaluating TL, objective function of the optimization, is explained and validated using analytical equations as comparison. The modeling of the acoustic barriers introduced inside the muffler is described.

Chapter 3 presents the optimization problem. The sensitivity number is derived and the analysis based on the sensitivity is explained. The evolutionary method (BESO) implementation aspects are presented. Filter scheme, sensitivity history and design variable update steps of the optimization are described. Finally, the evolutionary procedure proposed in this dissertation is summarized at the end of the chapter.

Chapter 4 exposes numerical examples and discusses the results of the optimization cases. Primarily BESO Hard-kill results are presented and analyzed. Secondarily, four optimization cases are presented using four different characteristic frequencies, this cases are studied and its final topologies are evaluated. Different meshes are tested to see the methods capability of reaching optimal topologies that are mesh independent.

Chapter 5 presents this dissertation's concluding remarks and suggestion for future works.

2 SILENCER ACOUSTICS: PERFORMANCE PARAMETERS, CONTINUUM FORMULATION AND DISCRETE MUFFLER MODELLING

Analysis of a muffler can be done using different methods, transfer matrix and three-pole method are examples of it. This chapter presents concepts on acoustic filter theory with focus on expansion chamber mufflers. The goal is to understand the theory and behavior of the expansion chamber. The data acquired using the theory here explained will be used in the next chapters for the optimization problem. The concepts and theory presented here can be found in Munjal (1987a), Wu and Wan (1996), Barron (2002) and Lee and Kim (2009).

2.1 Introduction

A silencer is an important equipment used for noise control in machinery exhaust and other sources involving gas flow (BARRON, 2002). Silencers can be passive or active. Passive silencers exploit wave reflection (reactive muffler) or wave absorption (dissipative mufflers) in order to attenuate sound and are mainly called mufflers. Active silencers use electronic techniques to create destructive interference and attenuate sound.

Basically a silencer uses geometric tools to creates wave reflections effectively decreasing the sound power output. The application of an optimization process in a reactive muffler seeks to maximize the wave reflection effect that diminishes sound power in the outlet of the silencer. The wave transmission phenomena inside the duct is governed by the Helmholtz equation.

The application of the Helmholtz equation yields the acoustic pressure in the frequency domain and has two important restrictions, energy dissipation effects are neglected and pressure wave amplitude must be relatively small in comparison with atmospheric pressure (BARRON, 2002). To analyze and solve the optimization problem proposed in this work it is necessary to solve the Helmholtz equation.

The reactive muffler model characteristic acoustic pressure field given by the Helmholtz equation is an important indicator of the muffler behavior. It can be said that the acoustic pressure field displayed by the muffler for any given frequency is a function of its attenuating properties. The objective of this chapter is not only to present the concepts of acoustic filters but to give all the mathematical modeling necessary to simulate the muffler behavior in the optimization problem conditions, that includes the FEM discretization of the Helmholtz equation.

2.2 Reactive Mufflers: Concept and Description

An acoustic filter consists of a single element or a set of elements located between a source of acoustic signals and the receiver (MUNJAL, 1987a), for example, the exhaust pipe between engine and atmosphere. As said before, reactive mufflers are silencers that use only wave reflections as tools to create sound attenuation. Two possible ways of achieving wave reflections in a duct are:

1. Connecting a Helmholtz resonator in the main duct.
2. Creating an abrupt change in cross-sectional area.

A reactive muffler that uses concept number 1 is called a side-branch muffler. Side-branch mufflers use Helmholtz resonators to reflect acoustic energy back to the source. In this work reactive mufflers that use concept number 2 are the main focus, they are expansion chamber mufflers.

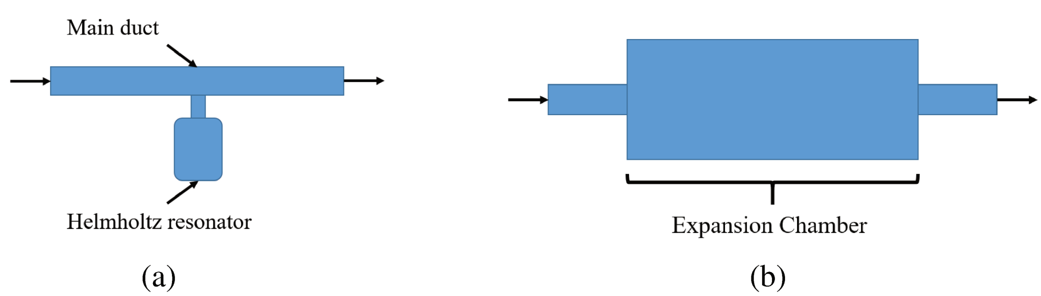

Figure 2.1: Examples of reactive mufflers. (a) A side-branch muffler diagram . (b) An expansion chamber muffler diagram.

The expansion chamber muffler presented in Fig. 2.1 b) is a single expansion chamber muffler. Depending on the performance required, the designer can use multiple expansion chambers or resonators. In the automotive industry these techniques are combined to create the highest acoustical performance without generating a pressure drop number high enough or low enough to harm the engines work, see Fig. 2.2.

In a reactive muffler, the principle of energy conservation requires that the rate of energy flow through the system is the same in all positions, making it sound paradoxical that the muffler

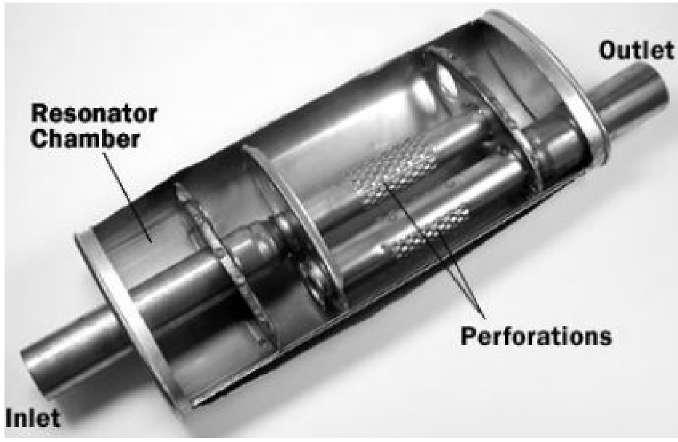

Figure 2.2: Typical reactive automotive muffler (POTENTE, 2005).

is able to attenuate sound since the energy would still be the same in the outlet. The answer to that paradox is that the reflection reduces the net energy flow in comparison with the unattenuated case (FAHY, 2000). Although the process of sound attenuation by wave reflection is clear, it is still hard to quantify the effect. Some performance parameters were created so that the wave reflection effect on the muffler could be properly accounted for.

2.3 Muffler performance parameters

The performance of an acoustic filter, in this case an expansion chamber muffler, can be measured using three parameters (MUNJAL, 1987a).

- Insertion Loss (IL)
- Level Difference (LD) or Noise Reduction (NR)
- Transmission Loss (TL)

Insertion loss by definition is the logarithmic ratio between the sound power in the outlet of a system without a silencer and the sound power of the same system with a silencer. Figure 2.3 shows two ducts, one has no silencer and has sound power W_1 in the outlet and the other has a silencer presenting W_2 in the outlet.

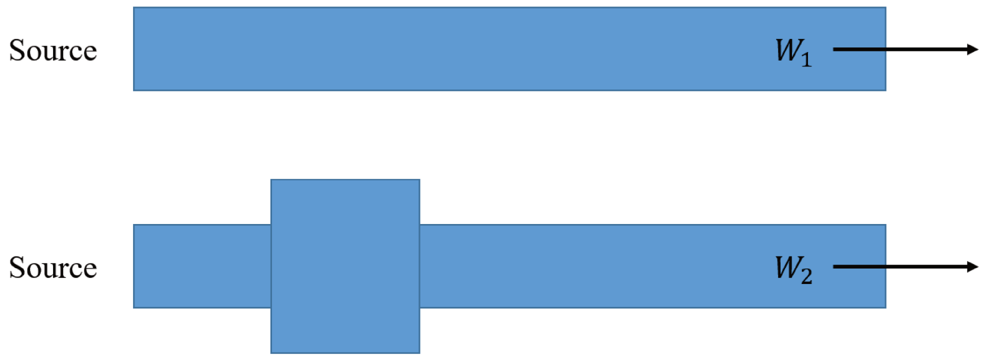

Figure 2.3: Insertion loss performance parameter definition.

$$IL = 10 \log_{10} \left(\frac{W_1}{W_2} \right) \tag{2.1}$$

Using Eq. 2.1 insertion loss of the silencer presented in Fig. 2.3 can be calculated. IL takes into account not only the attenuators performance but the alterations it brings to the entire system.

Level difference or noise reduction is the difference in sound pressure levels between two points of interest. As defined, LD is

$$LD = SPL_1 - SPL_2 \tag{2.2}$$

since,

$$SPL = 20 \log_{10} \frac{P_n}{2 \times 10^{-5}} \; dB \tag{2.3}$$

LD becomes,

$$LD = 20 \log_{10} \frac{P_1}{P_2} \; dB \tag{2.4}$$

where P_n is the acoustic pressure in the interest point n.

Level difference can be calculated using Eq. 2.4 and although IL is a comprehensive performance parameter this work uses transmission loss as its main performance parameter. Transmission loss detailed formulation and validation are done next.

2.3.1 Transmission Loss - Analytical formulation

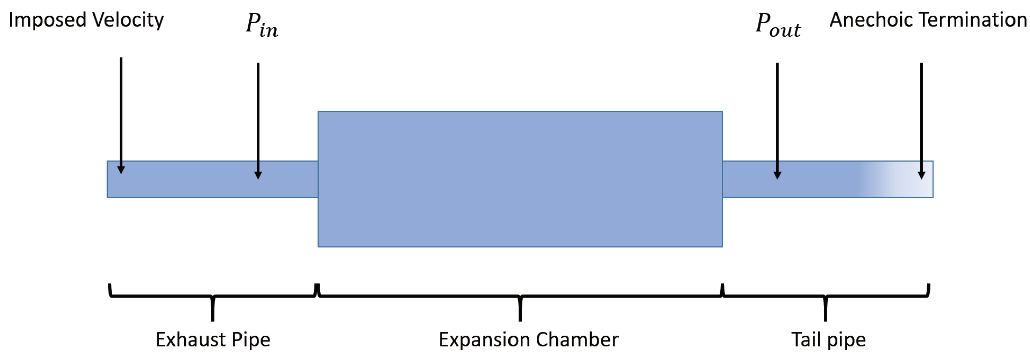

Figure 2.4: Expansion chamber muffler nomenclature.

Transmission Loss is an acoustical performance parameter, used to evaluate different acoustic filters, in this case, a muffler Fig. 2.4. TL can be described as the difference between power incident on the exhaust pipe and the power transmitted to the tailpipe that goes through the anechoic termination (MUNJAL, 1987a), Eq. 2.5 shows this relationship. Figure 2.4 shows the inlet duct and the outlet duct terminology. The inlet pipe or exhaust pipe receives the gases coming from the engine and direct them to the expansion chamber while the outlet duct or tail pipe directs the flow to the atmosphere. To represent inlet and outlet conditions 2 boundary conditions are used, imposed particle velocity and anechoic termination, both represented in Fig. 2.4.

$$TL = 10 \log \left| \frac{W_{in}}{W_{out}} \right| \tag{2.5}$$

where W_{in} is the incoming sound power and W_{out} is the outgoing sound power.

Sound power of a plane wave is proportional to the square of sound pressure amplitude and the waveguide cross-sectional area (WU AND WAN, 1996), thus Eq. 2.5 becomes

$$TL = 20 \log \left| \frac{P_{in}}{P_{out}} \right| + 10 \log \frac{A_{in}}{A_{out}} \tag{2.6}$$

where A_{in} and A_{out} are the cross-sectional areas of exhaust pipe and tail pipe respectively. In this work all muffler models have the same cross-sectional area, using that premise Eq. 2.6 can be reduced to

$$TL = 20 \log \left| \frac{P_{in}}{P_{out}} \right| \tag{2.7}$$

Equation 2.7 can be used to evaluate transmission loss in a silencer where exhaust and tail pipes have the same cross-sectional area. The same can be accomplished using analytical equations. Works such as (MUNJAL, 1987a), (BARRON, 2002) and (DAVIS *et al.*, 1954) present an analytical formulation for single and double expansion chamber mufflers. Analytical equations presented in this work assume the following:

- Sound pressures are small when compared with the absolute value of average pressure in the system.
- Tailpipe is terminated with its characteristic impedance avoiding reflected waves.
- The muffler walls neither conduct nor transmit sound energy.
- Only plane pressure waves are considered.
- Viscosity effects are neglected.

The assumptions made refer to cylindrical ducts but can be used in bi-dimensional cases as the one proposed in this work. For a single expansion chamber case in which exhaust pipe and tail pipe have the same diameter, TL can be calculated as

$$TL = 10 \times \log_{10} \left(1 + \frac{1}{4} \left(m - \frac{1}{m} \right)^2 sin^2 \left(kL \right) \right) \tag{2.8}$$

where,

$$m = \frac{d}{d_i}, k = \frac{2\pi f}{c}$$

d is the expansion chamber diameter, d_i is the inlet and outlet duct diameter, k is the wave number, f is the frequency and c is the speed of sound in the medium. In Davis *et al.* (1954) work m was an area ratio of the cylindrical mufflers, for the bi-dimensional case a width ratio is used. Evaluating Eq. 2.8 from 0 to 1200 Hz analytical TL muffler behavior can displayed, as seen in Fig. 2.5.

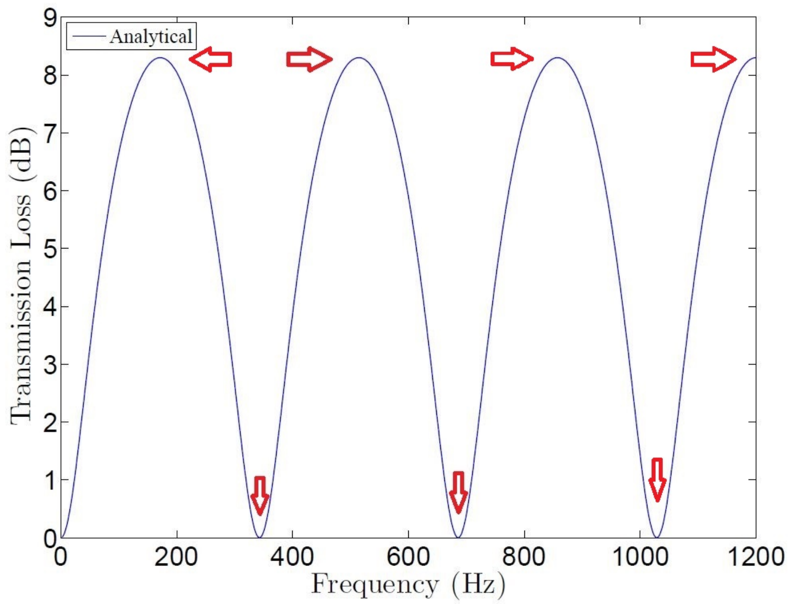

Figure 2.5: TL analytical function of a single expansion chamber muffler with $m = 5$.

The analytical transmission loss behavior show in Fig. 2.5 describes a typical pattern for an expansion chamber. The transmission loss curve shown have maximum TL of approximately 8 dB and minimum of 0 dB. In this work, a few of the frequencies that present peak TL (8 dB) and valley TL (0 dB) were choose to be studied in the optimization cases, they are 346 Hz, 518 Hz and 690 Hz.

In this work, the optimization process will add material inside the expansion chamber so it is possible that a double expansion chamber configuration appears. Figure 2.6 shows a 3D representation of a double expansion chamber and a 2D model with its main measures for the analytical formulation. Transmission loss can be calculated in an analytical manner for this kind of configuration. According to Barron (2002),

$$TL = 10 \times \log_{10} \left(G_1^2 + G_2^2 \right) \tag{2.9}$$

where,

$$G_1 = cos\left(2kL_2\right) - \left(m - 1\right) sin\left(2kL_2\right) tan\left(kL_1\right) \tag{2.10}$$

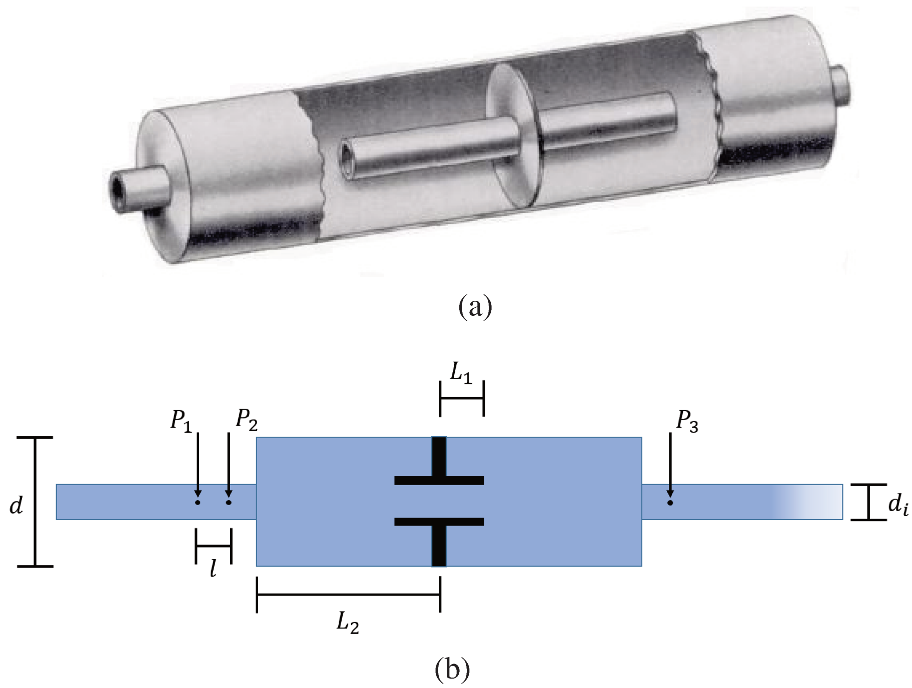

Figure 2.6: Double expansion chamber muffler. (a) A 3D rendering of a double expansion chamber muffler (DAVIS *et al.*, 1954). (b) Double expansion chamber variables of interest.

$$G_2 = \frac{1}{2}(m-1)\,tan\,(kL_1)\left[\left(m+\frac{1}{m}\right)cos\,(2kL_2) - \left(m-\frac{1}{m}\right)\right] + \frac{1}{2}\left(m+\frac{1}{m}\right)sin\,(2kL_2) \tag{2.11}$$

L_1 is half the length of the inner duct connecting both expansion chambers and L_2 is the length of both expansion chambers.

Equation 2.9 is evaluated from 0 Hz to 1200 Hz to display transmission loss behavior for a double expansion chamber with the same configuration presented in Fig. 2.6.

In Fig. 2.7 its possible to observe that the TL increases by a high margin when double expansion chambers are used. From 0 Hz to 170 Hz a peak TL of 3.5 dB is achieved, but for higher frequencies TL was magnified. In Fig. 2.7 all frequencies over 200 Hz present a TL higher than 8 dB, which was the maximum TL for single expansion chambers. Peak TL achieved was 25.6 dB at 446 Hz and approximately 81 dB at 858 Hz.

A double expansion chamber muffler can have a different configuration. Two expansion chambers connected by a duct can be seen as a double expansion chamber muffler. Figure 2.8

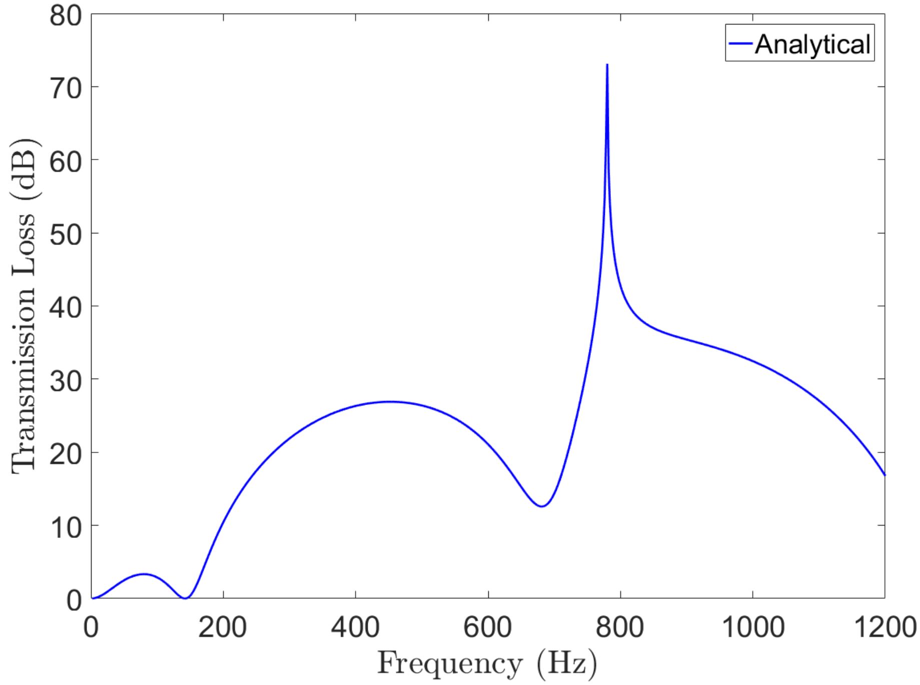

Figure 2.7: TL analytical function of a double expansion chamber muffler ($L_1 = 0.11$m, $L_2 = 0.25$m and $m = 5$).

presents this different configuration and its measurements. The analytical formulation presented before is not valid for this case. For configuration shown in Fig. 2.8 TL can be rewritten as,

$$TL = 10 \times \log_{10}\left(\frac{F_1^2 + F_2^2}{16m^2}\right) \tag{2.12}$$

where,

$$F_1 = (m+1)^2 cos\left[2k\left(L_1 + L_2\right)\right] - (m-1)^2 cos\left[2k\left(L_2 - L_1\right)\right] \tag{2.13}$$

$$\begin{split} F_2 = \frac{1}{2}\left(m + \frac{1}{m}\right)\left((m+1)^2 sin\left[2k\left(L_1 + L_2\right)\right] - (m-1)^2 sin\left[2k\left(L_2 - L_1\right)\right]\right) - \\ + \left(m - \frac{1}{m}\right)\left(m^2 - 1\right) sin\left(2kL_1\right) \end{split} \tag{2.14}$$

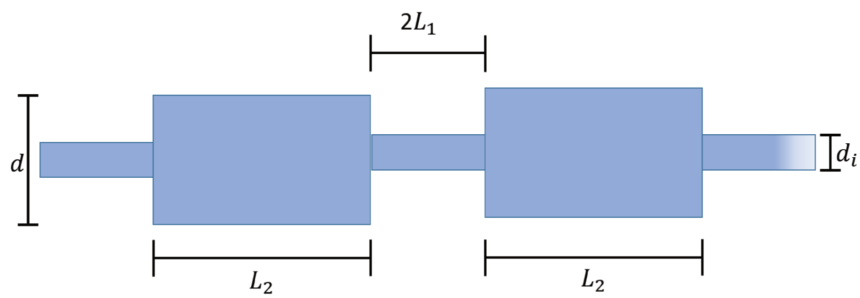

Figure 2.8: Double expansion chamber muffler with different configuration.

Evaluating Eq. 2.12 from 0 Hz to 1200 Hz the behavior of a muffler with configuration similar to Fig. 2.8 can be predicted. Figure 2.9 presents

Analyzing Fig. 2.9 is possible to see that a different behavior is achieved with the configuration presented in Fig. 2.8. In this case low TL is encountered in frequencies between 0 Hz and 200 Hz reaching only 4.1 dB at 112 Hz. From 200 Hz to 860 a higher TL area can be seen reaching 20.5 dB at 510 Hz and a smaller one reaching 18.3 dB at 1200 Hz.

The results presented above shows the variety of options the designer can consider when designing a muffler. Depending on project constraints, such as, muffler weight, pressure drop, working frequencies, etc. several configurations of muffler can be considered. For instance, if a muffler has working frequency between 400 Hz and 600 Hz and no weight constraints both double expansion chambers presented could be used. Both configurations shown present high TL between the working frequencies mentioned.

In order to evaluate transmission loss during the optimization process a finite element approach is used to discover the acoustic pressure distribution in the muffler. The analytical approaches presented here are not able to account for the different configurations that will appear while optimizing the muffler expansion chamber. Next section describes the FEM formulation.

2.4 Muffler Acoustic System - Continuum formulation

Consider an acoustic system as show in Fig. 2.10 where the domain $(\Omega_d \mathrm{U} \Omega_f)$ is a fluid domain governed by the Helmholtz equation Eq. 2.15 and the system has known boundary conditions

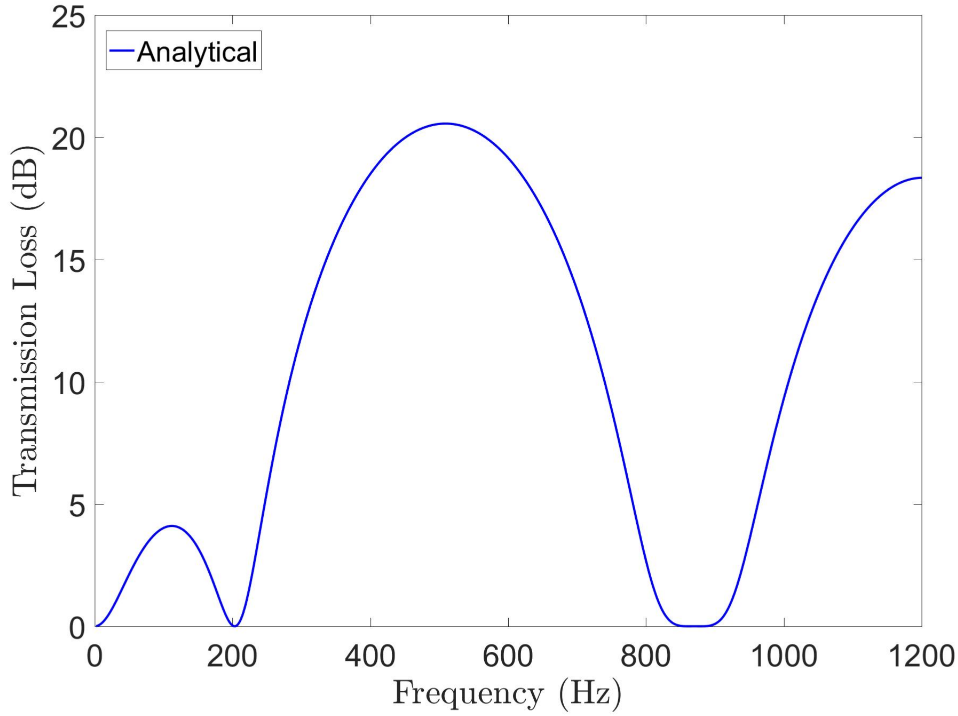

Figure 2.9: TL analytical function of a double expansion chamber muffler ($L_1 = 0.055$m and $L_2 = 0.195$m).

Eqs. 2.16, 2.17 and 2.18.

$$\nabla^2 P + \frac{\omega^2}{c^2} P = 0 \qquad \text{in } \Omega_d \mathrm{U} \Omega_f \tag{2.15}$$

$$\nabla P \cdot \mathbf{n} = \frac{\partial P}{\partial \mathbf{n}} \qquad \text{in } \Gamma_w \tag{2.16}$$

$$V_n = -\frac{1}{j\rho\omega}\frac{\partial P}{\partial \mathbf{n}} \qquad \text{in } \Gamma_i \tag{2.17}$$

$$P = \bar{Z} V_n = -\frac{\bar{Z}}{j\rho\omega}\frac{\partial P}{\partial \mathbf{n}} = -\frac{1}{j\rho\omega\bar{A}}\frac{\partial P}{\partial \mathbf{n}} \qquad \text{in } \Gamma_o \tag{2.18}$$

where $\mathbf{n}$ is the outward unit normal to the muffler domain, j is the imaginary unit, ρ is the air density, ω is the angular frequency in (rad/s), $\bar{Z}$ is the impedance, $\bar{A}$ is the admittance, P is the acoustic pressure, Ω_d is the design domain, Ω_f is the non-design fluid domain, V_n is the particle velocity, c is the sound velocity in the medium and the Γ boundaries are defined in Fig. 2.10.

The optimization objective is to maximize Transmission Loss in the muffler for different frequencies. To accomplish this goal the evaluation of the acoustic pressure field is necessary. Using the finite element method to approximate the continuum problem defined in Eqs. 2.15-2.18 the muffler acoustic problem takes the form of the following global discretized acoustic system

$$\left(\mathbf{K} + j\omega\mathbf{C} - \omega^2\mathbf{M}\right)\mathbf{p} = \mathbf{f} \tag{2.19}$$

where $\mathbf{K}$ is the fluid's acoustic stiffness matrix, $\mathbf{C}$ is a damping matrix , $\mathbf{M}$ is the fluid's acoustic mass matrix, $\mathbf{p}$ is the acoustic nodal pressure vector and $\mathbf{f}$ is the nodal load vector harmonically introduced in the system (Cook *et al.*, 2007), (Marburg and Nolte, 2008). Further work in this paper will show that $\mathbf{f}$ due to the boundary conditions used is a vector calculated according to the particle velocities imposed in the inlet Γ_i. Solving Eq. 2.19 the pressure field of the whole domain can be found.

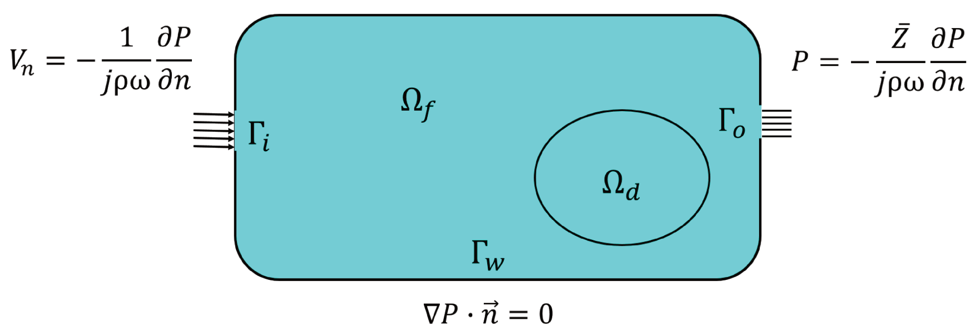

Figure 2.10: Acoustic domain and boundary conditions of the muffler system.

2.4.1 Finite element method for reactive mufflers

To apply the finite element method in the problem described above, a Weighted Residual method is used. The FEM approach described next will approximate the sound pressure field giving the necessary data to evaluate transmission loss in the acoustic muffler.

2.4.1.1 Reactive acoustic system: Descretized formulation

To find approximate solutions of the acoustic muffler system a FEM approach was used. In order to apply FEM a weighted residual formulation is used in the strong form of Eq. 2.15, so that a weak form is obtained. Using weight function Φ, Eq. 2.15 becomes,

$$\frac{1}{\rho}\int_{\Omega}\Phi\nabla^2 P d\Omega + \frac{\omega^2}{\rho c^2}\int_{\Omega}\Phi P d\Omega = 0 \tag{2.20}$$

Using Green's theorem the weak form of Eq. 2.20 can be rewritten as:

$$\frac{1}{\rho}\int_{\Gamma}\Phi\nabla P\cdot\mathbf{n}d\Gamma - \frac{1}{\rho}\int_{\Omega}\nabla\Phi\cdot\nabla P d\Omega + \frac{\omega^2}{\rho c^2}\int_{\Omega}\Phi P d\Omega = 0 \tag{2.21}$$

where $\mathbf{\Gamma}$ is the complete boundary of the domain presented in Fig. 2.10.

Using the Neumann boundary condition, Eq. 2.16, the weighted residual formulations becomes

$$\frac{1}{\rho}\int_{\Omega}\nabla\Phi\cdot\nabla P d\Omega - \frac{\omega^2}{\rho c^2}\int_{\Omega}\Phi P d\Omega = \frac{1}{\rho}\int_{\Gamma}\Phi\frac{\partial P}{\partial n}d\Gamma \tag{2.22}$$

Equation 2.22 is the weak form of the Helmholtz equation. In this work the muffler model will use three boundary conditions, rigid wall condition, imposed particle velocity and imposed impedance, respectively shown in Eq. 2.23.

$$\begin{cases} \nabla P\cdot\mathbf{n} = 0 \\ \quad V_n = 1 \\ \quad \bar{Z} = \rho c \end{cases} \tag{2.23}$$

Using the boundary conditions proposed in Eqs. 2.16, 2.17 and 2.18 the weak form Eq. 2.22 can be written as follows

$$\frac{1}{\rho}\int_{\Omega}\nabla\Phi\cdot\nabla P d\Omega - \frac{\omega^2}{\rho c^2}\int_{\Omega}\Phi P d\Omega = -\frac{1}{\rho}\left(\int_{\Gamma_i} j\rho\omega\Phi V_n d\Gamma_i + \int_{\Gamma_o} j\rho\omega\Phi\bar{A}P d\Gamma_o\right) \tag{2.24}$$

where the rigid wall boundary $\mathbf{\Gamma_w}$ integral vanishes accordingly with Eq. 2.23.

Using Galerkin's weighted residual approach the weight function and its gradient can be interpolated using the same set of shape functions as the sound pressure and the sound pressure gradient, such that

$$\begin{cases} \Phi = \mathbf{N}\boldsymbol{\phi_i} \\ P = \mathbf{N}\mathbf{p_i} \\ \nabla\Phi = \boldsymbol{\partial}\mathbf{N}\boldsymbol{\phi_i} = \mathbf{B}\boldsymbol{\phi_i} \\ \nabla P = \boldsymbol{\partial}\mathbf{N}\mathbf{p_i} = \mathbf{B}\mathbf{p_i} \end{cases} \tag{2.25}$$

where $\boldsymbol{\phi_i}$ is the vector of nodal test function magnitudes, $\mathbf{p_i}$ is the vector of nodal acoustic pressures, $\mathbf{N}$ is the set of shape functions and $\mathbf{B}$ their derivatives.

Applying Galerkin's approach from Eq. 2.25 in Eq. 2.24 the following system is reached

$$\left(\mathbf{K_g} + j\omega\mathbf{C_g} - \omega^2\mathbf{M_g}\right)\mathbf{p} = \mathbf{v} \tag{2.26}$$

with,

$$\mathbf{K_e} = \int_{\Omega_e} \mathbf{B}^t\mathbf{B}d\Omega_e \tag{2.27}$$

$$\mathbf{C_e} = \rho\bar{A}\int_{\Gamma_{oe}} \mathbf{N}^t\mathbf{N}d\Gamma_{oe} \tag{2.28}$$

$$\mathbf{M_e} = \frac{1}{c^2}\int_{\Omega_e} \mathbf{N}^t\mathbf{N}d\Omega_e \tag{2.29}$$

$$\mathbf{v} = -j\rho\omega\int_{\Gamma_i} \mathbf{N}^t V_n d\Gamma_i \tag{2.30}$$

where $\mathbf{K_e}$ is the fluid element stiffness matrix, Ω_e is the element fluid domain, $\mathbf{C_e}$ is the element damping matrix, Γ_{oe} is the outlet element boundary, $\mathbf{M_e}$ is the element mass matrix, $\mathbf{v}$ is the force equivalent vector in the inlet boundary Γ_i. Using the finite element methodology (Zienkiewicz and Taylor, 2000; Reddy, 1993) the global matrices presented in Eq. 2.26 can be written as follows.

$$\mathbf{K}_g = \mathop{\mathsf{A}}_{i=1}^{N} \mathbf{K}_e \tag{2.31}$$

$$\mathbf{C}_g = \mathop{\LARGE A}_{i=1}^{No} \mathbf{C}_e \tag{2.32}$$

$$\mathbf{M}_g = \mathop{\LARGE A}_{i=1}^{N} \mathbf{M}_e \tag{2.33}$$

where A is the assembly finite element operator, N is the number of elements and No is the number of elements in the outlet boundary.

2.5 Three-pole method

Transmission loss definition given in Eq. 2.7 shows that in order to calculate TL both P_{in} and P_{out} are needed. Using the finite element approach presented in this work all acoustic pressures in the fluid domain can be found. However, the acoustic pressure P_{in} found is affected by waves coming from the inlet region and by waves being reflected inside expansion chamber. Figure 2.11 shows the presence of acoustic pressure P_i, incident acoustic pressure coming from inlet, and P_r, incident acoustic pressure reflected from the expansion chamber, both constituting P_{in}. To evaluate TL the influence of P_r must be removed. Figure 2.11 also show the acoustic pressure in the outlet P_o. The anechoic termination in the outlet guarantees that there are no reflected waves making P_o the real acoustic pressure exiting the expansion chamber.

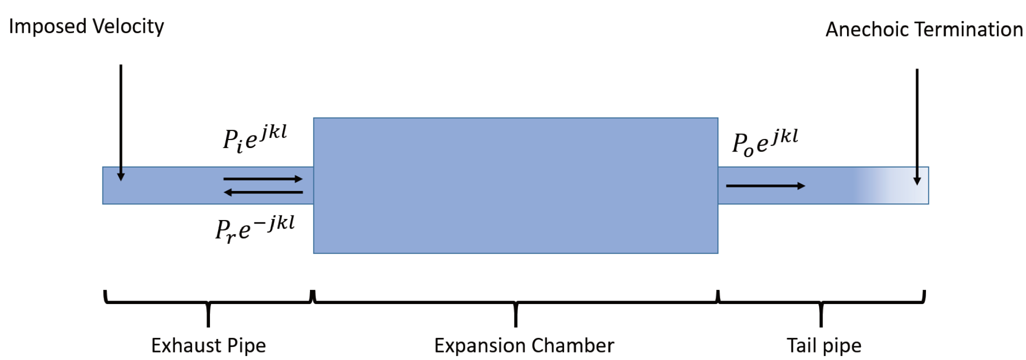

Figure 2.11: Incident, reflected and outward waves.

To calculate TL a four-pole method (Young and Crocker, 1975; Craggs, 1976) was created and widely used. Later, a three-pole method (Wu and Wan, 1996) was created and effectively

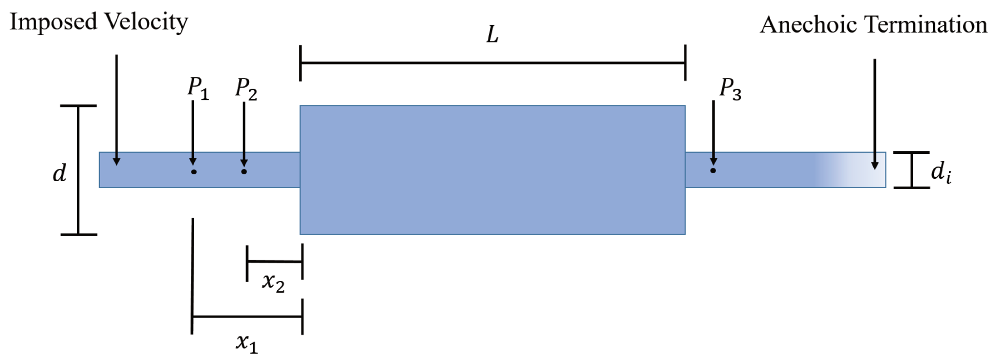

Figure 2.12: Muffler dimensions and Points of Interest for the three-pole method.

removed the influence of P_r when calculating transmission loss. Wu and Wan (1996) showed that using two acoustic pressure points in the inlet region the influence of P_r could be calculated and removed resulting in the desired P_{in}. Figure 2.12 shows the acoustic pressure points P_1 and P_2 used for P_{in} calculation. P_1 and P_2 can be calculated by the following equations.

$$P_1 = P_i e^{jkx_1} + P_r e^{-jkx_1} \tag{2.34}$$

$$P_2 = P_i e^{jkx_2} + P_r e^{-jkx_2} \tag{2.35}$$

where x_1 and x_2 are the distances each pressure point has from the expansion chamber, presented in Fig. 2.12.

Solving Eq. 2.34 and Eq. 2.35 for P_i and P_r, P_i can be found. Note that P_i is the acoustic pressure needed for evaluating TL, from this point forward this acoustic pressure will be refered as P_{in}.

$$P_{in} = \frac{1}{2jsin\left(k\left(x_1 - x_2\right)\right)} \left(P_1 e^{-jkx_2} - P_2 e^{-jkx_1}\right) \tag{2.36}$$

Rearranging Eq. 2.36 a definitive equation for P_{in} can be found.

$$P_{in} = \frac{P_1 - P_2 \cdot e^{-jk \cdot l}}{1 - e^{-j2k \cdot l}} \tag{2.37}$$

where k is the wave number and l is the axial distance between pressure points 1 and 2.

Since,

$$P_{out} = P_o$$

transmission loss described in Eq. 2.7 becomes

$$TL = 20 \times \log_{10} \left(\left| \frac{1}{P_o} \frac{P_1 - P_2 \cdot e^{-jk \cdot l}}{1 - e^{-j2k \cdot l}} \right| \right) \tag{2.38}$$

Transmission Loss in Eq. 2.38 can be calculated once the acoustic pressures in points 1, 2 and 3 are known.

2.6 Validating FEM muffler model

In this section the FEM approach presented before is used. The acoustic pressure distribution in the muffler is displayed for some distinguished frequencies and the three-pole method presented is compared with the given analytical equations.

2.6.1 Acoustic pressure distribution

Once the finite element system Eq. 2.26 is solved, the sound pressure for each finite element is obtained. To find the acoustic pressures using a FEM model some variables must be defined, for example, type of finite element, element size, expansion chamber muffler lengths and diameters.

In this work, all the examples use an element called Quad4. The Quad4 element is a rectangle with 4 nodes, as displayed in Fig. 2.13. Meshes (a) and (b) presented have 720 elements and 3120 elements respectively. All necessary measures of the expansion chamber muffler and element size used in the simulations of this section are exposed in Fig. 2.13. In the coarse mesh Fig. 2.13 (a) the element size is 10x10 mm. In the fine mesh, Fig. 2.13 (b), the element size is 5x5 mm. Both elements are square and identical for the whole domain. In consequence, the element can be calculated only one time reducing the computational cost of the finite element analysis.

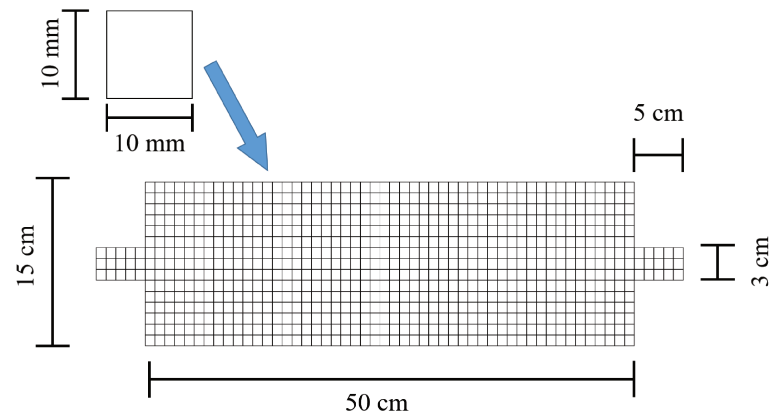

(a)

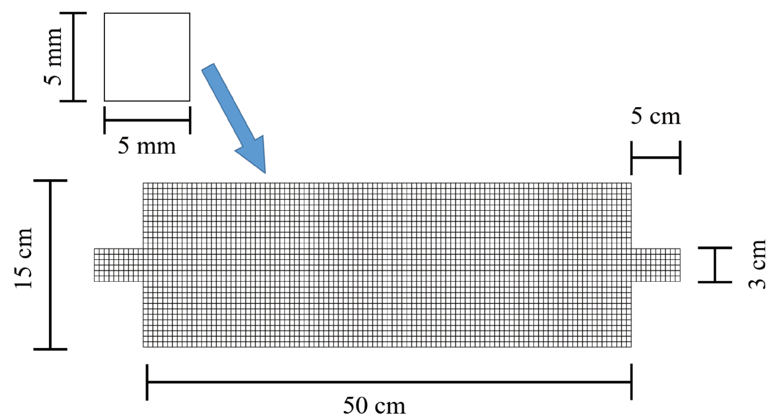

(b)

Figure 2.13: Finite element mesh and muffler model dimensions.(a) Mesh with 780 elements. (b) Mesh with 3120 elements.

To observe the sound pressure distribution, 2 frequencies (ω) were chose, 346 Hz and 690 Hz. These frequencies were chosen based on their influence in the transmission loss curves presented in Fig. 2.5. These frequencies corresponds to two acoustic modes of the muffler cavity and will be used later for optimization cases.

In Fig. 2.14 the results of solving the Helmholtz equation together with a finite element approach are presented. The absolute acoustic pressure fields encountered for each frequency with the two different meshes presented in Fig. 2.13 were similar as expected. The dynamic response at those frequencies is similar with expected mode shapes for the same frequencies and confirm the coherence of spatial distribution of the numerical results. Both meshes are subject of further studies and validation in the next subsection.

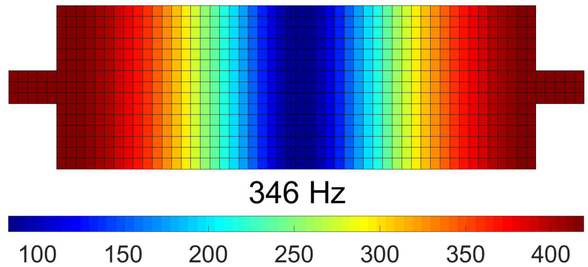

(a)

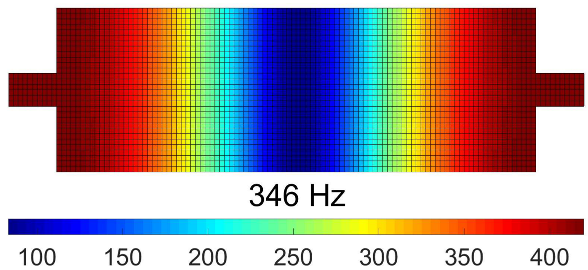

(b)

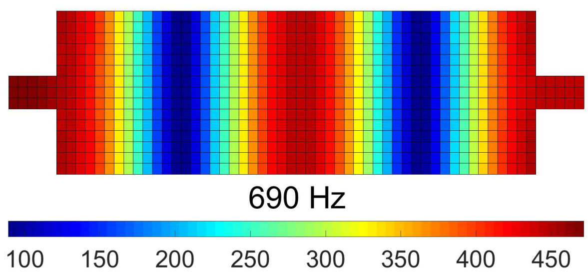

(c)

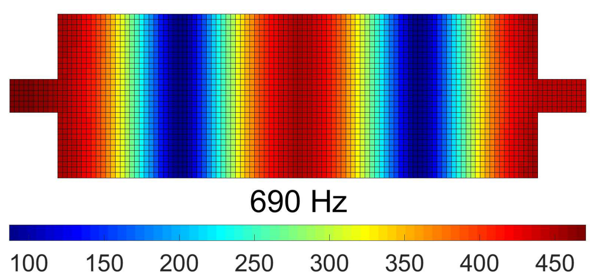

(d)

Figure 2.14: Absolute acoustic pressure distribution for two different acoustic modes of the single expansion chamber. (a) 346 Hz of frequency with 780 elements mesh. (b) 346 Hz of frequency with 3120 elements mesh. (c) 690 Hz of frequency with 780 elements mesh. (d) 690 Hz of frequency 3120 elements mesh.

2.6.2 Transmission Loss - Three-pole method Vs. Analytical

In this work three different analytical cases were presented, a single expansion chamber presented in Fig. 2.4, a double expansion chamber by adding a partition presented in Fig. 2.6 and a double expansion chamber by connecting two single expansion chambers presented in Fig. 2.8. Using the three-pole method calculated with Eq. 2.38 together with the finite element approach a comparison of the transmission loss curves and analytical TL response calculated with Eq. 2.8 for the single expansion chamber can be done using the two different meshes presented.

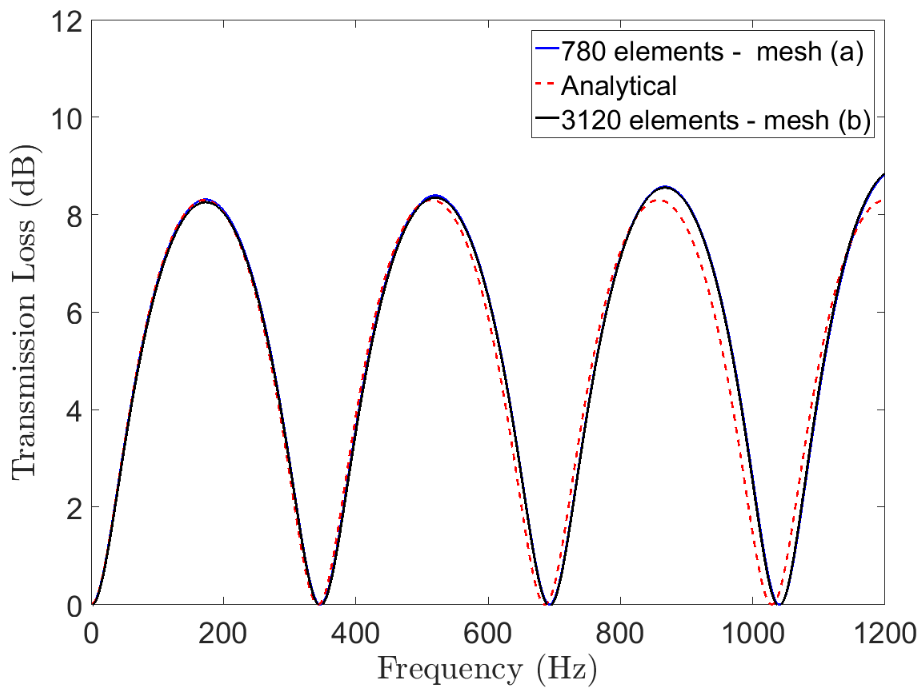

Figure 2.15: Comparison of analytical with three-pole method transmission loss using different finite element meshes.

In Fig. 2.15 the transmission loss curves for both meshes presented are shown. Since the behavior presented by both meshes in respect to the transmission loss is similar both mesh options could be used in the optimization cases. Although mesh (a) has the advantage of having a smaller number of elements inducing a cheaper computational cost, mesh (b) was chose and used for the optimization cases of this work. In Fig. 2.16 the TL behavior evaluated with mesh (b) is compared with the analytical solution. The finest mesh was chosen due to a higher resolution needed during the optimization process. Since a small percentage of volume $(5\% - 10\%)$ will be taken out of the design domain, rates of volume removal of each iteration will be of 10^{-1} order which require more refined meshes.

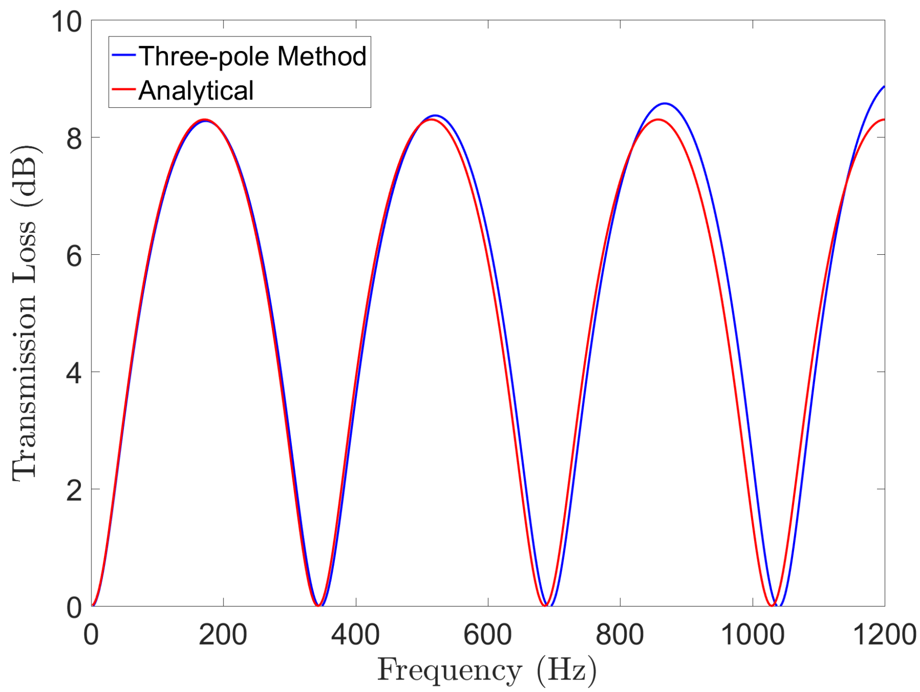

Figure 2.16: Comparison of analytical with three-pole method transmission loss.

In order to analyze the approximation error between both curves in Fig. 2.16 important data on peaks and valleys was compiled in Tab. 2.1.

Table 2.1: Peak and valley information: Transmission loss and frequency.

	TP Method TL (dB)	Frequency (Hz)	Analytical TL (dB)	Frequency (Hz)
2nd Peak	8.368	520	8.299	516
3rd Peak	8.573	868	8.299	856
4th Peak	8.87	1200	8.299	1200
2nd Valley	-0.00073	690	0	686
3rd Valley	-0.0062	1042	0.00209	1030

Observing both Fig. 2.16 and Tab. 2.1 two errors can be estimated, amplitude error and frequency error. The amplitude error is the difference in amplitude presented by the three-pole method when compared with the analytical formulation. The frequency error is the difference between frequencies presented by both curves in peaks and valleys. Both errors are estimated and summarized in Tab. 2.2.

Table 2.2: Peak and valley information: Transmission loss and frequency.

	Amplitude error (%)	Frequency error (%)
2nd Peak	0.8	0.77
3rd Peak	3.3	1.4
4th Peak	6.88	–
2nd Valley	–	0.58
3rd Valley	–	1.16

In the second peak of curves presented in Fig. 2.16 there is an amplitude error of 0.8% in the third and fourth peak this error grows to 3.3% and 6.88% as shown in Tab. 2.2. The amplitude errors in valleys is neglected as all transmission loss values can be rounded to 0. The frequency error presented also shows growth when higher frequencies are analyzed. The second peak of the tree-pole method curve presents 0.77% error in frequency when compared with the analytical curve. The third peak of the three-pole method have 1.4% error. The fourth peak is not shown completely therefore the frequency error is not evaluated.

The frequencies used in the optimization cases are in areas where the error is minimum. From 0 Hz until 690 Hz the error between the three-pole method with finite element approach and the analytical formulation is less than 1%. Based on these results, for practical purposes, it can be said that the FEM model is validated.

2.6.3 Double expansion chamber: Hard or Soft

For the double expansion chamber cases, rigid material was add to the empty chamber in order to match the characteristics described in Figs. 2.6 and 2.8. In Fig. 2.17 the double chamber configuration and its acoustic pressure distribution for 690 Hz are shown.

Using muffler FEM model Fig. 2.17 (a) and (b) a comparison between analytical TL and three-pole method TL can be done. Figure 2.18 shows the comparison between three-pole method calculated by Eq. 2.38 and double expansion chamber analytical Eq. 2.9 for muffler configuration Fig. 2.17(a). Figure 2.19 shows the same comparison for muffler configuration Fig. 2.17(b). In both figures a hard-kill approach was used to simulate rigid partitions inside the muffler. Using this approach the elements are eliminated from the finite element mesh and rigid wall boundary conditions are naturally included.

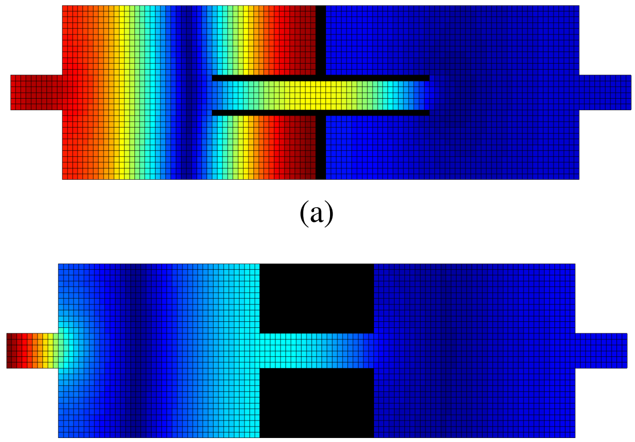

Figure 2.17: Double expansion muffler models as proposed in Fig. 2.6 and 2.8. (a) Model with partition creating two chambers ($L_1 = 0.11$m, $L_2 = 0.25$m and $m = 5$). (b) Model of two expansion chambers connected by duct ($L_1 = 0.055$m, $L_2 = 0.195$m and $m = 5$).

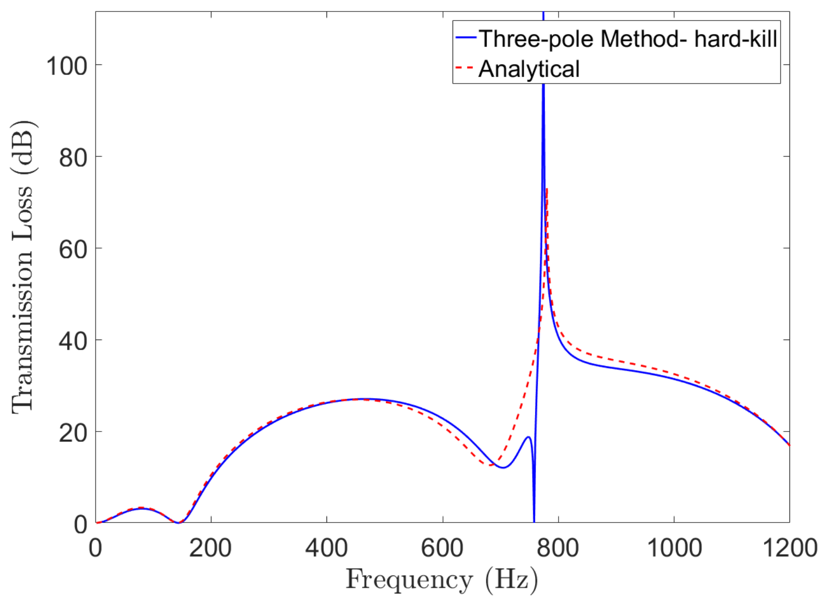

Figure 2.18: Comparison of analytical TL with three-pole method TL, muffler configuration (a).

It can be noticed that the deviation presented by the amplitude and frequency of TL curves in Figs. 2.18 and 2.19 are greater in this cases, particularly for the configuration Fig. 2.17(a), where the TL curve show more complex and irregular oscilations. The behavior of configuration Fig. 2.17(b) is more smooth and the deviation presented between the numeric and analytical solution

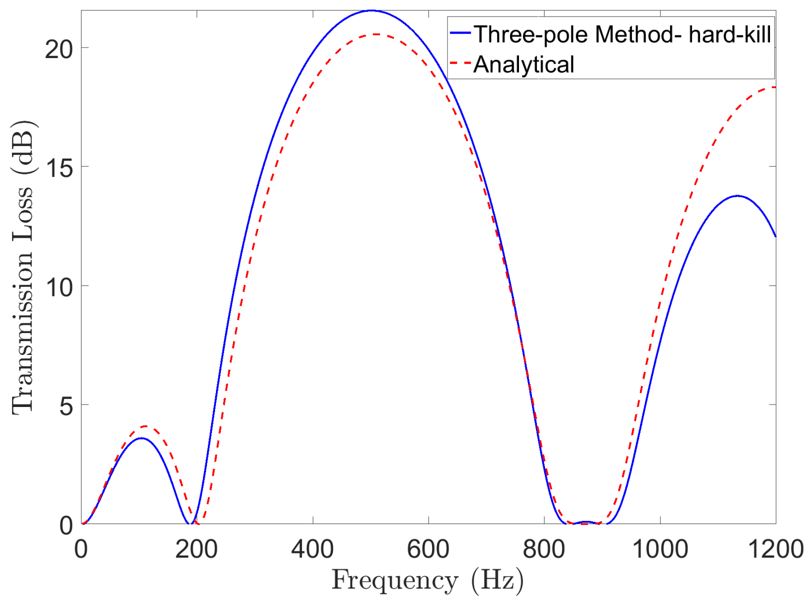

Figure 2.19: Comparison of analytical TL with three-pole method TL, muffler configuration (b).

are smaller.

In this work two approaches are used to simulate addition of material inside the expansion chamber. The hard-kill approach entirely removes fluid elements from the finite element mesh creating rigid walls while the soft-kill approach greatly diminishes the influence of the element by multiplying its stiffness and mass matrices by a small number. Equations 2.39 and 2.40 show how stiffness and mass matrices are evaluated when changing fluid elements, superscript f, to void elements, superscript v.

$$\mathbf{K}_e^v = \lambda \mathbf{K}_e^f \tag{2.39}$$

$$\mathbf{M}_e^v = \lambda \mathbf{M}_e^f \tag{2.40}$$

The λ variable in both equations penalize the fluid and mass matrices, the smaller λ gets the closer the element becomes to a complete void. For hard-kill approach λ is 0. In Figs. 2.20 and 2.21 the acoustic effects of hard and soft kill approaches are displayed. In Fig. 2.20 all incident waves reaching the void element are fully reflected demonstrating the hard-kill element behavior however in Fig. 2.21 incident waves are not fully reflected and have their magnitude diminished.

Figure 2.20: Illustration of hard-kill approach void element ($\lambda = 0$).

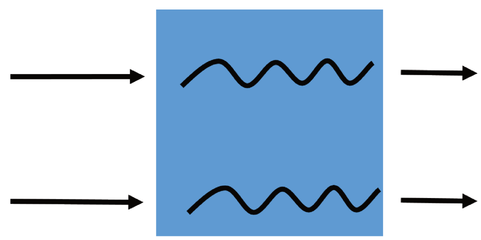

Figure 2.21: Illustration of soft-kill approach void element ($1 > \lambda > 0$).

The soft-kill approach approximates the hard-kill once a small enough number is used as penalization factor. The bigger the penalization the smaller the residue of the fluid element is left. The hard-kill method can sometimes create bad conditioned matrices due the complete removal of elements, this effect is avoided by the soft-kill method. The numerical singularities that can be proportioned by the hard-kill approach during the finite element analysis are prevented by the element residue left behind in the soft-kill approach. The Soft-kill approach has been widely used in structural optimization cases and its usage helps the objective function convergence.

The influence of the soft-kill approach in the transmission loss calculation for muffler (a) is demonstrated in Fig. 2.22. The different λ values used in Fig. 2.22 starting with 10^{-3} and decreasing demonstrates the different behaviors muffler partitions have in the TL parameter depending on the void elements used. The TL behavior changes until λ is small enough to characterize the hard-kill approach. This effect can be noticed observing the hard-kill behavior presented by the black line ($\lambda = 0$) in Fig. 2.22 as it is almost covered by the pink line ($\lambda = 10^{-5}$).

The influence of soft and hard-kill approaches in muffler model (b) is negligible as seen in

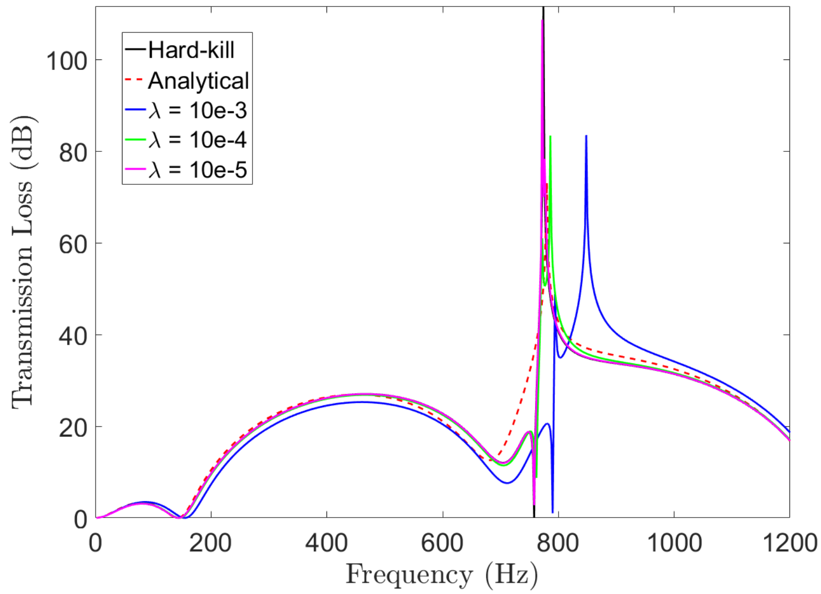

Figure 2.22: TL comparison using different soft-kill multipliers for muffler model (a).

Fig. 2.23. Due to the high amount of void elements together the soft-kill and hard-kill approaches have the same influence on the transmission loss behavior, making blue and black lines in Fig. 2.23 seem a single TL response curve.

In this chapter a brief review of expansion chamber muffler theory was done. The analytical formulation for single and double expansion chambers was presented. The acoustic problem continuum formulation was introduced and the boundary conditions for the muffler were described. The discrete formulation was explained and used to evaluate the acoustic pressure fields. A Three-pole method for evaluating TL was presented. Validation of the discrete formulation together with the three-pole method was done. Different modeling techniques for rigid elements inside the muffler were tested by analyzing their effects in the transmission loss parameters. The three-pole method proposed in this chapter was proved to be a viable and accurate option to evaluate TL during the optimization process. The next chapter will discuss the implementation of the optimization method.

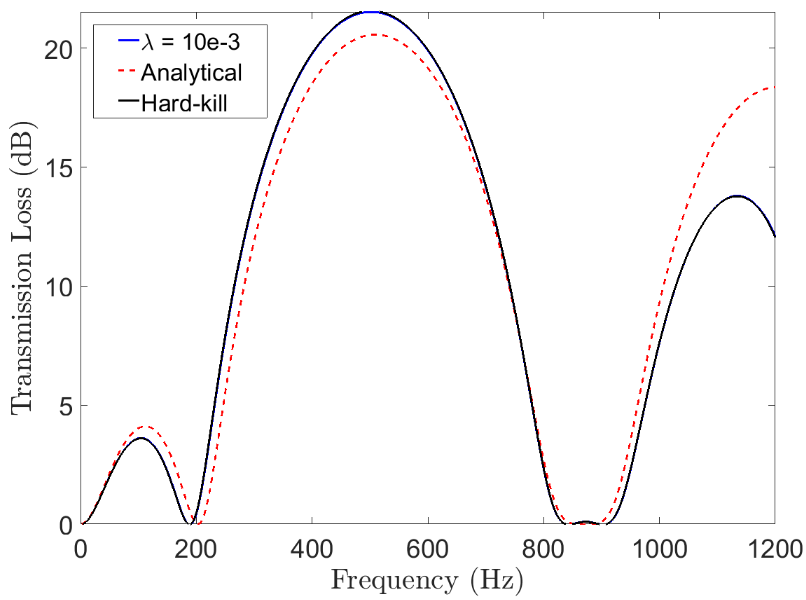

Figure 2.23: TL comparison using soft and hard-kill approach for muffler model (b).

3 BI-DIRECTIONAL EVOLUTIONARY TOPOLOGY OPTIMIZATION FOR MUFFLER DESIGN

Topology optimization can be done with several methods, SIMP, Level Set and BESO are examples . This chapter presents the acoustic muffler optimization problem and the methodology used in this work for the optimization itself. The adapted BESO method used in this work is thoroughly explained. The sensitivity number required for the optimization is derived and the necessary Bi-directional Structural Optimization method numerical implementation steps are introduced. The concepts and theory presented in this chapter can be found in Sigmund and Petersson (1998), Huang and Xie (2009), Huang and Xie (2010) and others.

3.1 Introduction

The BESO method proposed in Huang and Xie (2007) work was in fact first introduced as Evolutionary Structural Optimization (ESO) by (XIE AND STEVEN, 1993). The ESO methodology diverged from the widely used SIMP at the time. ESOs main proposal was to work with discrete design variables throughout the optimization instead of the continuum approach SIMP offered. In the ESO method there would be only void elements or filled elements, respectively elements with design variable 0 or 1.

The binary characteristic offered by the ESO is one of its great advantages when comparing optimization methods. This evolutionary approach is based on the gradual removal of less efficient elements in the structure, changing their design variables from 1 to 0. In order to remove the less efficient elements a sensitivity analysis of the structure is used to rank all elements in the design domain according with their importance.

A later work discussed flaws in the methodology (HUANG AND XIE, 2010). Checkerboard patterns, mesh dependency and non-optimal solutions were the main problems presented by the ESO evolutionary approach. The introduction of a filter scheme (SIGMUND AND PETERSSON, 1998) solved the mesh dependency and the checkerboard patterns. The logic ESO followed, gradual removal of inefficient elements, would not account for cases were later in the optimization a void element would become important to the structure, this caused the final topology to be an upgraded structure but not an optimum structure. To solve this issue an algorithm that could remove and add elements simultaneously was created, the BESO (HUANG AND XIE, 2007).

The term bi-directional is related to the ability of the new algorithm to reevaluate if void elements became important to the structure and change their design variable back to 1. The new evolutionary approach has been used since then in several optimization problems, such as, compliant mechanisms Li (2014), acoustic-structure interaction (PICELLI *et al.*, 2015), frequency response of fluid interaction systems (VICENTE *et al.*, 2015) and so on.

In this work, the BESO method is adapted to an acoustical problem. The empty expansion chamber presented in chapter 2 will have partitions added to it by the optimization process in order to maximize transmission loss.

3.2 Transmission Loss Maximization

To improve the performance of a reactive muffler its transmission loss have to be maximized. Works such as (LEE AND KIM, 2009), (YOON, 2013), (YEDEG *et al.*, 2016a) and several others use transmission loss function as at least one of the objective functions in the optimization process when optimizing reactive mufflers. In this work the BESO method is used with the goal of maximizing TL for different frequencies.

The reactive muffler optimization problem can be stated as

$$\text{Find:} \quad \mathbf{x} = x_i \qquad \text{where } x_i = x_{min} \text{ or } 1 \tag{3.1}$$

$$\text{Maximize:} \quad \mathbf{TL} \tag{3.2}$$

$$\text{Subject to:} \quad \begin{cases} \left(\mathbf{K}_g + j\omega\mathbf{C}_g - \omega^2\mathbf{M}_g\right)\mathbf{p} = \mathbf{v} \\ \\ V_f - \sum_{i=1}^{M} V_i x_i = 0 \end{cases} \tag{3.3}$$

The design variable x_i in Eq. 3.1 will change through the optimization process in order to describe a new material layout. In this work, x_i can assume two values, i.e. x_{min} indicating the absence of the fluid element or the presence of a rigid element and 1 indicating the presence of the fluid element. For the hard-kill method the x_{min} is changed to 0. The objective function in Eq. 3.2 is the Transmission Loss of the system, $\mathbf{TL}$ defined in Eq. 2.38. Equation 3.3 is a group of two equations, the global system equation and the volume constraint equation, with V_f being the final prescribed volume fraction and M is total number of elements used to describe the optimization domain Ω_d.

The $\mathbf{x}$ variable appears in the global system in Eq. 3.3 by using interpolation scheme presented in Eq. 3.4 and 3.5.

$$\mathbf{K}_g = \mathop{\mathsf{A}}_{i=1}^{N} x_i^{\Lambda} \mathbf{K}_e \tag{3.4}$$

$$\mathbf{M}_g = \mathop{\mathsf{A}}_{i=1}^{N} x_i^{\Lambda} \mathbf{M}_e \tag{3.5}$$

where Λ is a penalization factor.

Using the interpolation scheme presented the sensitivity analysis can be evaluated as shown in the next section.

3.3 Sensitivity Analysis

In order to maximize a reactive muffler transmission loss parameter by removing or adding elements it is necessary to know what elements are less or more efficient in the expansion chamber. The sensitivity analysis is a rank of the elements based on their efficiency inside the muffler.

In this work the sensitivity used in order to maximize the objective function is gradient-based. The derivative of the objective function Eq. 2.38 can be written as

$$\alpha_e = \frac{\partial TL(\omega, x_i)}{\partial x_i} = \frac{10}{ln10}\left(\frac{\partial \mid P_{in} \mid^2}{\partial x_i}\frac{1}{\mid P_{in} \mid^2} - \frac{\partial \mid P_o \mid^2}{\partial x_i}\frac{1}{\mid P_o \mid^2}\right) \tag{3.6}$$

During the optimization process the sensitivities of filled elements ($x_i = 1$) and void elements ($x_i = x_{min}$) are calculated. Taking in consideration that the acoustic pressures calculated are complex, P_{in} squared becomes

$$P_{in}^2 = \frac{1}{\gamma}\big(P_{1Re} - P_{2Re}cos\big(kl\big) - P_{2Im}sin\big(kl\big)\big)^2 + \frac{1}{\gamma}\big(P_{1Im} - P_{2Im}cos\big(kl\big) + P_{2Re}sin\big(kl\big)\big)^2 \quad (3.7)$$

and accordingly,

$$P_o^2 = P_{3Re}^2 + P_{3Im}^2 \quad (3.8)$$

with γ being,

$$\gamma = \big(1 - cos\big(2kl\big)\big)^2 + \big(sin\big(2kl\big)\big)^2 \quad (3.9)$$

where subscripts (Re) and (Im) mean real and imaginary components respectively.

In order to evaluate the sensitivity the derivative terms of eq. 3.6 need to be calculated as well. Equations bellow show how those terms can be expanded.

$$\begin{aligned}\frac{\partial \mid P_{in} \mid^2}{\partial x_i} =& \frac{2}{\gamma}\left(P_{1Re} - P_{2Re}cos\left(kl\right) - P_{2Im}sin\left(kl\right)\right)\left(\frac{\partial P_{1Re}}{\partial x_i} - \frac{\partial P_{2Re}}{\partial x_i}cos\left(kl\right) - \frac{\partial P_{2Im}}{\partial x_i}sin\left(kl\right)\right) \\ &+ \frac{2}{\gamma}\left(P_{1Im} - P_{2Im}cos\left(kl\right) + P_{2Re}sin\left(kl\right)\right)\left(\frac{\partial P_{1Im}}{\partial x_i} - \frac{\partial P_{2Im}}{\partial x_i}cos\left(kl\right) + \frac{\partial P_{2Re}}{\partial x_i}sin\left(kl\right)\right)\end{aligned} \quad (3.10)$$

$$\frac{\partial \mid P_o \mid^2}{\partial x_i} = 2\frac{\partial P_{3Re}}{\partial x_i}P_{3Re} + 2\frac{\partial P_{3Im}}{\partial x_i}P_{3Im} \quad (3.11)$$

To calculate Eq. (3.10) and Eq. (3.11), the differentiations of acoustic pressure in the three points, P_1, P_2 and P_o are necessary. Those can be found by differentiating the governing equation system in Eq. (3.3) as:

$$\frac{d\mathbf{p}}{dx_i} = -\left(\mathbf{K}_g + j\omega\mathbf{C}_g - \omega^2\mathbf{M}_g\right)^{-1}\frac{d}{dx_i}\left(\mathbf{K}_g + j\omega\mathbf{C}_g - \omega^2\mathbf{M}_g\right)\mathbf{p} \quad (3.12)$$

where $\mathbf{v}$, the source therm, is considered constant.

The computational cost to solve Eq. 3.12 is significant. To avoid this computational cost, Chu *et al.* (1996) and Vicente *et al.* (2015) used a different scheme to calculate the derivative of defined variables. In this work, the adjoint approach is applied. In order to determine the change of response in specific degrees of freedom $\mathbf{p_j}$ of the system due to the i_{th} element removal, a vector $\mathbf{f_j}$ can be introduced. $\mathbf{f_j}$ is locator vector, it is composed of zeros and a single one located in the position of the specific degree of freedom wanted. The following can be written

$$\frac{d\mathbf{p_j}}{dx_i} = \mathbf{f}_j^t \cdot \frac{d\mathbf{p}}{dx_i} \tag{3.13}$$

The substitution of the global system derivative from Eq. 3.12 into Eq. 3.13 yields

$$\frac{d\mathbf{p_j}}{dx_i} = \mathbf{f_j}^t \mathbf{H}^{-1} \frac{d\mathbf{H}}{dx_i} \mathbf{p} \tag{3.14}$$

where,

$$H = \left(\mathbf{K}_g + j\omega \mathbf{C}_g - \omega^2 \mathbf{M}_g\right)$$

The system's global equation where only the locator vector $\mathbf{f_j}$ acts can be written as

$$\mathbf{p_j} = \mathbf{H}^{-1} \mathbf{f_j} \tag{3.15}$$

With the substitution of Eq. 3.15 in Eq. 3.14 the pressure derivates necessary to calculate the sensitivity can be found:

$$\frac{d\mathbf{p_j}}{dx_i} = -\mathbf{p_j}^t \frac{d\mathbf{H}}{dx_i} \mathbf{p} \tag{3.16}$$

where the global system's matrix $\mathbf{H}$ derivative in respect to the design variable x_i, can be calculated in local form as follows:

$$\frac{d\mathbf{H}}{dx_i} = \frac{d\mathbf{K}_g}{dx_i} - \omega^2 \frac{d\mathbf{M}_g}{dx_i} \tag{3.17}$$

where,

$$\frac{d\mathbf{K}_g}{dx_i} = \Lambda x_i^{\Lambda - 1} \mathbf{K}_e \tag{3.18}$$

$$\frac{d\mathbf{M}_g}{dx_i} = \Lambda x_i^{\Lambda-1}\mathbf{M}_e \tag{3.19}$$

Using Eqs. 3.18 and 3.19 in Eq. 3.17 the following equation is obtained.

$$\frac{d\mathbf{p_j}}{dx_i} = -\left(\Lambda x_i^{\Lambda-1}\right)\mathbf{p_j}^t\left(\mathbf{K}_e - \omega^2\mathbf{M}_e\right)\mathbf{p} \tag{3.20}$$

Once the pressure derivative Eq. 3.20 is found, the derivatives of P_{in}^2, Eq. 3.10, and P_o^2, Eq. 3.11, can be evaluated and the global sensitivity Eq. 3.6 can be rewritten as

$$\alpha_e = \frac{\partial TL(\omega, x_i)}{\partial x_i} = \Lambda x_i^{\Lambda-1}\frac{10}{ln10}\left(\frac{\partial \mid P_{in}\mid^2}{\partial x_i}\frac{1}{\mid P_{in}\mid^2} - \frac{\partial \mid P_o\mid^2}{\partial x_i}\frac{1}{\mid P_o\mid^2}\right) \tag{3.21}$$

The sensitivity analysis can be simplified as follows:

$$\alpha_e = \frac{1}{\Lambda}\frac{\partial TL}{\partial x_i} = \begin{cases} \frac{10}{ln10}\left(\frac{\partial |P_{in}|^2}{\partial x_i}\frac{1}{|P_{in}|^2} - \frac{\partial |P_o|^2}{\partial x_i}\frac{1}{|P_o|^2}\right) & x_i = 1 \\ x_{min}^{\Lambda-1}\frac{10}{ln10}\left(\frac{\partial |P_{in}|^2}{\partial x_i}\frac{1}{|P_{in}|^2} - \frac{\partial |P_o|^2}{\partial x_i}\frac{1}{|P_o|^2}\right) & x_i = x_{min} \end{cases} \tag{3.22}$$

Using the sensitivity analysis described in Eq. 3.22 the importance of each element can be displayed. Figure 3.1 shows the sensitivity distribution in an empty expansion chamber for different frequencies. The sensitivity distribution gives a insight of where most of the void elements will be concentrated. The removal of elements with smaller sensitivity number raises transmission loss and the removal of elements with higher sensitivity number decreases the systems TL.

3.4 Acoustic Topology Optimization Numerical Implementation

In this work the acoustic topology optimization will be done using the Bi-directional evolutionary structural optimization (BESO) method (Huang and Xie, 2010). The BESO approach used in this work follows the scheme presented in the flow chart of Fig. 3.2.

The FEM analysis step, necessary to evaluate the acoustic pressure and transmission loss of

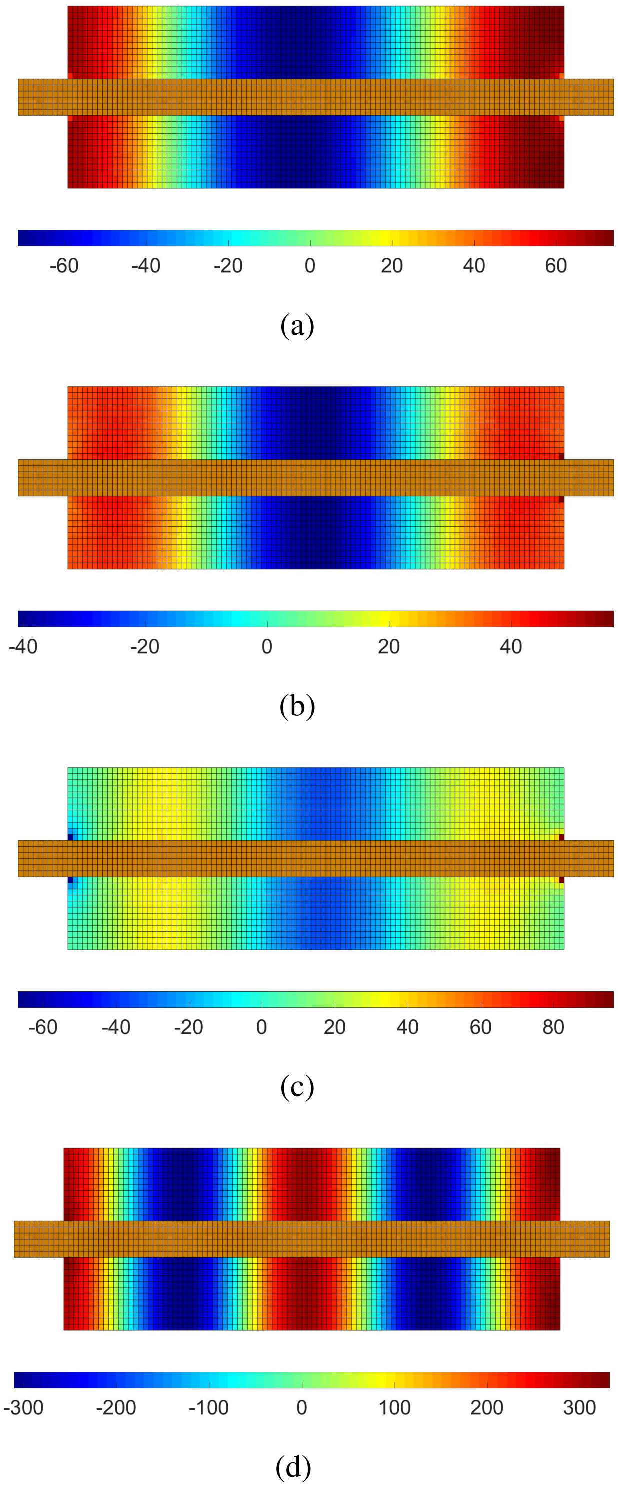

Figure 3.1: Sensitivity number distribution for four different frequencies. (a) 346 Hz. (b) 420 Hz. (c) 518 Hz. (d) 690 Hz.

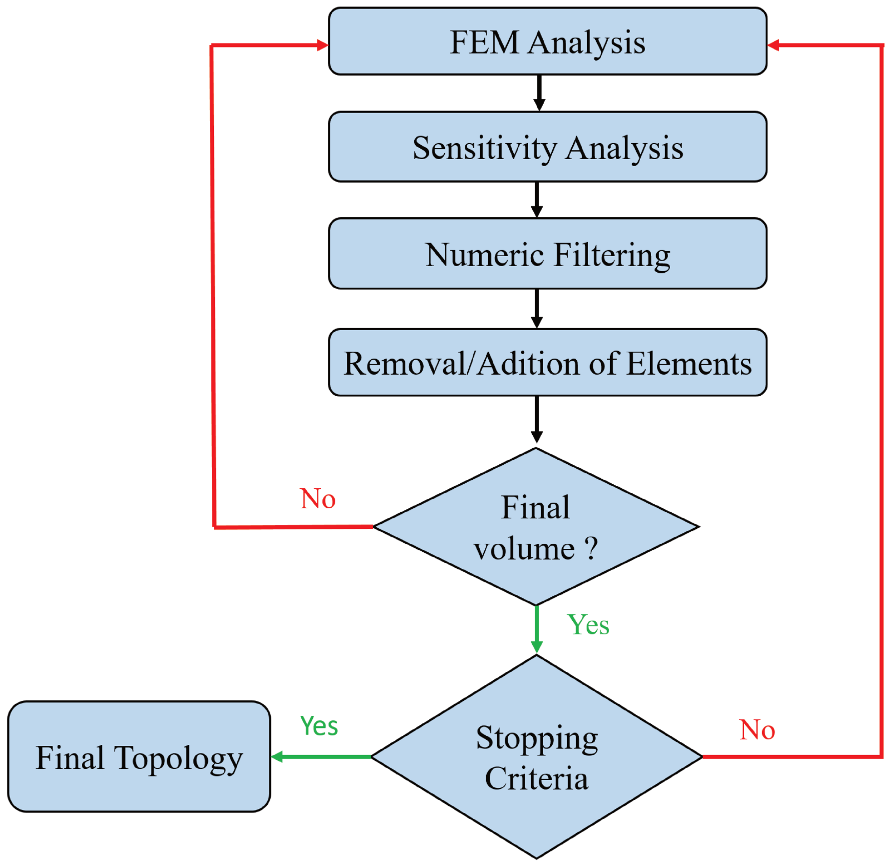

Figure 3.2: BESO method flow chart.

the reactive muffler and Sensitivity analysis step, necessary to rank all finite elements based on their efficiency in Fig. 3.2 were already detailed previously. In this section the remaining implementation steps are discussed.

3.4.1 Filter scheme

A filter scheme has been used in topology optimization in order to avoid numerical instabilities and mesh-dependency problems (Sigmund and Petersson, 1998). These problems, checkerboard patterns for instance, are caused by the usage of low order bi-linear finite elements often inducing discontinuities throughout the element borders (Jog and Haber, 1996), (Diaz and Sigmund, 1995). In order to avoid the aforementioned problems, a spatial linear filter is used to smooth the sensitivity number (Huang and Xie, 2007). Figure 3.3 depicts the checkerboard pattern and a typical topology that undergoes its effects.

Figure 3.3: Deficiencies presented in the BESO method. (a) Checkerboard pattern. (b) Typical topology with checkerboard pattern.

In this work the filter scheme presented by Huang and Xie (2010) is used to. After calculating the sensitivity number (α_e) using the formulation presented in this paper, the filtering procedure can be started by using that number to find a sensitivity for each node of the mesh (α_n) by applying the following equation.

$$\alpha_n = \frac{\sum_{i=1}^{nec} A_e \alpha_e}{\sum_{i=1}^{nec} A_e} \tag{3.23}$$

where A_e is the area of each element and nec is the total number of elements connected to the nth node. Note that in this paper all elements have the same area, in this case eq. 3.23 becomes the mean sensistivity of the elements connected to the nth node.

Following the creation of α_n, a sub-domain is created using the r_{min} parameter. The circular sub-domain Ω_r with radius r_{min} centered in each elements centroid envelopes ner elements that will influence the element sensitivity. Figure 3.4 highlights all nodes that will influence the element in consideration.

A new filtered elemental sensitivity α_e^f can be found as follows

$$\alpha_e^f = \frac{\sum_{j=1}^{ner} w(r_n) \alpha_n}{\sum_{j=1}^{ner} w(r_n)} \tag{3.24}$$

where r_n is the distance from each node to the element currently at the sub-domain center and $w(r_n)$ is the weight factor based in the nodes distance, that is, $(r_n - r_{min})$ so that the furthest the

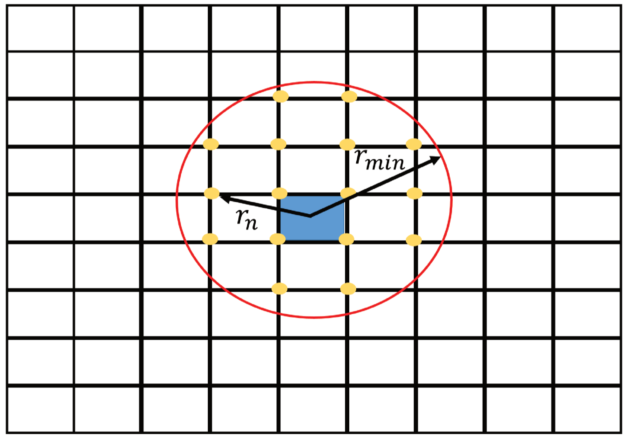

Figure 3.4: Sub-domain Ω_r created by r_{min}.

node is from the sub-domain center the lower its weight factor is.

3.4.2 Sensitivity history

The sensitivity history is a tool that can be used to help stabilize the optimization process (HUANG AND XIE, 2007). The final sensitivity number used in the optimization can be found applying the following

$$\alpha_e^h = \frac{(\alpha_e^f)^i + (\alpha_e^f)^{i-1}}{2} \tag{3.25}$$

where i is the current iteration number. The usage of the sensitivities history as a tool to facilitate convergence is already used effectively in the field, (HUANG AND XIE, 2010).

3.4.3 Design variables update

The design variables update, step 4 in fig. 3.2 uses the evolutionary ratio (ER) parameter in Eq. 3.26 to determine the next iteration volume V^{i+1}. The volume difference $V^i - V^{i+1}$ defines the the ammount of volume/elements to be added or removed accordingly with the volume constraint established and the initial condition. In this work all elements start with $x_i = 1$ which means the chamber is filled with fluid elements.

$$V^{i+1} = V^i - ER \tag{3.26}$$

Sorting α_e^h in a descending order facilitates the process of choosing the elements to be added or removed. In a compact way to describe the process, after sorting the sensitivities a threshold is created where the elements underneath it, the most negative elements in this case, are removed by switching their design variable x_i from 1 to x_{min} and the elements above it have their design variable changed to 1. This sensitivity threshold is called α^{th}.

The elements above α^{th} mentioned have their design variable x_i switched to 1 based on another optimization parameter named maximum volume addition ratio AR_{max}. During the optimization process volume addition ration (AR) is calculated based on the number of elements above the threshold. If AR is smaller than the prescribed AR_{max} than all elements above α^{th} can be switched back to $x_i = 1$, otherwise, the AR_{max} is used to evaluate how many elements must return, using this number the elements with design variable $xmin$ that have the highest sensitivity are switched to 1.

Its important to notice that the volume is descending to the volume constraint specified V_f while there are void elements (x_{min}) being turned to solid elements (1) and vice-versa which means that ER parameter must be respected, otherwise the volume constraint would never be met. (XIE AND STEVEN, 1997) and (HUANG *et al.*, 2010) developed and detailed the procedure needed for BESO method variable design update used in this work.

3.4.4 Stopping Criteria

Once the prescribed final volume V_f is reached, the volume is then kept constant throughout the next iterations and a stopping criteria is used to evaluate the convergence of the objective function. The stopping criteria verifies that the variation of the objective function is within a prescribed error τ, if so, than the optimization is finished and a final topology is reached. The variation mentioned earlier can be evaluated as follows

$$error = \frac{|\sum_{j=1}^{N}(TL)^{i-j+1} - \sum_{j=1}^{N}(TL)^{i-N-j+1}|}{\sum_{j=1}^{N}(TL)^{i-j+1}} \leq \tau \tag{3.27}$$

where, TL^i is the objective function value in the ith iteration and N is the prescribed number of iterations the error will take in consideration.

3.4.5 Numerical implementation summary

The optimization algorithm can be summarized in a few steps once all the BESO concepts and muffler acoustics theories are presented. The evolutionary iterative procedure is described as follows.

1. Define BESO optimization parameters: V_f, ER, AR_{max}, r_{min}, τ and N.
2. Create a discrete domain using a finite element mesh considering particle velocity (V_n) and imposed impedance ($\bar{Z}$) boundary conditions.
3. Perform FEM analysis by solving the reactive muffler acoustic system Eq. 2.26 and finding the acoustic pressure vector ($\mathbf{p}$).
4. Evaluate the objective funtion (TL) of the current iteration using Eq. 2.38.
5. Perform the sensitivity analysis as described in section 3.3 and use numeric filter described in section 3.4.1 to smooth the sensitivity number.
6. Determine the target volume fraction for the next iteration using Eq. 3.26 .
7. Remove and add fluid elements in accordance with section 3.4.3.
8. Repeat steps 3-7 until the final volumeV_f is achieved and the convergence criteria Eq. 3.27 is met.

In this chapter all implementation aspects of the BESO method for transmission loss maximization were presented. Next chapter presents numerical examples of the acoustic muffler optimization problem and discussions of such examples.

4 NUMERICAL EXAMPLES AND DISCUSSION

This section presents the results obtained in this research for the muffler design optimization problem. The (BESO) method is used for different optimization cases and the results are then analyzed accordingly.

In tab. 4.1 all necessary muffler dimensions and properties used are presented.

Table 4.1: Muffler dimensions and interest points coordinates.

Variable	Description	Value
d	Acoustic chamber diameter	$0.15m$
d_i	Exhaust/Tail pipes diameter	$0.03m$
L	Acoustic chamber length	$0.5m$
l	Distance between P_1 and P_2	$0.01m$
c	Sound velocity in air	$343m/s$
ρ	Air density	$1.21kg/m^3$

The optimization frequencies used were picked based on the highest, medium and lowest transmission loss presented in the empty expansion chamber. Figure 4.1 shows the valleys and peaks of the analytical and FEM TL function highlighting the frequencies studied in this chapter.

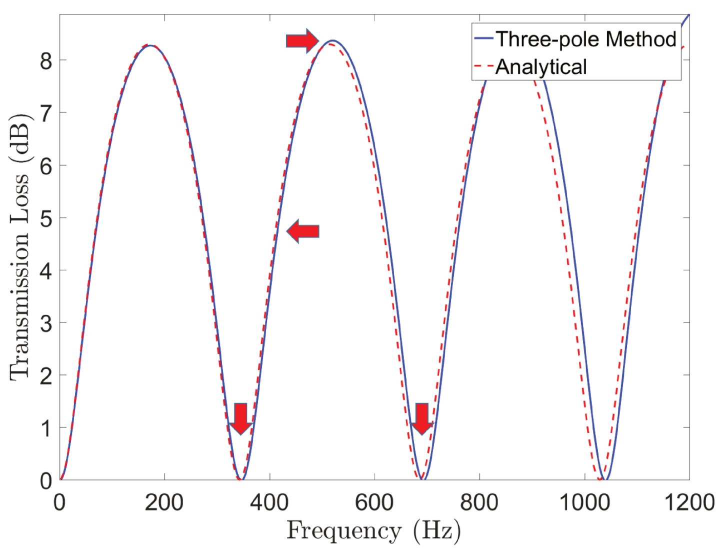

Figure 4.1: Transmission loss for the empty expansion chamber, analytical vs. FEM.

The BESO parameters used for the optimization cases are presented in Tab. 4.2. When testing different parameters the alterations are mentioned. The starting expansion chamber is filled with fluid, while the optimization iterations are ran the expansion chamber starts to be filled with void elements creating rigid walls.

Table 4.2: BESO parameters for the examples 1, 2 and 3.

Variable	Description	Value
V	Initial volume	100%
V_f	Final volume fraction	95%
ER	Evolutionary volume ratio	0.1%
AR_{max}	Maximum addition ratio	0.1%
r_{min}	Filter radius	3 mm
τ	Stopping criteria tolerance	1×10^{-4}
N	Stopping criteria parameter	10
Λ	Optimization penalty factor	3
x_{min}	Void element value	10^{-1}

Next sections present optimization cases using hard-kill and soft-kill.

4.1 BESO: Hard-Kill void elements

In this section, the Hard-Kill void elements are used for modeling the rigid elements inside the muffler expansion chamber during the optimization. For all optimization cases tested in this work the Hard-kill approach was not capable of meeting the convergence criteria of Eq. 3.27. Figures 4.2, 4.3, 4.4 and 4.5 show the evolution of the objective function for the 4 different frequencies used in the optimization cases.

The oscillating pattern observed in the objective function and volume evolution curves presented is caused by the repetitive creation of holes in the partitions created during the optimization process. Figure 4.6 displays the effect mentioned before showing the topologies before and after the holes appearance during the optimization. It is important to notice that while the convergence criteria using the Hard-Kill approach is not met the optimization procedure provided final topologies that are similar to optimum topologies later shown in this work. In Fig. 4.7 a red line is drawn to emphasize that the convergence criteria would be met by avoiding the creation of holes and that would explain the effectiveness of the final topologies even without convergence.

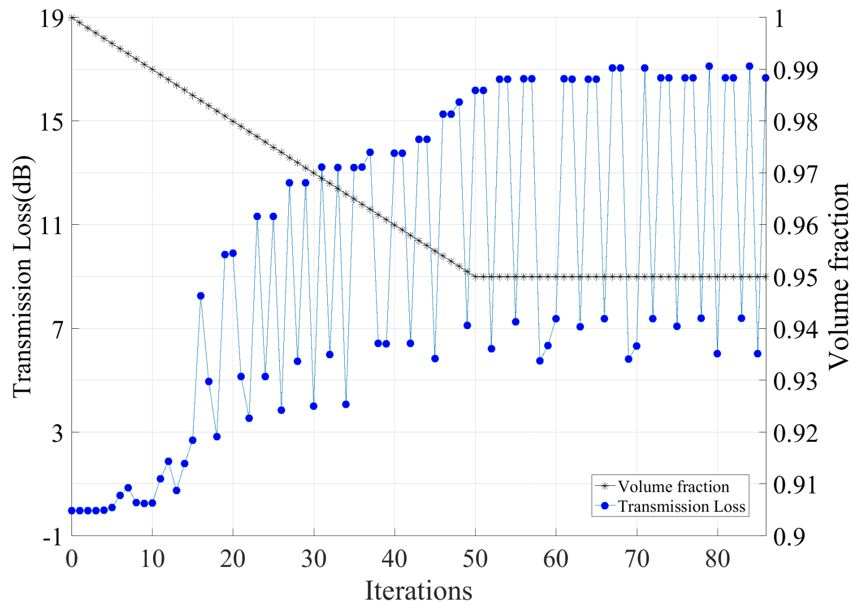

Figure 4.2: Transmission loss and volume evolution during the optimization procedure for 346 Hz.

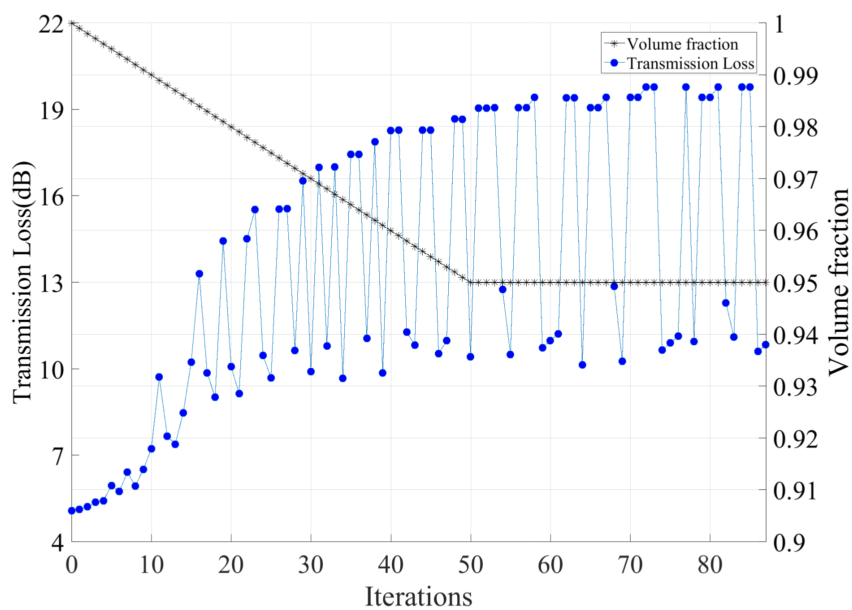

Figure 4.3: Transmission loss and volume evolution during the optimization procedure for 420 Hz.

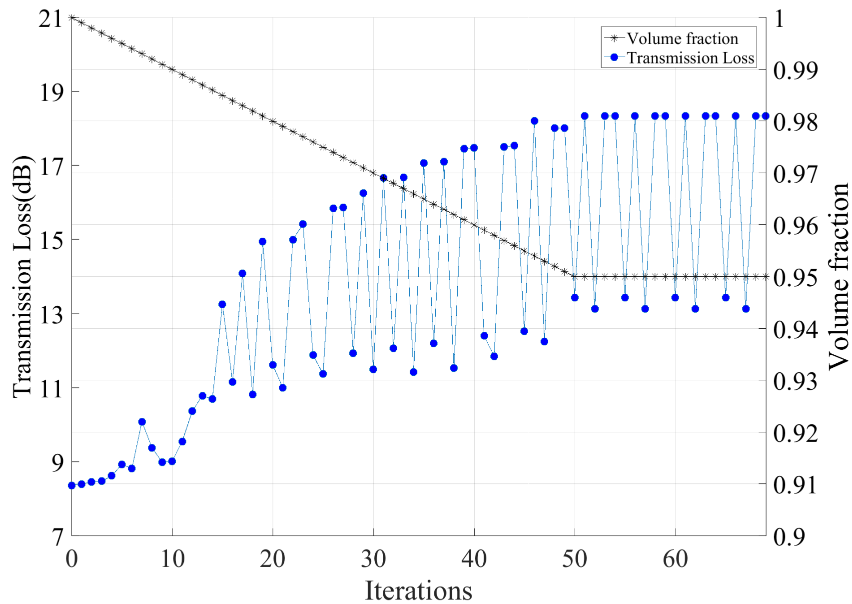

Figure 4.4: Transmission loss and volume evolution during the optimization procedure for 518 Hz.

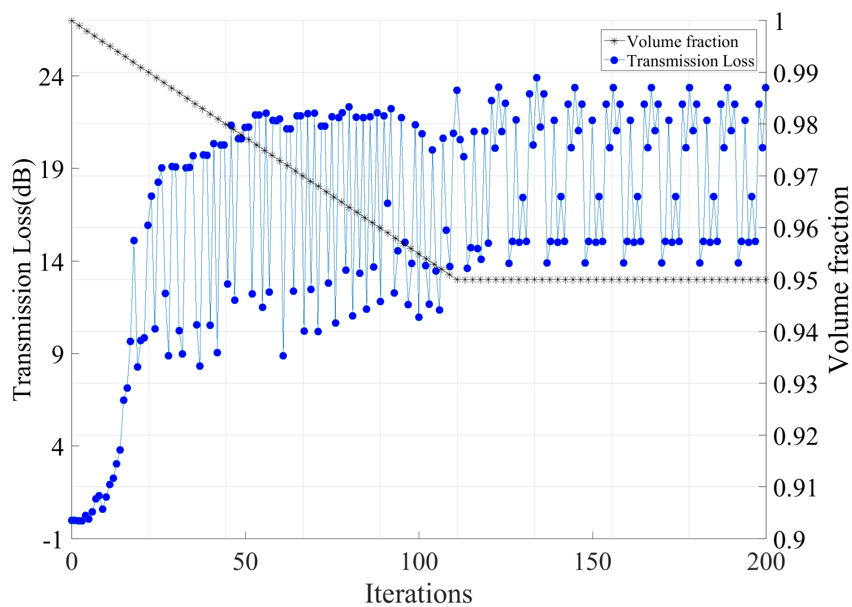

Figure 4.5: Transmission loss and volume evolution during the optimization procedure for 690 Hz.

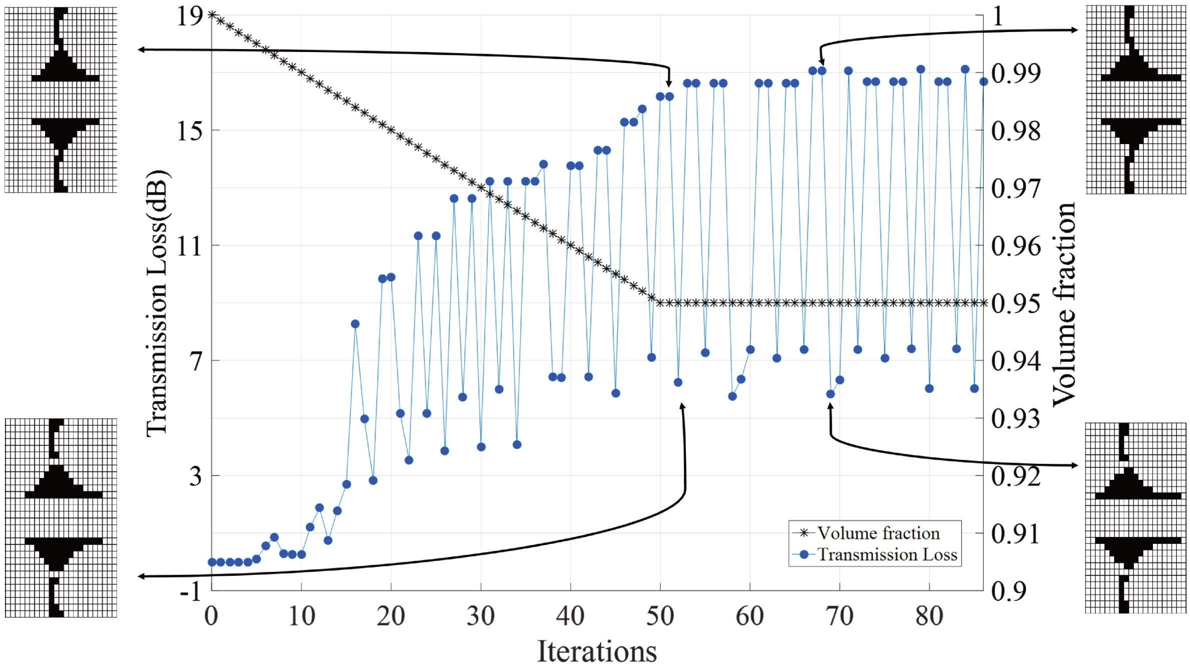

Figure 4.6: Transmission loss and volume evolution during the optimization procedure for 346 Hz displaying iterations 51-52 and 68-69.

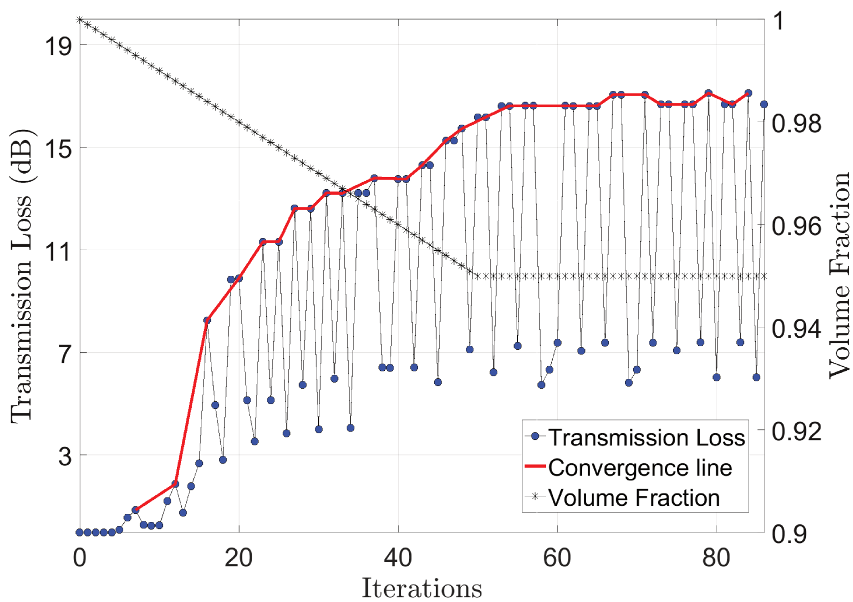

Figure 4.7: Transmission loss and volume evolution during the optimization procedure for 346 Hz emphasizing evolution without creating holes in the partitions.

The objective function oscillating pattern created during the optimization process could indicate that the interpolation scheme used is not well suited for the dynamic problem with hard-kill approach. The usage of another filter scheme could also be a remedy to this issue. The solution of this convergence problem is not further studied in this work.

4.2 BESO: Soft-Kill void elements

In this section the Soft-Kill void elements are used for modeling the rigid elements inside the muffler expansion chamber.

4.2.1 Example 1: Muffler Design for 1st low TL frequency

In this example the first valley frequency ($\omega = 346Hz$) of the TL curve is used for the optimization. Since transmission loss approaches zero at the picked frequency the sound pressure coming from the inlet goes through the muffler almost unchanged.

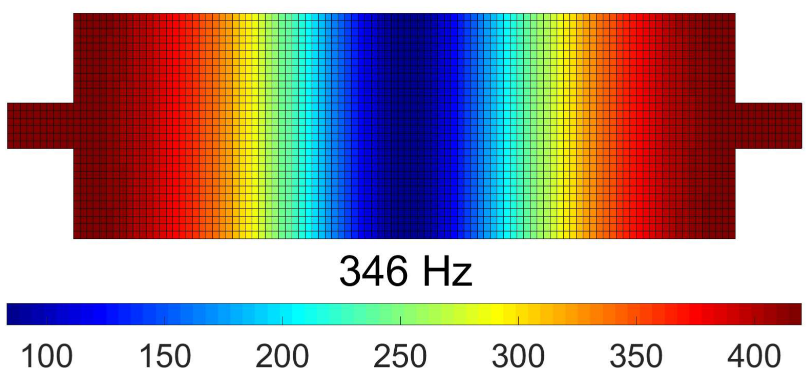

Figure 4.8: Absolute acoustic pressure distribution in the muffer for 346 Hz.

Figure 4.8 shows the absolute acoustic pressure distribution inside the muffler. A similar sound pressure is seen in inlet and outlet of the muffler, this effect is caused by the zero TL presented by this example's frequency.

The final topology for this optimization case is presented in Fig. 4.9 with the corresponding acoustic pressure distribution. Trough the optimization process a rigid wall was created separating the single expansion chamber in two different chambers. It can be observed that the right side chamber has a bigger length than the left side chamber. A similar topology was found by Lee and Kim (LEE AND KIM, 2009).

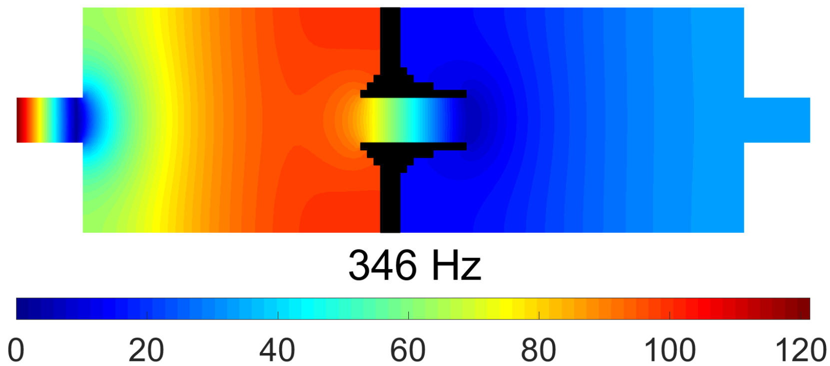

Figure 4.9: Acoustic Pressure distribution in the optimized muffler of example 1.

The evolution of the objective function and volume fraction are shown in Fig. 4.10 together with intermediary topologies. Between iterations 14 and 22 the objective function becomes unstable, that effect is caused because of the progression of the wall in construction. During the process the wall are not continuous, once they have been fully built the objective function stabilizes in a ascending pattern and then converges after the volume constraint $V_f = 95\%$ at the $50th$ iteration is satisfied. After the $50th$ iteration the topology has reached stability and only a feel changes are made in the topology until the convergence criteria is met, the transmission loss variation in this stage is negligible.

Once the final topology is reached is possible do analyze its effectiveness calculating the Transmission Loss parameter for a range of frequencies. Figure 4.11 shows the behavior of example 1 final topology for frequencies ranging from 1 Hz to 1200 Hz. The first transmission loss valley became a point with approximately 16.4 dB instead of 0 dB, moreover, other frequencies had their TL maximized, for instance in 518 Hz the whole peak of 8 dB was maximized to barely 20 dB.

Maximizing transmission loss guarantees a smaller sound pressure level in the outlet region. Throughout the optimization, while TL is maximized the sound pressure level in the outlet is expected to get lower until a final topology is found. Figure 4.12 shows the evolution of sound pressure level response in the outlet throughout the optimization, and as expected the sound pressure curve is minimized.

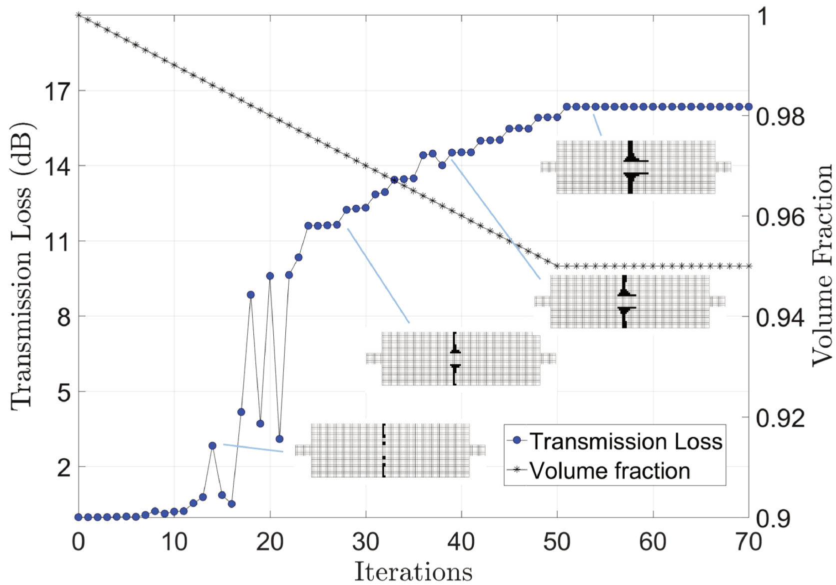

Figure 4.10: Evolution of the objective function and volume fraction for example 1.

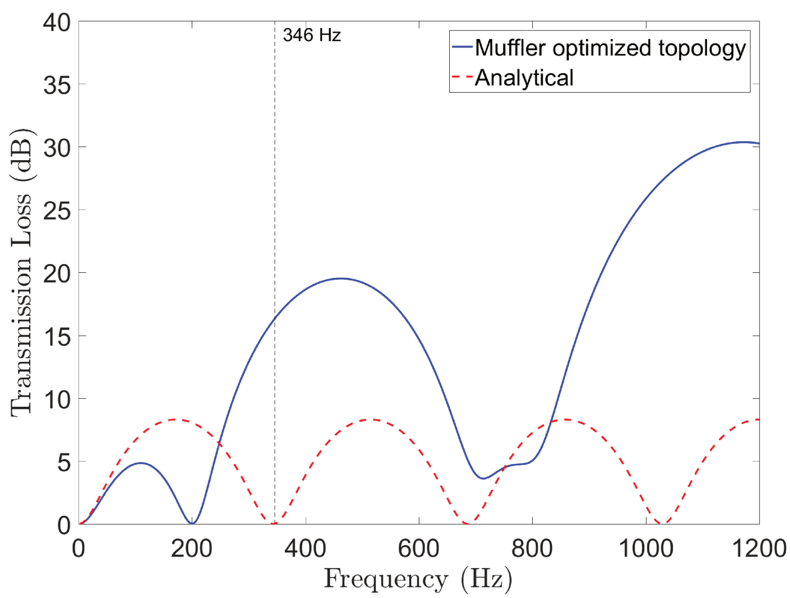

Figure 4.11: Transmission Loss for the optimized topology of example 1 in a frequency range in contrast with the prior empty chamber.

The results presented attest that the topology found not only maximizes TL for the given frequency but have a good behavior in other frequency ranges. The simulated effectiveness and the ease of construction of the optimized topology attest to the usage of the method proposed for design of acoustic mufflers.

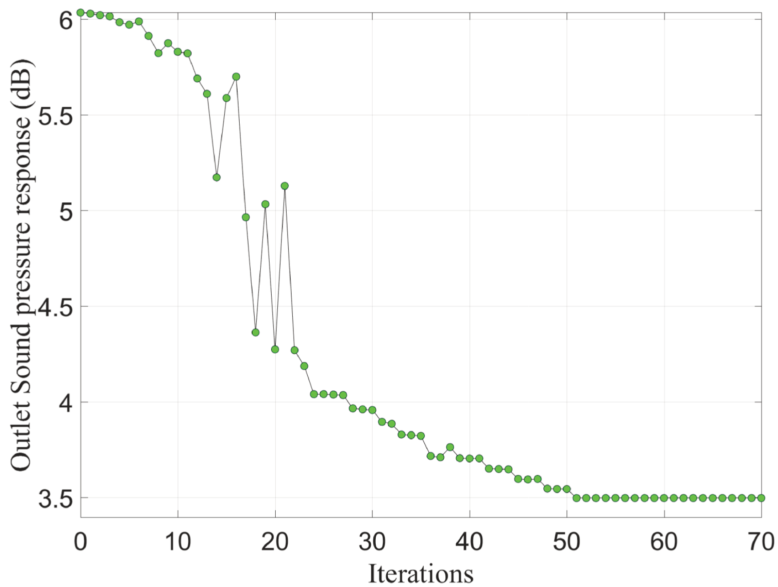

Figure 4.12: Outlet sound pressure level evolution in example 1.

The sound pressure level response in the outlet can be plotted for a range of frequencies, in fig. 4.13 the initial outlet response and the final outlet response are shown.

The motion and expansion of the sound modes in the acoustic chamber depicted in fig. 4.13 due to the optimization is a good indicator that the acoustic filter was enhanced. In this example, the third mode approached the second while the first was minimized, this created two zones of lower sound pressure level response.

4.2.2 Example 2: Muffler Design for non peak TL frequency

In this example the frequency ($\omega = 420Hz$) used for optimization corresponds to a TL value that is neither peak nor valley in the empty chamber case.

Figure 4.14 shows the absolute acoustic pressure distribution inside the muffler. The distribution of absolute acoustic pressure changed from what was observed in example 1. The low pressure zone moved to the right side of the expansion chamber while another low pressure zone appeared

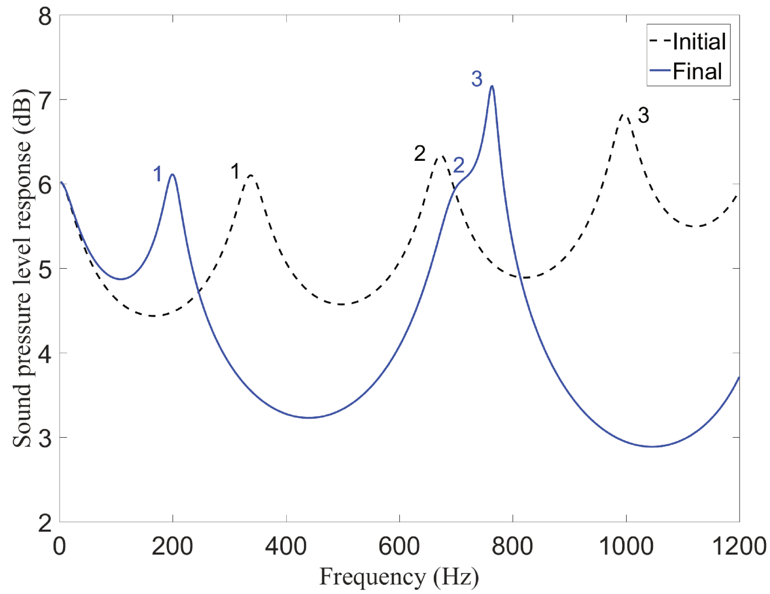

Figure 4.13: Outlet sound pressure level for a range of frequencies in example 1.

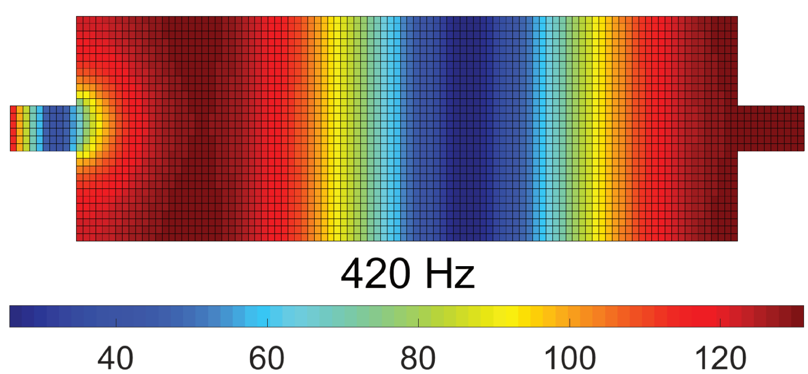

Figure 4.14: Acoustic Pressure distribution in the muffler for 420 Hz.

at the muffler inlet.

The BESO parameters used in this case are presented in Tab. 4.2. The same starting conditions are used, the chamber is filled with fluid and rigid elements are inserted in order to maximize TL.

The final topology for this optimization case is presented in Fig. 4.15 with the corresponding acoustic pressure distribution. Trough the optimization process a rigid wall was created.

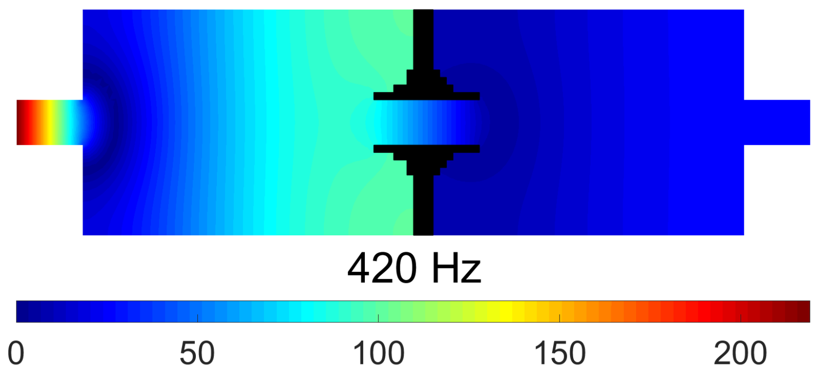

Figure 4.15: Acoustic Pressure distribution in the optimized muffer of example 2.

The evolution of the objective function and volume fraction are shown in Fig. 4.16 together with some intermediary topologies. Between iterations 12 and 24 the objective function becomes unstable, that effect is caused because of the progression of the wall in construction as it happened in the first optimization case. Once the wall has been fully built the objective function stabilizes in an ascending pattern and then converges after the volume constraint $V_f = 95\%$ at the $50th$ iteration is satisfied. After the $50th$ iteration the topology has reached stability and only a feel adjustments are made until the convergence criteria is met at the $69th$ iteration, the transmission loss variation in this stage is negligible.

Once the final topology is reached is possible do analyze its Transmission Loss effectiveness for a range of frequencies. Figure 4.17 shows the behavior of example 2 final topology for frequencies ranging from 1 Hz to 1200 Hz. The middle transmission loss became a point with approximately 19.1 dB instead of 6 dB, moreover, other frequencies had their TL maximized as it happened in example 1. The behavior of the muffler produced in example 2 is similar to the muffler in example 1, however, it's possible to notice that in example 2 the most prominent peak is slightly shifted to the left expanding the area with higher TL by a small amount.

Since the frequency picked for this example already had 6 dB of TL before the optimization began, the sound pressure in the outlet is expected to be smaller than the previous example in the first iterations and that sound pressure is minimized through the optimization. In Fig. 4.18 the evolution of the sound pressure in the outlet is presented.

The sound pressure level response in the outlet can be plotted for a range of frequencies, in Fig. 4.19 the initial outlet response and the final outlet response are shown.

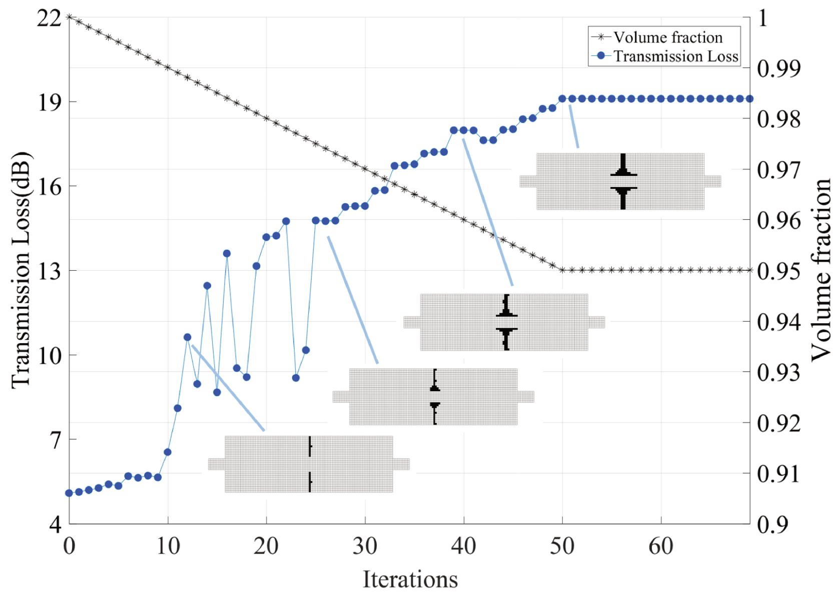

Figure 4.16: Evolution of the objective function and volume fraction for example 2.

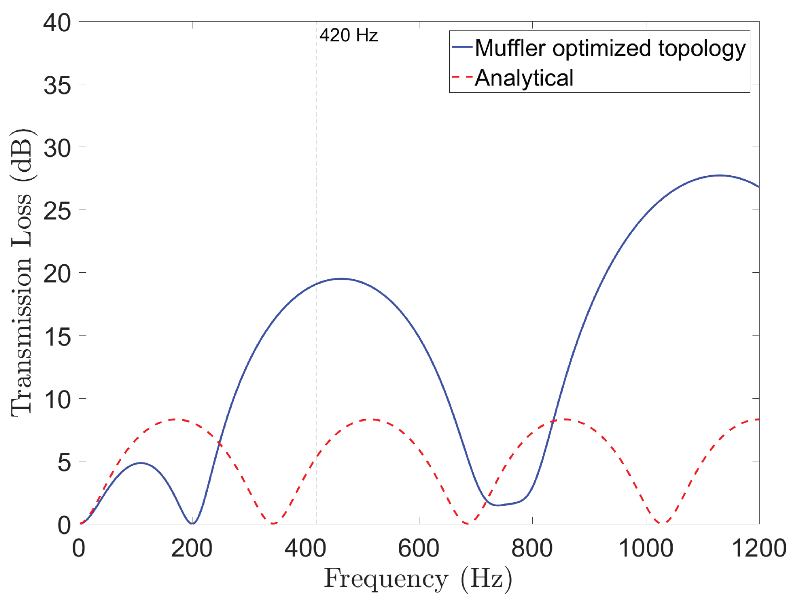

Figure 4.17: Transmission Loss for the optimized topology of example 2 in a frequency range in contrast with analytical empty chamber TL.

The motion and expansion of the sound modes in the acoustic chamber depicted in Fig. 4.19 due to the optimization is a indicator that the acoustic filter was enhanced. In this example, the third

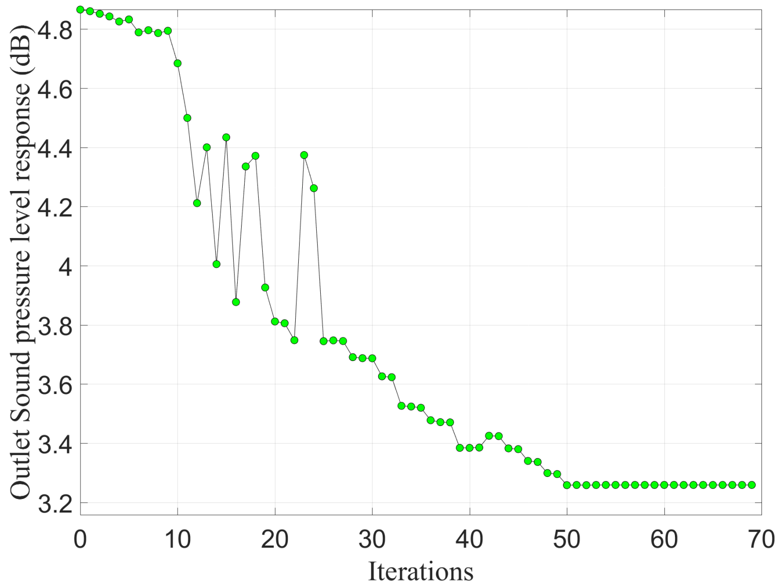

Figure 4.18: Outlet sound pressure level evolution in example 2.

mode moves closer to second mode, although the second mode movement is negligible. Just as in the first example, two low sound pressure level zones were expanded indicating a better muffler performance.

4.2.3 Example 3: Muffler Design for peak TL frequency

In this example the frequency ($\omega = 518Hz$) used for optimization corresponds to a TL value that corresponds to a peak TL in the empty chamber case.

Figure 4.20 shows the absolute acoustic pressure field in the muffler with a higher TL value. The acoustic pressure in the outlet is reduced unlike the first example were there is a significant pressure concentration.

In accordance with the other examples, BESO parameters presented in tab. 4.2 are used and the optimization is started with the domain in the same initial conditions.

The final topology for this optimization case is presented in Fig. 4.21 with the corresponding sound pressure distribution. In this example the position of the wall is shifted to the right when

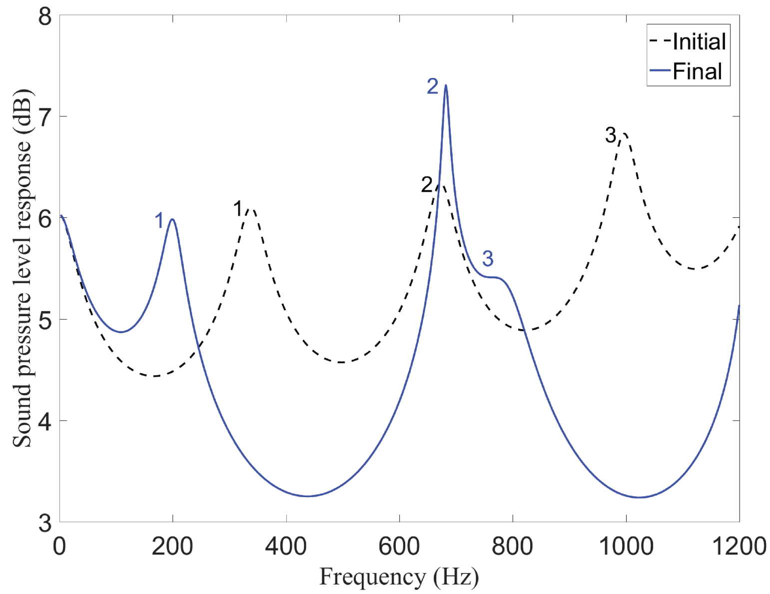

Figure 4.19: Outlet sound pressure level for a range of frequencies in example 2.

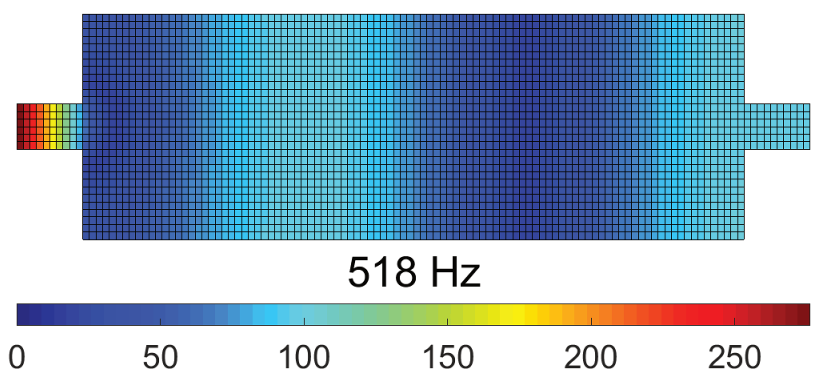

Figure 4.20: Acoustic Pressure distribution in the muffler for 518 Hz.

compared with example 2, a pattern can already be noticed in the position of the wall being create in the optimization.

The evolution of the objective function and volume fraction are shown in Fig. 4.22 together with some intermediary topologies. Between iterations 15 and 21 the objective function becomes unstable, that effect was already perceived in past examples and it is due to the progression of the wall in construction. Once the wall has been fully built the objective function stabilizes in

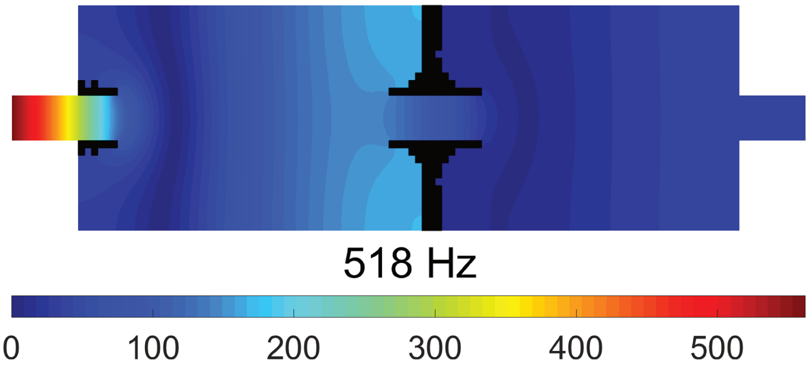

Figure 4.21: Acoustic Pressure distribution in the optimized muffer of example 3.

a ascending pattern and then converges at iteration 77 after the volume constraint $V_f = 95\%$ is satisfied at the $50th$ iteration. After the $50th$ iteration the topology has reached stability and only a feel adjustments are made until the convergence criteria is met at the $77th$ iteration, at this stage the extension together with the topology variation of the inlet tube have a significant influence in the outlet pressure.

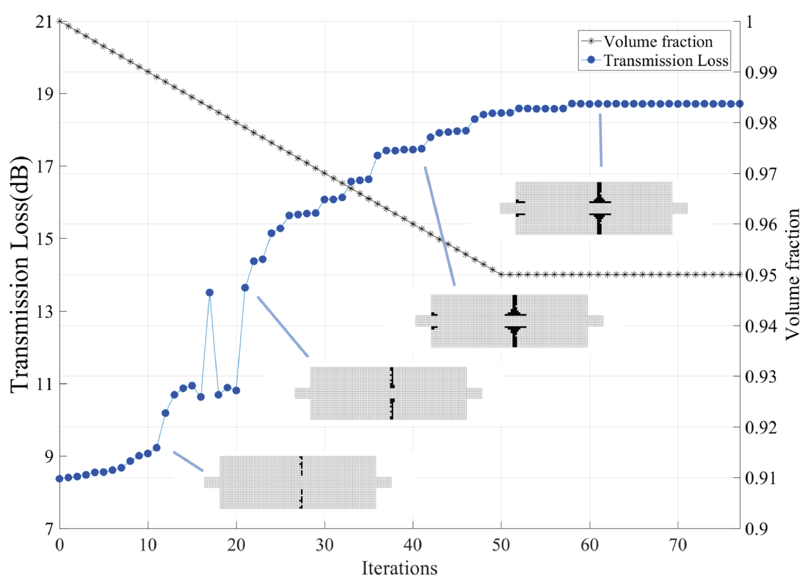

Figure 4.22: Evolution of the objective function and volume fraction for example 3.

Once the final topology is reached is possible do analyze its Transmission Loss effectiveness for a range of frequencies. Figure 4.23 shows the behavior of example 3 final topology for frequencies ranging from 0 Hz to 1200 Hz. The peak transmission loss became a point with approximately 18.7 dB instead of 8.3 dB, moreover, other frequencies had their TL maximized as it happened in example 1 and 2. The behavior of the muffler produced in example 3 is very similar to the muffler in example 1 and 2, however, it's possible to notice that in example 3 the most prominent peak is slightly shifted to the left expanding the area with higher TL and the maximum TL for that peak was also raised.

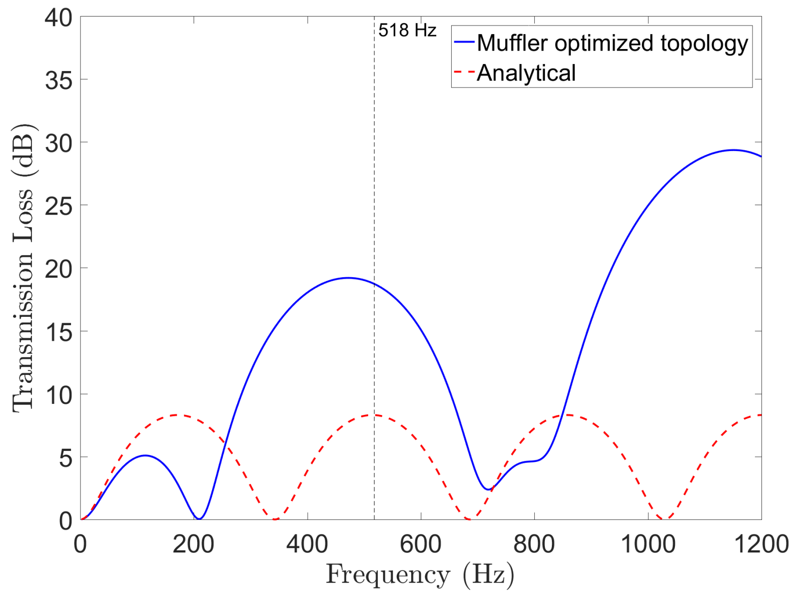

Figure 4.23: Transmission Loss for optimized topology of example 3 in a frequency range in contrast with the prior empty chamber.

Since the frequency picked for this example already had 8.3 dB of TL before the optimization began, the sound pressure in the outlet is expected to be even smaller than the previous examples in the first iterations. In Fig. 4.24 the evolution of the sound pressure in the outlet is presented, although the expected result is the minimization effect of the sound pressure in the outlet, it is possible to notice that the sound pressure in the outlet is slightly raised at the end of the optimization.

As seen in Fig. 4.22, TL continues its ascendant pattern even while the outlet pressure is raised fig. 4.24, this outcome is caused by the extension of the inlet tube, which causes an unexpected increment in the inlet pressure thus causing the effect described above. The inlet sound pressure becomes higher enough that even a increment in the outlet sound pressure still would still mean the maximization of the TL which is another form of enhancing the muffler properties.

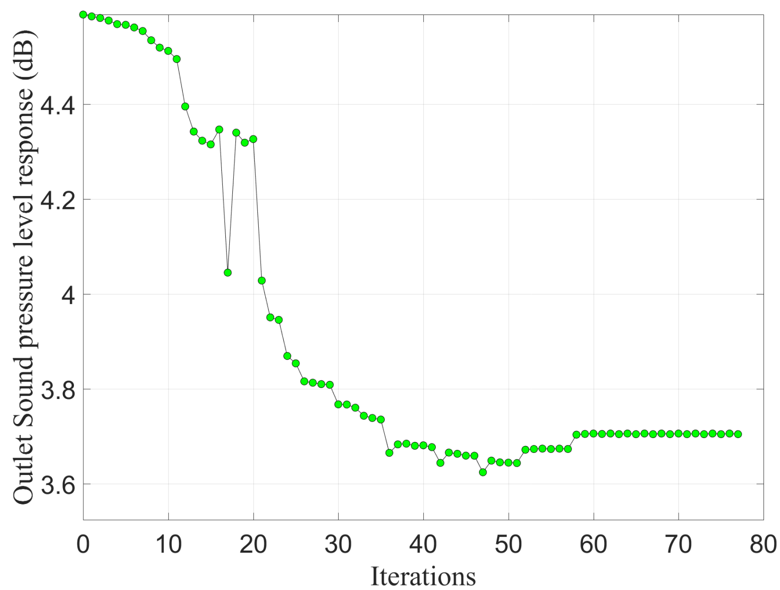

Figure 4.24: Outlet sound pressure level evolution in example 3.

The sound pressure response in the outlet can be plotted for a range of frequencies, in fig. 4.25 the initial outlet response and the final outlet response are shown. In this example, the first mode has its frequency reduced while the second mode slightly shifts having a decrease in frequency as well. The third mode is reduced to the point a fourth mode appears. This changes in acoustic modes created lower acoustic pressure level areas mainly between approximately 200 Hz and 600 Hz and frequencies higher than 1000 Hz.

4.2.4 Example 4: Muffler Design for valley TL in higher frequency

In this example, the frequency ($\omega = 690Hz$) used for optimization corresponds to a TL value that corresponds to a valley TL in the empty chamber case, however the chosen frequency is almost 2 times bigger than the one from example 1.

Figure 4.26 shows the absolute acoustic pressure field in the muffler, as expected, with a TL close to 0 dB the acoustic pressure in the outlet is similar to the one in the entrance. Two low pressure zones can be identified.

BESO optimization parameters presented in tab. 4.2 are used with a single difference, the final

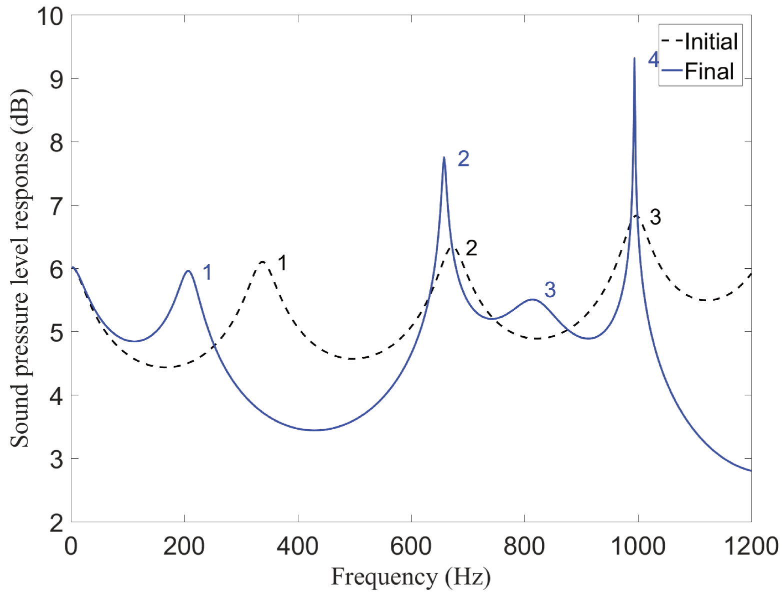

Figure 4.25: Outlet sound pressure for a range of frequencies in example 3.

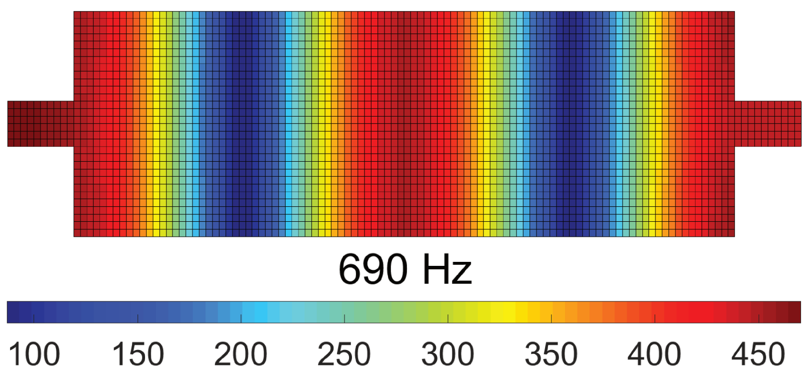

Figure 4.26: Acoustic Pressure distribution in the muffer for 690 Hz.

volume fraction used is 94%. This update in the final volume parameter was made to accommodate the trend the frequency of $690Hz$ has, as is tends to build two different barriers more volume was allowed in order to help the optimization process in creating two well defined walls. The optimization is started with the domain in the same initial conditions.

The final topology for this optimization case is presented in Fig. 4.27 with the corresponding acoustic pressure distribution. In this example, two barriers are created effectively creating 3

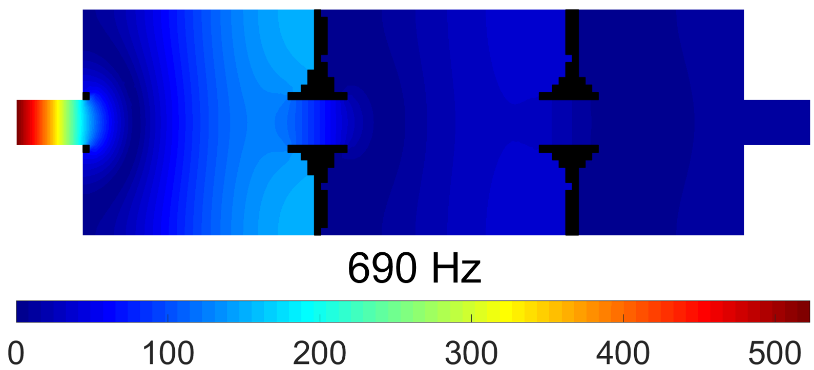

Figure 4.27: Acoustic Pressure distribution in the optimized muffer of example 4.

different acoustic chambers.

The evolution of the objective function and volume fraction are shown in Fig. 4.28 together with some intermediary topologies. Between iterations 14 and 26 the objective function becomes unstable, that effect was already perceived in past examples and it is due to the progression of the wall in construction, another significant jump in the objective function is noticed between iterations 43 and 46, this jump is caused by the conclusion of the second wall. Once both walls are fully built the objective function stabilizes and then converges at iteration 99 after the volume constraint $V_f = 94\%$ is satisfied at the $60th$ iteration.

Once the final topology is reached is possible do analyze its Transmission Loss effectiveness for a range of frequencies. Figure 4.29 shows the behavior of example 4 final topology for frequencies ranging from 1 Hz to 1200 Hz. The valley transmission loss became a point with approximately 31.2 dB instead of 0 dB, moreover, other frequencies had their TL maximized as it happened in the other examples. The behavior of the muffler produced in example 4 has inferior performance in frequencies ranging from 0 Hz to approximately 400 Hz. In higher frequencies, the TL observed is bigger for every frequency when compared with the empty chamber.

In Fig. 4.30 the evolution of the sound pressure in the outlet is presented and the minimization of the sound pressure can be observed as well as in examples 1 and 2.

The sound pressure response in the outlet can be plotted for a range of frequencies, in fig. 4.31 the initial outlet response and the final outlet response are shown. In this example, the second mode approaches the first mode while the third have its frequency decreased just a little. This movement

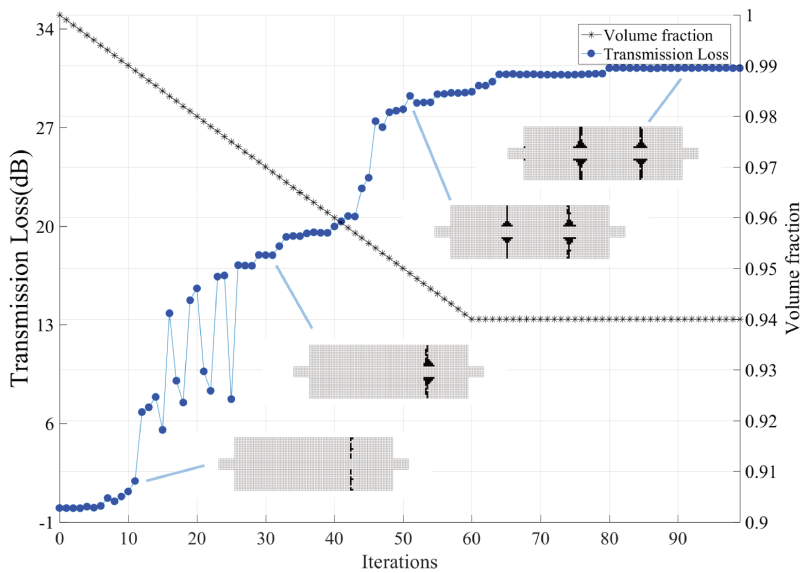

Figure 4.28: Evolution of the objective function and volume fraction for example 4.

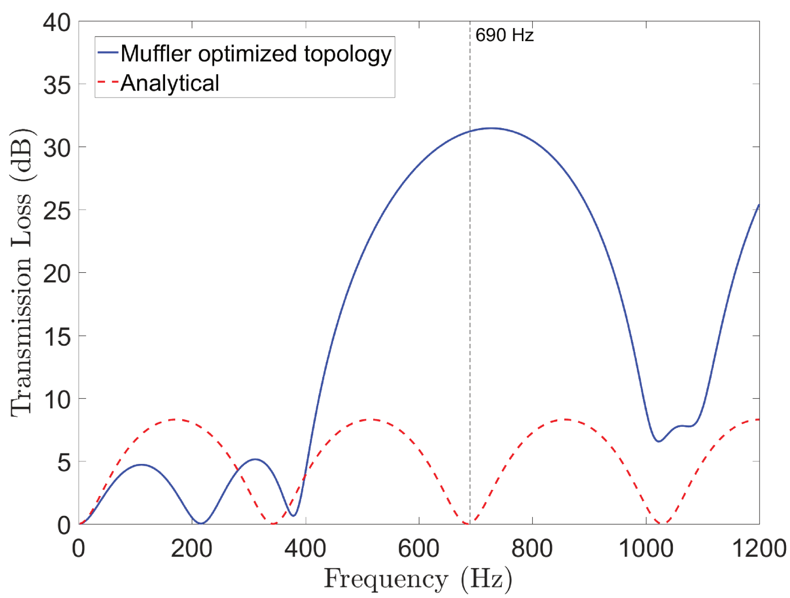

Figure 4.29: Transmission Loss for optimized topology of example 4 in a frequency range in contrast with the prior empty chamber.

creates a large area where low sound pressure levels are achieved. Its also visible that a fourth mode has appeared.

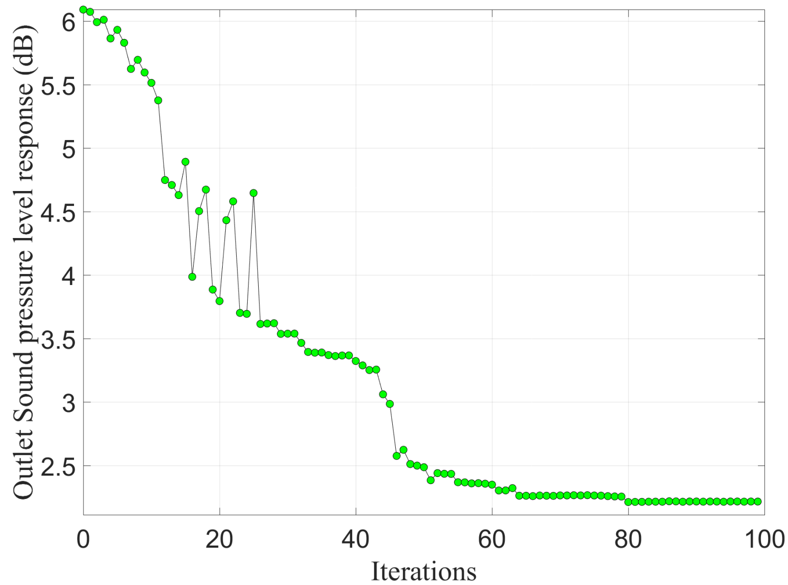

Figure 4.30: Outlet sound pressure level evolution in example 4.

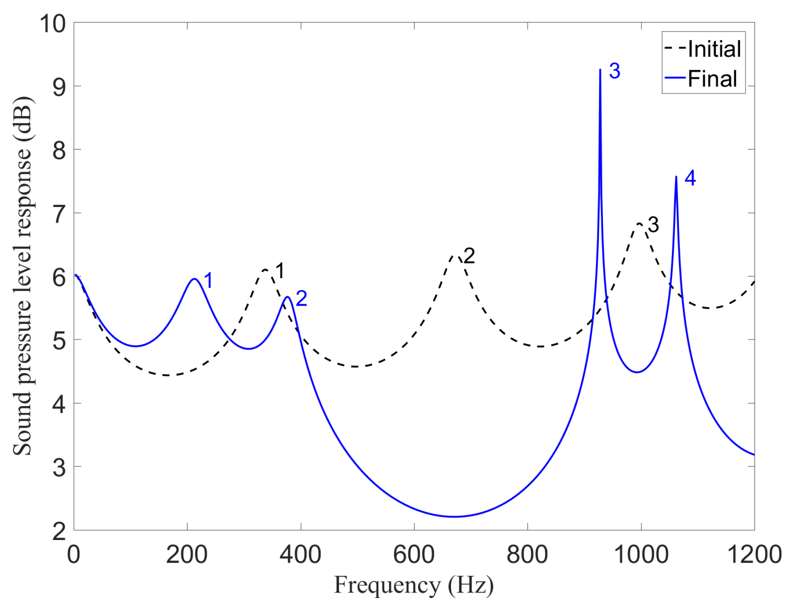

Figure 4.31: Outlet sound pressure level for a range of frequencies in example 4.

4.2.4.1 Different final volumes V_f

For the specific case of $\omega = 690$ Hz the final volume was changed to facilitate convergence. As said before, when using a final volume fraction of 95% the optimization attempted to create 3 cavities by using four barriers but the amount of void elements allowed, only 5%, made the optimization process nearly 60 iterations longer than the other examples. In Fig. 4.32 the objective function evolution of this case is presented. The topologies found with 95% and 94% were similar.

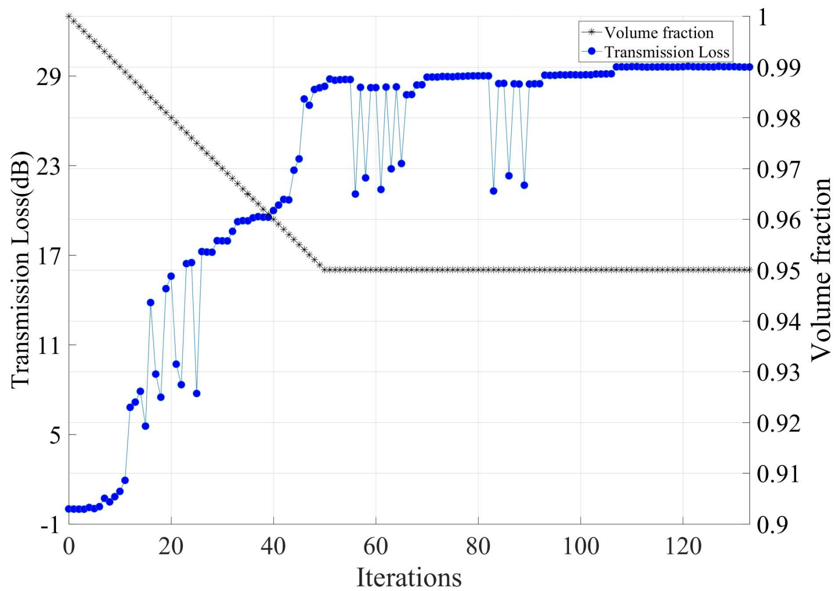

Figure 4.32: Objective function and volume fraction evolution for the case with 95% $\mathbf{V_f}$.

Two other final volume fractions were tested, 92% and 90%. The results can be seen in Figs.4.33 and 4.34.

In both new final volume fractions tested there was increase in the transmission loss function. The increase in TL was caused by the extension of the inlet duct allowed by the extra volume of rigid elements. The designer can choose the weight of the system and study the cost-benefit of heaving heavier or lighter expansion chambers with higher or lesser TL.

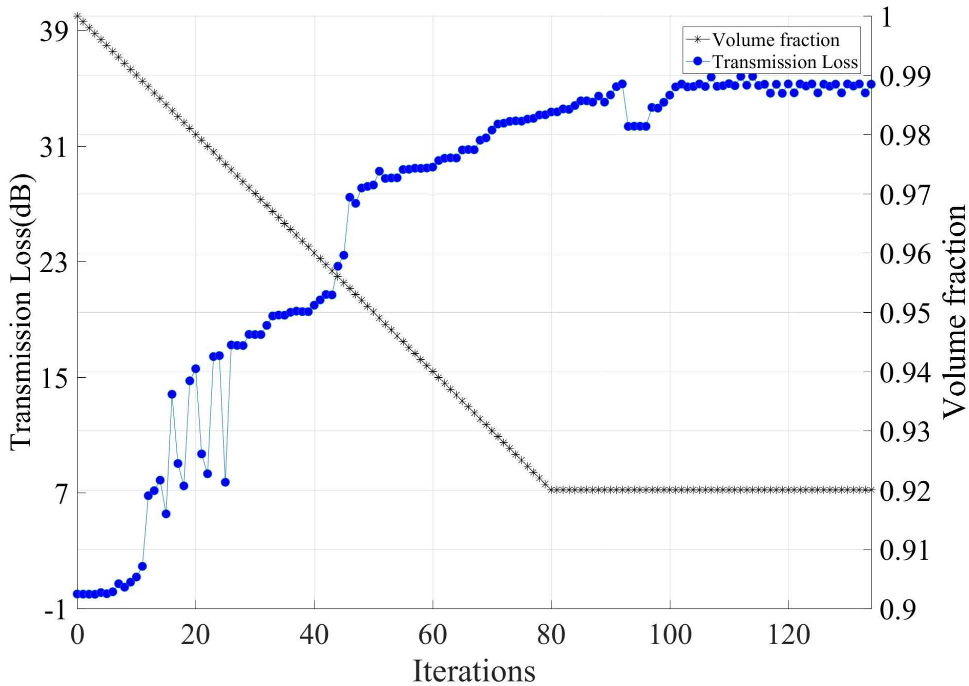

(a)

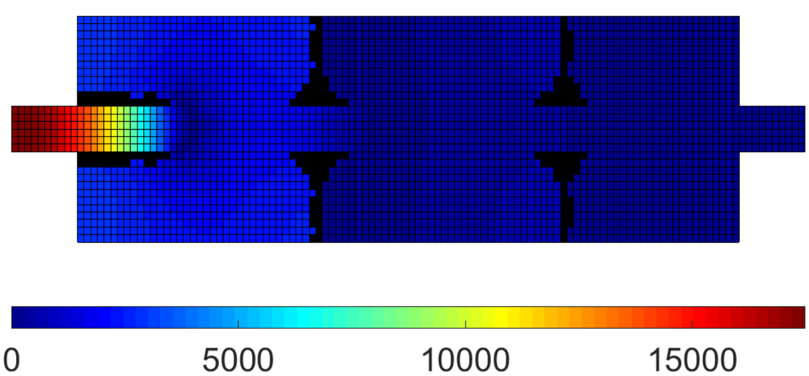

(b)

Figure 4.33: (a)Objective function and volume fraction evolution for $\mathbf{V_f}$ =92%. (b) Final topology achieved with $\mathbf{V_f}$ =92%.

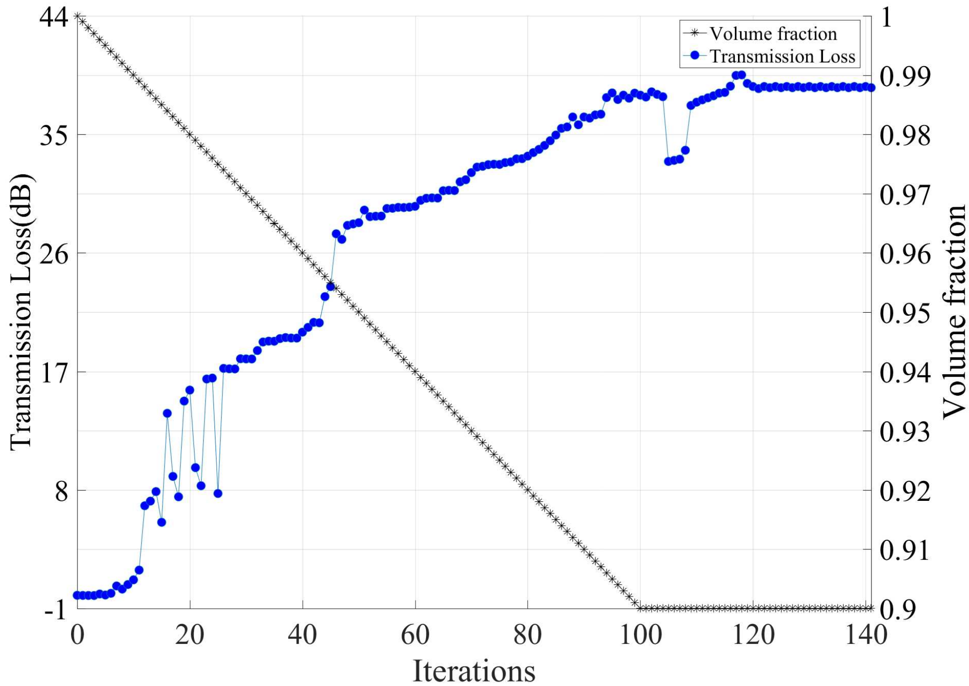

(a)

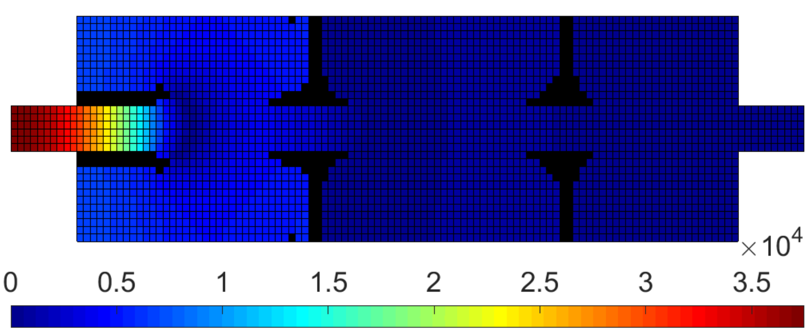

(b)

Figure 4.34: (a)Objective function and volume fraction evolution for $\mathbf{V_f}$ =90%. (b) Final topology achieved with $\mathbf{V_f}$ =90%.

4.3 Mesh dependency analysis

In this section, a finer mesh is used in order to observe the optimization process convergence and final topologies reached. Figure 4.35 (a) shows the evolution of the TL objective function and volume throughout the optimization for the frequency of 346 and Fig. 4.35 (b) the final topology obtained. The usage of a finite element mesh with 12480 elements provided a smooth convergence avoiding the creation of holes in the partitions as observed in the examples presented in the previous section. The final topology presented is similar to the case where a thicker mesh was used showing that the numeric filter used avoided mesh dependency.

Figure 4.36 (a) shows the evolution of the TL objective function during the optimization process for the frequency of 690 Hz. Different from previous section example the convergence of the TL function show no signs of holes appearing in the partition walls during the optimization. The final topology found using a finer mesh for the case of 690 Hz presented in Fig. 4.36 (b) is similar to the topology shown in the previous section as well.

The usage of a finer mesh provided a smoother convergence curve for both examples and no significant mesh dependency was found in the topologies presented in Figs. 4.35 (b) and 4.36 (b) showing the capability of the proposed methodology to achieve optimum results using different mesh sizes.

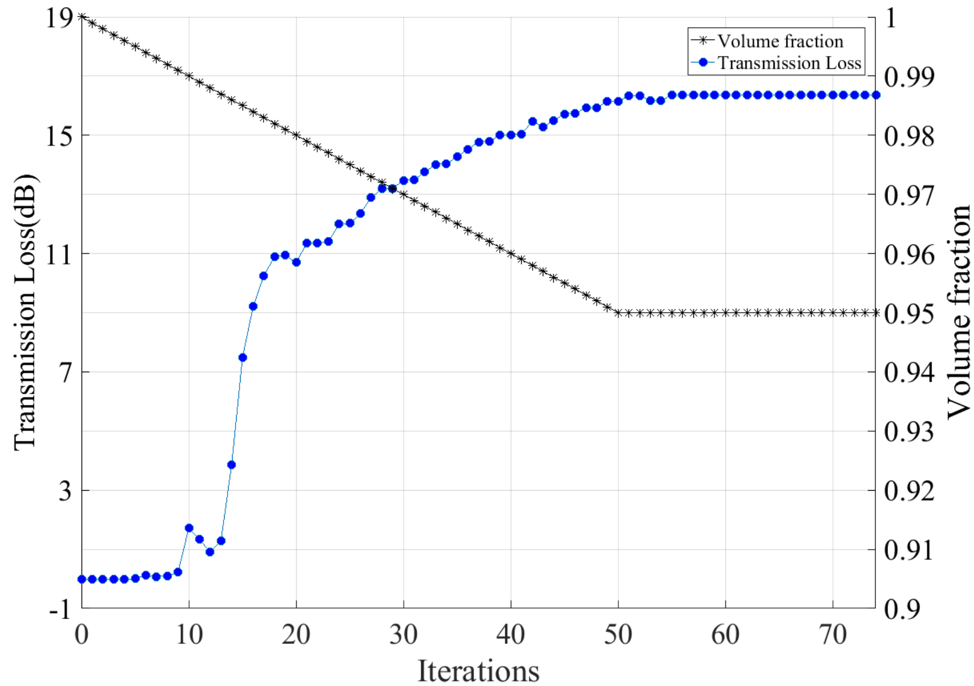

(a)

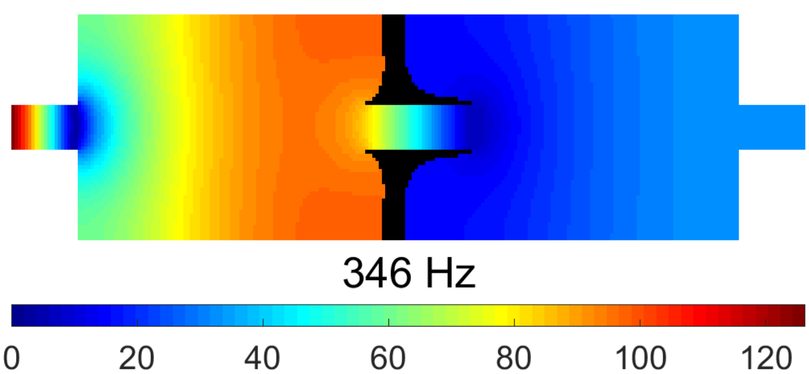

(b)

Figure 4.35: (a)Objective function and volume fraction evolution for optimizing 346 Hz frequency using 12480 elements mesh. (b) Final topology achieved for the frequency of 346 Hz and $V_f = 95\%$.

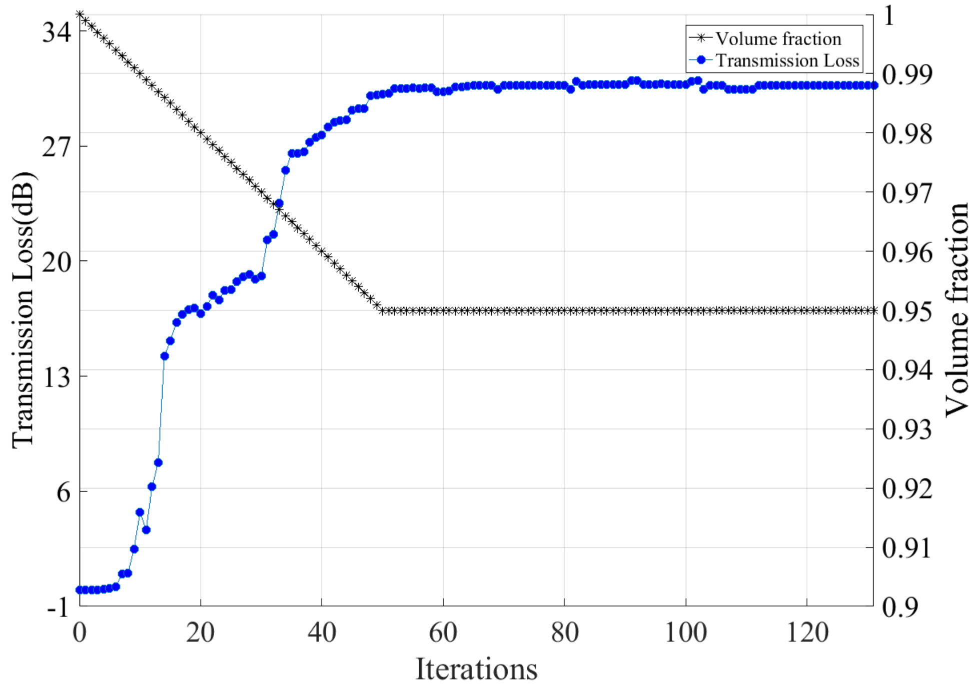

(a)

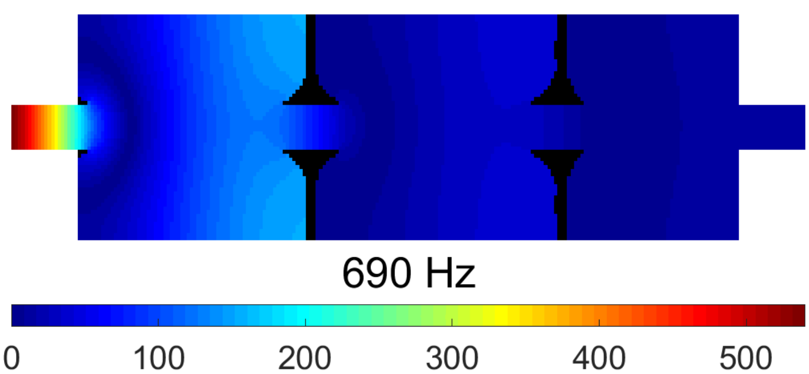

(b)

Figure 4.36: (a)Objective function and volume fraction evolution for optimizing 690 Hz frequency using 12480 elements mesh. (b) Final topology achieved for the frequency of 690 Hz and $V_f = 95\%$.

5 CONCLUSIONS AND SUGGESTED FUTURE WORKS

In this chapter, concluding remarks are presented based on the development of this work, which had as its main goal, the numerical implementation of an algorithm for acoustic mufflers design using the BESO method. Finally, a few suggestions for future research are listed.

5.1 Conclusions

This work presented a study of evolutionary optimization of acoustic mufflers. A discrete model of an acoustic muffler was created using a finite element approach and the acoustic pressure field inside the expansion chamber was visualized. Transmission loss performance parameter was presented and three-pole method of TL evaluation was proposed and validated considering analytical equations for single and double expansion chambers. The discrete finite element model developed was then used together with an evolutionary optimization method to maximize transmission loss in reactive mufflers.

The acoustic topology optimization was done using the evolutionary method BESO. The sensitivity analysis based on the TL three-pole method derivative was proven adequate for this problem. The ranked sensitivity number as seen in the numerical examples section guided the optimization in order to maximize TL and guided a minimization pattern for the outlet sound pressure level.

The topology optimization proposed was studied from a design of acoustic mufflers point of view. The topologies found not only maximized transmission loss but also were feasible and could be manufactured for an industry application. The final topologies encountered presented high transmission loss for the prescribed working frequency and in addition, high TL was found in other frequencies.

The binary characteristic of the BESO approach favored the computational cost and the number of iterations until convergence criteria was met. The highest number of iterations necessary after the final volume was achieved was 70 iterations for one of the 690 Hz cases where V_f was 95%. For most of the numerical examples presented in this dissertation, a smaller number of iterations was presented.

5.2 Suggestions for future research

Important suggestions for future works continuing this research field are summarized in the list bellow:

- Study the addition of Helmholtz resonators to the muffler in a post-processing algorithm, avoiding low TL in specific frequencies.
- Study the influence of adding porous materials inside the muffler during the optimization process. A multi-material optimization with fluid, porous and rigid elements is suggested.
- Study more complex muffler models. In the literature, there are already some cases with perforated ducts for instance.
- Create and study 3D muffler models and compare the results found with the 2D models, if similar, the results would show that a less expensive 2D model could be used effectively in muffler design through optimization methods.
- Add acoustic-structure interaction in the muffler model, considering the partitions inside the muffler vibration.
- Study optimization case with acoustic, thermic and flow objective functions and compare the final topologies. In the literature, there are cases of coupled analysis.
- Study the effect of micro-scale approach material design for noise attenuation inside the muffler. A micro-scale optimized material could be used for example to coat the rigid partitions in the acoustic muffler.

REFERENCES

ALLAIRE, G.; JOUVE, F. and TOADER, A.M. Structural optimization using sensitivity analysis and a level-set method. **Journal of Computational Physics**, v. 194, n. 1, 363 – 393, 2004.

BARBIERI, R. and BARBIERI, N. Finite element acoustic simulation based shape optimization of a muffler. **Applied Acoustics**, v. 67, n. 4, 346 – 357, 2006.

BARRON, R.F. **Industrial noise control and acoustics**. CRC Press, 2002.

BENDSøE, M.P. Optimal shape design as a material distribution problem. **Structural optimization**, v. 1, n. 4, 193–202, 1989.

BENDSøE, M.P. and KIKUCHI, N. Generating optimal topologies in structural design using a homogenization method. **Computer methods in applied mechanics and engineering**, v. 71, n. 2, 197–224, 1988.

BILAWCHUK, S. and FYFE, K. Comparison and implementation of the various numerical methods used for calculating transmission loss in silencer systems. **Applied Acoustics**, v. 64, n. 9, 903–916, 2003.

CHU, D.; XIE, Y.; HIRA, A. and STEVEN, G. Evolutionary structural optimization for problems with stiffness constraints. **Finite Elements in Analysis and Design**, v. 21, n. 4, 239 – 251, 1996.

COOK, R.D. *et al.* **Concepts and applications of finite element analysis**. John Wiley & Sons, 2007.

CRAGGS, A. A finite element method for damped acoustic systems: An application to evaluate the performance of reactive mufflers. **Journal of Sound and Vibration**, v. 48, n. 3, 377 – 392, 1976.

DAVIS, D.D.J.; M., S.; M., M. and L., S. **Theoretical and experimental investigation of mufflers with comments on engine exhaust muffler system**. NACA Report 1192, 1954.

DIAZ, A. and SIGMUND, O. Checkerboard patterns in layout optimization. **Structural optimization**, v. 10, n. 1, 40–45, 1995.

DÜHRING, M.B. **Topology Optimization for Acoustic Problems**, pp. 375–385. Springer Netherlands, Dordrecht, 2006.

DÜHRING, M.B.; JENSEN, J.S. and SIGMUND, O. Acoustic design by topology optimization. **Journal of Sound and Vibration**, v. 317, n. 3-5, 557 – 575, 2008.

FAHY, F.J. **Foundations of engineering acoustics**. Academic press, 2000.

GARCÍA, A. and FAUS, L. Statistical analysis of noise levels in urban areas. **Applied Acoustics**, v. 34, n. 4, 227 – 247, 1991.

GENUIT, K. The sound quality of vehicle interior noise: a challenge for the NVH-engineers. **International Journal of Vehicle Noise and Vibration**, v. 1, n. 1-2, 158–168, 2004.

GERGES, S.; JORDAN, R.; THIEME, F.; BENTO COELHO, J. and ARENAS, J. Muffler modeling by transfer matrix method and experimental verification. **Journal of the Brazilian Society of Mechanical Sciences and Engineering**, v. 27, n. 2, 132–140, 2005.

HUANG, X. and XIE, Y.M. Convergent and mesh-independent solutions for the bi-directional evolutionary structural optimization method. **Finite Elements in Analysis and Design**, v. 43, n. 14, 1039–1049, 2007.

HUANG, X. and XIE, Y.M. Bi-directional evolutionary topology optimization of continuum structures with one or multiple materials. **Computational Mechanics**, v. 43, n. 3, 393–401, 2009.

HUANG, X. and XIE, Y.M. **Evolutionary Topology Optimization of Continuum Structures: Methods and Applications**. Wiley, 2010.

HUANG, X.; ZUO, Z.H. and XIE, Y.M. Evolutionary topological optimization of vibrating continuum structures for natural frequencies. **Computers & structures**, v. 88, n. 5, 357–364, 2010.

JANG, G.W. and LEE, J.W. Topology optimization of internal partitions in a flow-reversing chamber muffler for noise reduction. **Structural and Multidisciplinary Optimization**, pp. 1–16, 2016.

JOG, C.S. and HABER, R.B. Stability of finite element models for distributed-parameter optimization and topology design. **Computational Mechanics**, v. 130, 203–226, 1996.

JURAGA, I.; PAVIOTTI, M. and BERGER, B. The environmental noise directive at a turning point. In **Proceedings of EuroNoise Conference (2015, Maastricht, The Netherlands)**, pp. 1041–44. 2015.

KIM, K.H. and YOON, G.H. Optimal rigid and porous material distributions for noise barrier by acoustic topology optimization. **Journal of Sound and Vibration**, v. 339, 123 – 142, 2015.

KREBBER, W.; GENUIT, K. and SOTTEK, R. Sound quality of vehicle exterior noise. In **Proceeding of Forum Acusticum**. 2002.

LEE, J.W. Optimal topology of reactive muffler achieving target transmission loss values: Design and experiment. **Applied Acoustics**, v. 88, 104 – 113, 2015.

LEE, J.W. and JANG, G.W. Topology design of reactive mufflers for enhancing their acoustic attenuation performance and flow characteristics simultaneously. **International Journal for Numerical Methods in Engineering**, v. 91, n. 5, 552–570, 2012.

LEE, J.W. and KIM, Y.Y. Topology optimization of muffler internal partitions for improving acoustical attenuation performance. **International Journal for Numerical Methods in Engineering**, v. 80, n. 4, 455–477, 2009.

LEE, J.W. and OH, K.S. Optimal topology of a reactive muffler in the presence of temperature gradient. In **The 21st International Congress on Sound and Vibration**. 2014.

LI, Y. **Topology optimization of compliant mechanisms based on the BESO method**. 2014. PhD Thesis. RMIT University.

MARBURG, S. and NOLTE, B. **Computational acoustics of noise propagation in fluids: finite and boundary element methods**, v. 578. Springer, 2008.

MOURA, M.S.; OLIVEIRA, A.R.G. and ICHANO, J.N. Melhora dos parâmetros acústicos reais através de ferramentas de predição em sistemas de exaustão. **SAE Technical Paper Series**, 2008.

MUNJAL, M. **Acoustics of Ducts and Mufflers With Application to Exhaust and Ventilation System Design**. A Wiley-Interscience publication. Wiley, 1987a.

MUNJAL, M. A simple numerical method for three-dimensional analysis of simple expansion chamber mufflers of rectangular as well as circular cross-section with a stationary medium. **Journal of Sound and vibration**, v. 116, n. 1, 71–88, 1987b.

MUNJAL, M.L. Recent advances in muffler acoustics. **International Journal of Acoutics and Vibration**, v. 18, n. 2, 71–85, 2013.

OH, J.E. and CHA, K.J. Noise reduction of muffler by optimal design. **KSME international journal**, v. 14, n. 9, 947–955, 2000.

PEAT, K. Evaluation of four-pole parameters for ducts with flow by the finite element method. **Journal of Sound and Vibration**, v. 84, n. 3, 389–395, 1982.

PICELLI, R.; VICENTE, W.M.; PAVANELLO, R. and XIE, Y.M. Evolutionary topology optimization for natural frequency maximization problems considering acoustic-structure interaction. **Finite Elements in Analysis and Design**, v. 106, 56 – 64, 2015.

POTENTE, D. General design principles for an automotive muffler. In **Proceedings of ACOUSTICS**, pp. 153–158. 2005.

PRAGER, W. and ROZVANY, G.I. Optimization of structural geometry. **Dynamical systems**, pp.

265–293, 1977.

PRASAD, M. and CROCKER, M. Studies of acoustical performance of a multi-cylinder engine exhaust muffler system. **Journal of Sound and Vibration**, v. 90, n. 4, 491–508, 1983.

QUERIN, O.; STEVEN, G. and XIE, Y. Evolutionary structural optimisation (eso) using a bidirectional algorithm. **Engineering Computations**, v. 15, n. 8, 1031–1048, 12 1998.

REDDY, J.N. **An introduction to the finite element method**, v. 2. McGraw-Hill New York, 1993.

SIGMUND, O. **Design of Materials Structures Using Topology Optimization**. Department of Solid Mechanics, Technical University of Denmark, 1994.

SIGMUND, O. Tailoring materials with prescribed elastic properties. **Mechanics of Materials**, v. 20, n. 4, 351 – 368, 1995.

SIGMUND, O. A 99 line topology optimization code written in matlab. **Structural and Multidisciplinary Optimization**, v. 21, n. 2, 120–127, 2001.

SIGMUND, O. and PETERSSON, J. Numerical instabilities in topology optimization: a survey on procedures dealing with checkerboards, mesh-dependencies and local minima. **Structural optimization**, v. 16, n. 1, 68–75, 1998.

SULLIVAN, J.W. and CROCKER, M.J. Analysis of concentric-tube resonators having unpartitioned cavities. **The Journal of the Acoustical Society of America**, v. 64, n. 1, 207–215, 1978.

TAO, Z. and SEYBERT, A. A review of current techniques for measuring muffler transmission loss. Technical report, SAE Technical Paper, 2003.

VICENTE, W.M.; PICELLI, R.; PAVANELLO, R. and XIE, Y.M. Topology optimization of frequency responses of fluid-structure interaction systems. **Finite Elements in Analysis and Design**, v. 98, 1 – 13, 2015.

VICENTE, W.M.; ZUO, Z.H.; PAVANELLO, R.; CALIXTO, T.K.L.; PICELLI, R. and XIE, Y.M. Concurrent topology optimization for minimizing frequency responses of two-level hierarchical structures. **Computer Methods in Applied Mechanics and Engineering**, v. 301, 116 – 136, 2016.

WADBRO, E. and BERGGREN, M. Topology optimization of an acoustic horn. **Computer Methods in Applied Mechanics and Engineering**, v. 196, n. 1-3, 420 – 436, 2006.

WANG, M.Y.; WANG, X. and GUO, D. A level set method for structural topology optimization. **Computer Methods in Applied Mechanics and Engineering**, v. 192, n. 1-2, 227–46, 2003.

WU, T. and WAN, G. Muffler performance studies using a direct mixed-body boundary element method and a three-point method for evaluating transmission loss. **Journal of Vibration and Acoustics**, v. 118, 479–484, 1996.

XIE, Y. and STEVEN, G. A simple evolutionary procedure for structural optimization. **Computers & Structures**, v. 49, n. 5, 885 – 896, 1993.

XIE, Y.M. and STEVEN, G.P. Basic evolutionary structural optimization. In **Evolutionary Structural Optimization**, pp. 12–29. Springer, 1997.

YEDEG, E.L.; WADBRO, E. and BERGGREN, M. Interior layout topology optimization of a reactive muffler. **Structural and Multidisciplinary Optimization**, v. 53, n. 4, 645–656, 2016a.

YEDEG, E.L.; WADBRO, E.; HANSBO, P.; LARSON, M.G. and BERGGREN, M. A nitsche-type method for helmholtz equation with an embedded acoustically permeable interface. **Computer Methods in Applied Mechanics and Engineering**, v. 304, 479 – 500, 2016b.

YOON, G.H. Acoustic topology optimization of fibrous material with delany-bazley empirical material formulation. **Journal of Sound and Vibration**, v. 332, n. 5, 1172 – 1187, 2013.

YOUNG, C.I.J. and CROCKER, M.J. Prediction of transmission loss in mufflers by the finite element method. **The Journal of the Acoustical Society of America**, v. 57, n. 1, 144–148, 1975.

ZHOU, M. and ROZVANY, G. On the validity of eso type methods in topology optimization. **Structural and Multidisciplinary Optimization**, v. 21, n. 1, 80–83, 2001.

ZIENKIEWICZ, O.C. and TAYLOR, R.L. **The finite element method: solid mechanics**, v. 2. Butterworth-heinemann, 2000.

ZUO, Z.H.; XIE, Y.M. and HUANG, X. An improved bi-directional evolutionary topology optimization method for frequencies. **International Journal of Structural Stability and Dynamics**, v. 10, n. 01, 55–75, 2010.

CONEM 2016

CONEM 2016
CONGRESSO NACIONAL DE ENGENHARIA MECÂNICA
ABCM 40 anos
Associação Brasileira de Engenharia e Ciências Mecânicas
21 - 25 AGOSTO DE 2016
FORTALEZA - CEARÁ

Evolutionary Topology Optimization for Acoustic Mufflers

Felipe M Azevedo, fazevedo@fem.unicamp.br[1]
Renato Picelli, renato.picelli@gmail.com[2]
William Vicente, vicente@fem.unicamp.br[1]
Renato Pavanello, pava@fem.unicamp.br[1]

[1]University of Campinas, Rua Mendeleyev 200, 13083-860 Campinas,Brazil
[2]Cardiff School of Engineering, Cardiff University Queen's Buildings, The Parade CARDIFF CF24 3AA, Wales, UK.

Abstract: *This article introduces an evolutionary topology optimization approach applied to design acoustic mufflers. The main goal is to find the best configuration of barriers inside typical acoustic mufflers used in the automotive industry. The acoustic medium is governed by Helmholtz equation and rigid wall boundary conditions are introduced to represent acoustic barriers. In order to find a configuration of acoustic barriers that minimize the Transmission Loss function of the muffler an Evolutionary Structural Optimization (ESO) method will be used.*
To represent the acoustic domain inside the muffler, several boundary conditions are implemented, such as, normal imposed velocity, imposed pressure and imposed impedance as anechoic termination or infinite outlet. The continuum problem is solved in the frequency domain and it is discretized using the finite element method. Using ESO method a simple topology is reached, which maximizes the Transmission Loss function for different frequencies. The results reached are then compared with results available in the literature, considering different boundary conditions and excitation frequencies. The influence of fluid element discretization and of rejection parameters in the ESO method in the obtained topologies are presented. This work will be escalated to solve acoustic cloaking device problems.
Palavras-chave: *Topology Optimization, ESO Method,Transmission Loss, Acoustic Mufflers*

1. INTRODUCTION

In the past few decades, topology optimization has been used to improve and find the best responses in vibroacoustic systems using coupled and uncoupled formulation (Bendsoe and Sigmund, 2004; Huang and Xie, 2010). One of those systems is represented by the expansion chamber named mufflers, currently used in sound attenuation in vehicle exaust systems, that will be studied in this paper and has been studied in several publications (Munjal, 1987; Lee and Kim, 2009).

A number of authors have been devoted to study the problem of acoustic mufflers modeling and to propose different design approaches to optimize the acoustic muffler. Yedeg *et al.* (2015) muffler model has a perforated pipe connecting inlet and outlet and Lee and Jang (2012) muffler model couples flow and acoustic equations for the optimization problem. The principal design approaches used are based on Solid Isotropic Material with Penalization (SIMP) method (Dühring *et al.*, 2008; Yedeg *et al.*, 2015), or evolutionary structural optimization (ESO) method (Silva, 2007; Silva and Pavanello, 2010).

Actually the optimization of acoustic domains has been an important topic and investigations concerning noise attenuation became a major issue in the present days. In this scenario muffler type devices studies grew in importance, Barbieri and Barbieri (2005) used base shape optimization to improve Transmission Loss (TL) in a muffler, Lee and Kim (2009) used MMA to create barriers or partitions in expansion chambers maximizing transmission loss effectively reducing sound pressure levels in the outlet portion of the chamber.

In this work an evolutionary structural optimization (ESO) method is proposed to maximize TL and minimize acoustic pressure level in the outlet of a single expansion chamber of one automotive muffler.

2. ANALYTICAL AND APPROXIMATE TRANSMISSION LOSS IN A MUFFLER

An automotive exhaust system, two-dimensional muffler Fig. 1, presents a Transmission Loss (TL) function that can be analytically calculated by the following equation (Selamet and Radavich, 1997),

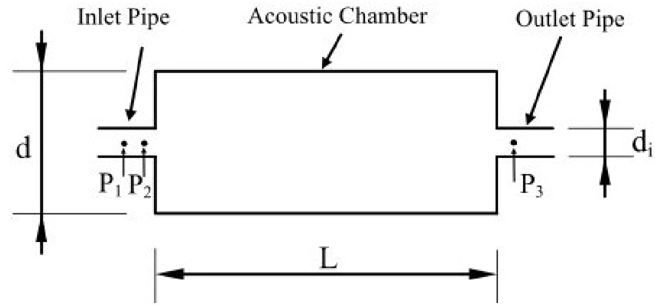

Figure 1: **Single Expansion Chamber Muffler**

$$TL = 10 \times Log_{10}\left(1 + \frac{1}{4}\left(m - \frac{1}{m}\right)^2 \cdot sin^2\left(k \cdot L\right)\right) \tag{1}$$

where,

$$m = \frac{d}{d_i}, k = \frac{2\pi f}{c} \tag{2}$$

and where d is the acoustic chamber diameter, d_i is the inlet and outlet pipes diameter, k is the wave number, f is the frequency and c is the speed of sound in the medium.

Using Eq. (1) to predict the TL function for a muffler with, $L = 0.5$m, $d = 0.15$m and $d_i = 0.03$m, considering that the domain is filled with air ($c = 343$m/s) for a frequency range, results shown in Fig. 2 are obtained.

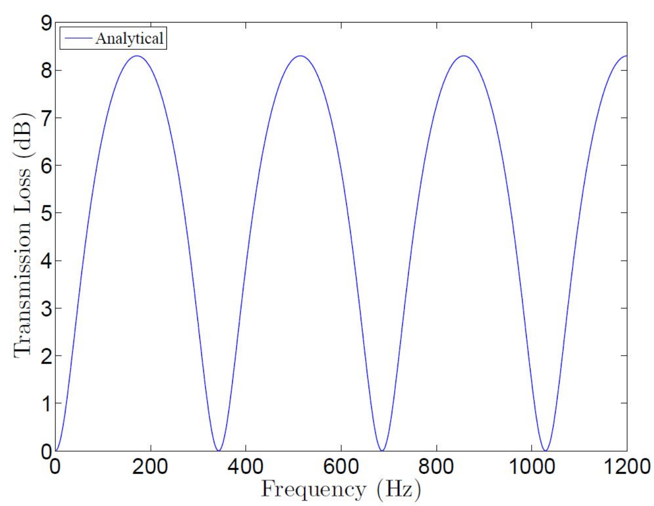

Figure 2: **TL analytical function of a single expansion chamber Eq.** (1)

The analytical model for TL function is no longer valid when rigid wall conditions are included inside the muffler acoustic chamber (Lee and Kim, 2009). In order to obtain an approximated solution the Finite Element Method is used and another equation is stated to find the TL function for an acoustic chamber with rigid barriers, Eq. (3);

$$TL = 20 \times Log_{10}\left(\left|\frac{1}{P_3}\frac{P_1 - P_2 \cdot e^{-jk \cdot l}}{1 - e^{-j2k \cdot l}}\right|\right) \tag{3}$$

where l is the distance between points 1 and 2, P_1 and P_2 are pressures in the inlet pipe and P_3 is the pressure in the outlet pipe as shown in Fig. 1. The $j = \sqrt{-1}$ is the imaginary unit.

Problem formulation and corresponding finite element discretization are discussed in the next section.

3. MUFFLER DEVICE: GOVERNING EQUATION AND FINITE ELEMENT MODEL

The governing equation of steady-state linear acoustic problems in frequency domain, valid inside the muffler acoustic chambers is the Helmholtz equation (Dühring *et al.*, 2008):

$$\nabla^2 P_{(x,y)} + \frac{\omega^2}{c^2} P_{(x,y)} = 0 \tag{4}$$

where ω is the angular frequency in (rad/s), P is the acoustic pressure and ∇^2 is the Laplacian operator. Equation (4) is valid in the acoustic domain shown in Fig. 3 in $(\Omega_d \mathrm{U} \Omega_f)$.

The weighted residual formulation for Eq. (4) can be written as;

$$\frac{1}{\rho}\int_\Omega \Phi \cdot \nabla^2 P d\Omega + \frac{\omega^2}{\rho c^2}\int_\Omega \Phi \cdot P d\Omega = 0 \tag{5}$$

where ρ is the air density, ϕ is the Weight Function and Ω_f is the fluid domain with Ω_d being a partition of it, represented in Fig. 3.

Rearranging the first term of Eq. (5) and using the Divergence Theorem, Eq. (5) can be written as:

$$\frac{1}{\rho}\int_\Gamma \Phi \cdot \nabla P \cdot \vec{n} d\Gamma - \frac{1}{\rho}\int_\Omega \nabla\Phi \cdot \nabla P d\Omega + \frac{\omega^2}{\rho c^2}\int_\Omega \Phi \cdot P d\Omega = 0 \tag{6}$$

Since,

$$\nabla P \cdot \vec{n} = \frac{\partial P}{\partial n} \tag{7}$$

Eq. (6) can be rearranged as:

$$\frac{1}{\rho}\int_\Omega \nabla\Phi \cdot \nabla P d\Omega - \frac{\omega^2}{\rho c^2}\int_\Omega \Phi \cdot P d\Omega = \frac{1}{\rho}\int_\Gamma \Phi \cdot \frac{\partial P}{\partial n} d\Gamma \tag{8}$$

where Γ is the boundary of the acoustic domain.

For the problem stated in this paper two boundary conditions will be introduced, see Fig. 3, Ω_f is the full domain filled with fluid and Ω_d represents part of the domain where partitions will be introduced. The Ω_d region is the design domain for the evolutionary optimization method. Two boundary conditions are imposed: Normal velocity V_n in boundary Γ_i, expressed in Eq. (9), and normal impedance $\bar{Z}$ in boundary Γ_o, expressed in Eq. (10).

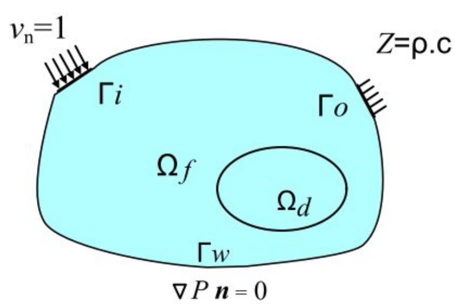

Figure 3: **Acoustic domain and Boundary conditions**

$$V_n = -\frac{1}{j\rho\omega}\frac{\partial P}{\partial n} \tag{9}$$

$$P = \bar{Z} V_n = -\frac{\bar{Z}}{j\rho\omega}\frac{\partial P}{\partial n} = -\frac{1}{j\rho\omega\bar{A}}\frac{\partial P}{\partial n} \tag{10}$$

where V_n is a vector of imposed velocities in Γ_i and $\bar{A}$ is acoustic admittance in Γ_o. To completely represent the whole boundary boundary problem rigid wall natural conditions $(\nabla P n = 0)$ are imposed in Γ_w.

Applying Eq. (9) and Eq. (10) in Eq. (8) we have

$$\frac{1}{\rho}\int_{\Omega}\nabla\Phi\cdot\nabla P d\Omega-\frac{\omega^2}{\rho c^2}\int_{\Omega}\Phi\cdot P d\Omega=-\frac{1}{\rho}\left(\int_{\Gamma_i} j\rho\omega\Phi V_n d\Gamma_i+\int_{\Gamma_o} j\rho\omega\Phi\bar{A}P d\Gamma_o\right) \tag{11}$$

Using the finite element method is possible to approximate Eq. (11). Using Galerkin's method the system response equation for the stated problem is:

$$\left(\left[\mathbf{K}\right]+j\omega\left[\mathbf{C}\right]-\omega^2\left[\mathbf{M}\right]\right)\cdot\left\{\mathbf{P}\right\}=\left\{\mathbf{V_{ni}}\right\} \tag{12}$$

where,

$$\left[\mathbf{K}\right]=\int_{\Omega}\left[\mathbf{B}\right]^t\left[\mathbf{B}\right]d\Omega \tag{13}$$

$$\left[\mathbf{C}\right]=\rho\bar{A}\int_{\Gamma_o}\left[\mathbf{N}\right]^t\left[\mathbf{N}\right]d\Gamma_o \tag{14}$$

$$\left[\mathbf{M}\right]=\frac{1}{c^2}\int_{\Omega}\left[\mathbf{N}\right]^t\left[\mathbf{N}\right]d\Omega \tag{15}$$

$$\left\{\mathbf{V_{ni}}\right\}=-j\rho\omega\int_{\Gamma_i}\left[\mathbf{N}\right]^t V_n d\Gamma_i \tag{16}$$

and $[\mathbf{N}]$ is the vector containing the shape functions for the acoustic element discretization with $[\mathbf{B}]$ being its derivatives (Desmet and Vandepitte, 2005), $[\mathbf{K}]$ is the acoustic stiffness matrix, $[\mathbf{C}]$ is the equivalent damping matrix relative to the output boundary condition, $[\mathbf{M}]$ is the mass matrix and $[\mathbf{V_{ni}}]$ is the vector relative to inlet conditions.

In this work, linear 4 node elements are used. Figure 4 shows the mesh used.

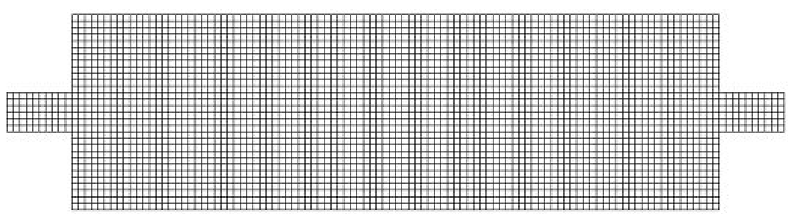

Figure 4: **Muffler Mesh with 3120 elements measuring 0.005m.**

Equation (12) can be used to verify the TL behavior for our domain previous to the addition of partitions, using the boundary conditions presented in Fig. 3, ($V_n = 1$) in the entire inlet and ($Z = \rho c$) in the entire outlet. Figure 5 shows a comparison of results achieved with Eq. (1) and results from the formulation developed in this section.

4. EVOLUTIONARY ACOUSTIC OPTIMIZATION PROBLEM FOR TL MAXIMIZATION:

In this section the evolutionary acoustic optimization problem is stated and the sensitivity analysis is derived. In this work an Evolutionary Topology optimization strategy is adopted, considering discrete values 1 or 0 which correspond to acoustic and void elements respectively, in a discretized form of the equation system, this approach is called "hard kill" in the literature. This method avoids intermediate density elements during the optimization procedure Huang and Xie (2010).

4.1 Problem statement

The objective is to maximize the amplitude of the TL function for a predefined frequency. The desing variable x_i represents the presence ($x_i = 1$) or absence ($x_i = 0$) of our particular fluid element. When the fluid element is removed, a rigid wall boundary condition is naturally imposed on the system, representing the local inclusion of a rigid barrier.

Considering volume constraints for barriers inclusion, the evolutionary optimization problem can be stated as:

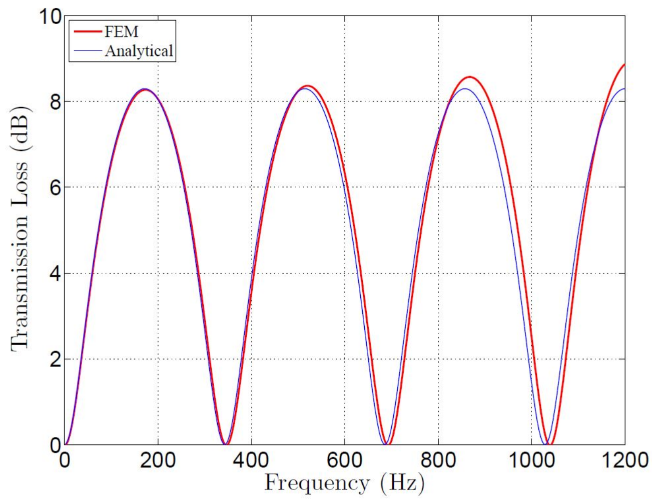

Figure 5: **Comparison between analytical TL and FEM approximated TL.**

$$\text{Maximize } \mathbf{TL} = 20 \times Log_{10}\left(\left|\frac{1}{P_3}\frac{P_1 - P_2 \cdot e^{-jk\cdot l}}{1 - e^{-j2k\cdot l}}\right|\right)$$

$$\text{Subject to: } \left(\left[\mathbf{K}\right] + j\omega\left[\mathbf{C}\right] - \omega^2\left[\mathbf{M}\right]\right)\cdot\left\{\mathbf{P}\right\} = \left\{\mathbf{V_{ni}}\right\}$$

$$V_f - \sum_{i=1}^{nel} v_i x_i = 0$$

$x_i = 0$ or 1

In the ESO method a gradient-based optimizer is necessary in order to evaluate the relevance of each element after the model analysis. This optimizer is generally called sensitivity and its calculation is described in the next section.

4.2 Transmission Loss Sensitivity Analysis

The sensitivity number is the objective function derivative with respect to the design variable, since transmission loss can be written as,

$$TL(\omega, x_i) = 10 \times log_{10}\left(\frac{\mid Pin\mid^2}{\mid Pout\mid^2}\right) \tag{17}$$

the derivative is,

$$\frac{\partial TL(\omega, x_i)}{\partial x_i} = \frac{10}{ln10} \times \left(\frac{\partial \mid P_{in}\mid^2}{\partial x_i}\cdot\frac{1}{\mid P_{in}\mid^2} - \frac{\partial \mid P_{out}\mid^2}{\partial x_i}\cdot\frac{1}{\mid P_{out}\mid^2}\right) \tag{18}$$

where P_{in} is,

$$P_{in} = \left|\left(\frac{P_1 - P_2\cdot e^{-jk\cdot l}}{1 - e^{-j2k\cdot l}}\right)\right| \tag{19}$$

and P_{out} is,

$$P_{out} = \mid P_3\mid \tag{20}$$

Since P_{in} and P_{out} in Eq. (19) and Eq. (20) are complex numbers, they can be expanded as follows:

$$P_{in}^2 = \frac{1}{\gamma}\left(P_{1Re} - P_{2Re}\cdot cos\left(k\cdot l\right) - P_{2Im}\cdot sin\left(k\cdot l\right)\right)^2 + \frac{1}{\gamma}\left(P_{1Im} - P_{2Im}\cdot cos\left(k\cdot l\right) + P_{2Re}\cdot sin\left(k\cdot l\right)\right)^2 \tag{21}$$

$$P_{out}^2 = P_{3Re}^2 + P_{3Im}^2 \tag{22}$$

with γ defined as,

$$\gamma = \big(1 - cos\big(2k \cdot l\big)\big)^2 + \big(sin\big(2k \cdot l\big)\big)^2 \tag{23}$$

where subscripts (Re) and (Im) mean real and imaginary parts respectively.

To calculate Eq. (21) and Eq. (22) derivatives for sensitivity analysis, the differentiations of acoustic pressure in the three points, P_1, P_2 and P_3 are necessary. Those can be found by differentiating the governing equation system Eq. (24) as:

$$\left\{\frac{d\mathbf{P}}{dx_i}\right\} = -\left(\left[\mathbf{K}\right] + j\omega\left[\mathbf{C}\right] - \omega^2\left[\mathbf{M}\right]\right)^{-1} \cdot \frac{d}{dx_i}\left(\left[\mathbf{K}\right] + j\omega\left[\mathbf{C}\right] - \omega^2\left[\mathbf{M}\right]\right) \cdot \left\{\mathbf{P}\right\} \tag{24}$$

where $\left\{\mathbf{V_{ni}}\right\}$ is constant with respect to x_i.

According to Chu *et al.* (1996), Vicente *et al.* (2015) and Vicente *et al.* (2016) in order to determine the change of response in especific degrees of freedomP_j of the system due to the i_{th} element removal, a vector F_j can be introduced. F_j is composed of zeros and a single one for the specific degree of freedom.

Thus we can write the following equations:

$$\frac{dP_j}{dx_i} = \mathbf{F}_j^t \cdot \frac{dP}{dx_i} \tag{25}$$

$$Z = \left(\left[\mathbf{K}\right] + j\omega\left[\mathbf{C}\right] - \omega^2\left[\mathbf{M}\right]\right) \tag{26}$$

Substituting Eq. (24) in Eq. (25):

$$\frac{dP_j}{dx_i} = F_j^t \cdot Z^{-1} \cdot \frac{dZ}{dx_i} \cdot \left\{P\right\} \tag{27}$$

Since the systems response where only F_j acts can be written as,

$$P_j = Z^{-1} \cdot F_j \tag{28}$$

Eq. (27) becomes:

$$\frac{dP_j}{dx_i} = -P_j^t \cdot \frac{dZ}{dx_i} \cdot \left\{P\right\} \tag{29}$$

where $\frac{dZ}{dx_i}$ is the response matrix of the i_{th} element, and can be calculated in local form, element by element.

Equation (29) aproximates $\frac{dP_i}{dx_i}$ avoiding huge computational costs and enabling $\frac{dTL}{dx_i}$ evaluation.

5. NUMERICAL RESULTS

The objective of this section is to validate the formulation and implementation of the optimization method, finite element model and TL evaluation, the numerical results presented by Lee and Kim (2009) are used for comparison.

The proposed example is represented in Fig. 1, with the configuration presented in section 2. It is a bi-dimensional representative acoustic model, for a simple automotive muffler. Table 1 shows ESO parameters used to optimize the system.

Table 1: **ESO Parameters.**

Evolutionary Ratio (ER)	0.166%
Final Volume (V_f)	97 %

The topology optimization strategy proposed in this article is applied for four different frequencies, those are relative to peak and valley values in Fig. 5.

It is possible to see that the final topologies produced in this work, shown in Fig. 6, are similar to the ones presented by Lee and Kim (2009). Figure 7 shows the evolution of the Transmission loss function amplitude through the optimization process for ($\omega = 519.5$ Hz).

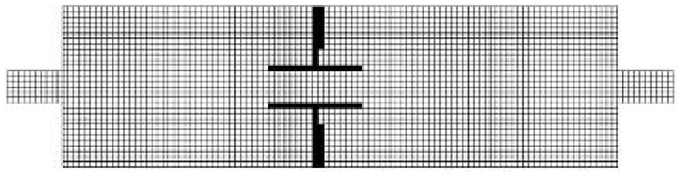

(a)

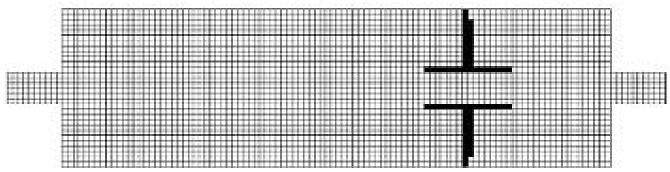

(b)

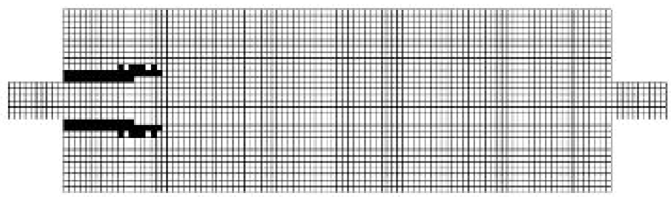

(c)

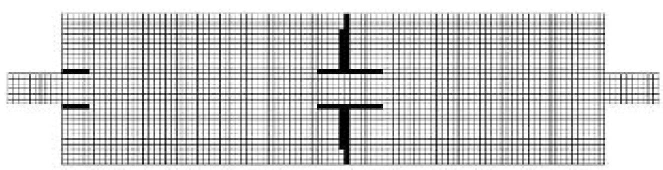

(d)

Figure 6: **Final topologies using ESO method ; (a): topology for a frequency of 346 Hz; (b): topology for a frequency of 693 Hz; (c): topology for a frequency of 173 Hz; (d): topology for a frequency of 519.5 Hz.**

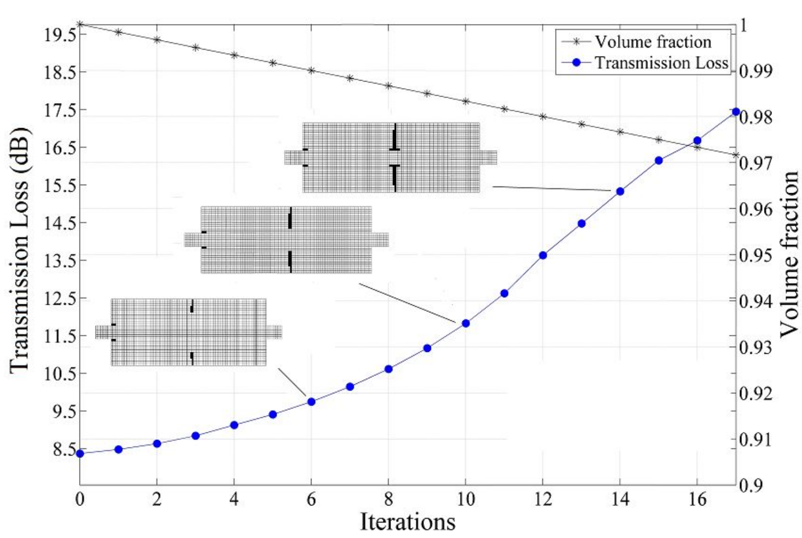

Figure 7: **TL evolution for 520 Hz example**

At the end of the optimization the maximum TL obtained for 519.5 Hz was 18 dB. Figure 8 shows TL response for a range of frequencies for mufflers presented in Fig. 6.

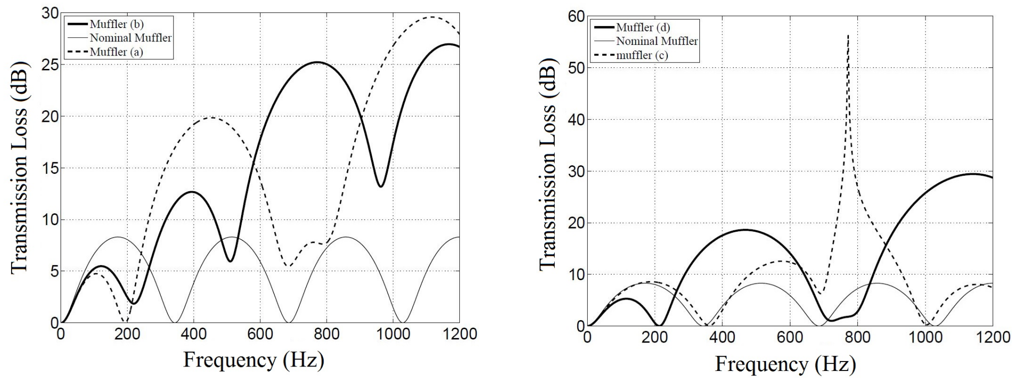

(a) (b)

Figure 8: **(a) TL responses for Mufflers (a) and (b); (b)TL responses for Mufflers (c) and (d)**

According to the results presented here the ESO approach was validated. One of the reasons results displayed in this paper do not agree completely with other publications is different methods being used, Lee and Kim (2009) used SIMP method to find the barrier layout, and different numerical parameters, in this work an ESO approach was used, an approach prior to Bi-directional Evolutionary Structural Optimization (BESO) method.

6. CONCLUSION

The main objective of this work is to propose an evolutionary methodology for acoustic otimization of automotive mufflers. A sensitivity analysis of the optimization problem has been presented considering an evolutionary approach. In order to maximize the Tranmission Loss, the optimiztion process has added attenuation barriers in the expansion chamber interior. For different frequencies, the results presented show the capability of the proposed methodology to maximize noise attenuation in the studied system. As a further work, the Bi-directional evolutionary structure optimization should be implemented for a more detailed analysis of the muffler optimization and different acoustic problems, for example, cloaking devices design.

7. ACKNOWLEDGMENTS

The authors are grateful to FAPESP (São Paulo Research Foundation, grant numbers 2013/08293-7, 2013/00085-6 and 2015/18607-4) and CAPES for the financial support of this work.

8. REFERÊNCIAS

Barbieri, R. and Barbieri, N., 2005. "Finite element acoustic simulation based shape optimization of a muffler". *Applied Accoustics*, Vol. 67, pp. 346–357.

Bendsoe, M.P. and Sigmund, O., 2004. *Topology Optimization: Theory Methods and Applications*. Springer.

Chu, D.N., Xie, Y.M., Hira, A. and Steven, G.P., 1996. "Evolutionary structural optimization for problems with stiffness constraints". *Finite Elements in Analysis and Design*, Vol. 21, pp. 239–251.

Desmet, W. and Vandepitte, D., 2005. *Finite Element Method for Acoustics*. LMS International.

Dühring, M.B., Jensen, J.S. and Sigmund, O., 2008. "Acoustic design by topology optimization". *Journal of Sound and Vibration*, Vol. 317, pp. 557–575.

Huang, X. and Xie, Y.M., 2010. *Evolutionary Topology Optimization of Continuum Structures: Methods and Applications*. Wiley.

Lee, J.W. and Jang, G.W., 2012. "Topology design of reactive mufflers for enhancing their acoustic attenuation performance and flow characteristics simultaneously". *International Journal for Numerical Methods in Engineering*, Vol. 91, pp. 552–570.

Lee, J.W. and Kim, Y.Y., 2009. "Topology optimization of muffler internal partitions for improving acoustical attenuation performance". *International Journal for Numerical Methods in Engineering*, Vol. 80, pp. 455–477.

Munjal, M.L., 1987. *Acoustic of Duct and Muffler with Application to Exhaust and Ventilation System Design*. Wiley.

Selamet, A. and Radavich, P.M., 1997. "The effect of length on the acoustic attenuation performance of concentric expansion chambers: Analytical, computacional and experimental investigation". *Journal of Sound and Vibration*, Vol. 201, pp. 407–426.

Silva, F.I., 2007. *Síntese Computacional de Absorvedores Acústicos Poroelásticos*. Ph.D. thesis, Universidade Estadual de Campinas.

Silva, F.I. and Pavanello, R., 2010. "Synthesis of porous-acoustic absorving systems by an evolutionary optimization method". *Engineering Optimization*, Vol. 42:10, pp. 887–905.

Vicente, W.M., Picelli, R., Pavanello, R. and Xie, Y.M., 2015. "Topology optimization of frequency responses of fluid-structure interaction systems". *Finite Elements in Analysis and Design*, Vol. 98, pp. 1–13.

Vicente, W.M., Zuo, Z.H., Pavanello, R., Calixto, T.K.L., Picelli, R. and Xie, Y.M., 2016. "Concurrent topology optimization for minimizing frequency responses of two-level hierarchical structures". *Computer Methods in Applied Mechanics and Engineering*, Vol. 301, pp. 116–136.

Yedeg, E.L., Wadbro, E. and Berggren, M., 2015. "Interior layout topology optimization of a reactive muffler". *Structural and Multidisciplinary Optimization*.

9. AUTHORAL RESPONSIBILITIES

The authors are solely responsible for the content of this work.

ENGOPT 2016

EngOpt 2016 - 5^{th} International Conference on Engineering Optimization
Iguassu Falls, Brazil, 19-23 June 2016.

A Bi-directional Evolutionary Topology Optimization method applied for Acoustic Mufflers Design

Felipe Azevedo, fazevedo@fem.unicamp.br[1]
Renato Picelli, PicelliR@cardiff.ac.uk[2]
William Vicente, vicente@fem.unicamp.br[1]
Renato Pavanello, pava@fem.unicamp.br[1]

[1]University of Campinas, Campinas,Brazil
[2]Cardiff School of Engineering, Wales, UK.

Abstract

This article introduces an evolutionary topology optimization approach applied to design acoustic mufflers. The main goal is to find the best configuration of barriers inside typical acoustic mufflers used in the automotive industry that minimizes sound pressure level in the outlet of the muffler. The acoustic medium is governed by Helmholtz equation and rigid wall boundary conditions are introduced to represent acoustic barriers. In order to minimize sound pressure level in a specific location of the muffler this work uses Transmission Loss (TL) function maximization in the work domain as strategy. Maximizing TL guarantees that the sound pressure level at the outlet of the muffler is reduced. To find the configuration of acoustic barriers that maximizes the Transmission Loss function of the muffler a Bi-directional Evolutionary Structural Optimization (BESO) method will be used.

To represent the acoustic domain inside the muffler, a few boundary conditions are implemented, such as, normal imposed velocity, imposed impedance as anechoic termination or infinite outlet and rigid wall conditions. The continuum problem is solved in the frequency domain and it is discretized using the finite element method. Using BESO method simple topologies are reached, which maximizes the Transmission Loss function for different frequencies. The influence of the fluid element discretization and the rejection parameters in the BESO method are presented. This work will be escalated to solve acoustic cloaking device problems.

Keywords: Transmission Loss, BESO, Acoustic, Barriers, Sound pressure.

1 Introduction

In the last two decades, topology optimization has been in a wide variety of problems, including the improvement of responses in vibroacoustic systems using coupled and uncoupled formulation [1, 2]. One of those problems is the expansion chambers named mufflers, currently used in sound attenuation in vehicle exhaust systems. Mufflers were a extensive subject of study in [3] and furthermore studied in optimizations problems for interior barrier optimization [4, 5].

Several authors worked the problem of modeling acoustic mufflers and proposed different design approaches to optimize acoustic mufflers. A muffler model that has a perforated pipe connecting inlet and outlet, Berggren et al. [6], and a muffler model that couples flow and acoustic equations for the optimization problem, Jang and Lee [7], are examples o models used. The works published on the subject use in majority, a design approach based on Solid Isotropic Material with Penalization (SIMP) method [8, 6]. In this work an bi-directional evolutionary structural optimization (BESO) and (ESO) methods [9, 10] are used.

The optimization of acoustic domains has been an important topic and investigations concerning noise attenuation became a major issue, since new regulations for noise control are being enforced. In this scenario muffler type devices studies grew in importance, Barbieri and Barbieri [11] used base shape optimization to improve Transmission Loss (TL) in a muffler, Lee and Kim [5] used MMA to create barriers or partitions in expansion chambers maximizing transmission loss effectively reducing sound pressure levels in the outlet portion of the chamber.

In a previous work, muffler optimization was done using (ESO) method and it will be used as reference. This work is a further study on muffler optimization using (BESO) method to maximize TL in a more robust manner. The (BESO) method has been used in multi-physics structures and problems such as buoyant structures [12] and natural frequency maximization considering acoustic-structure interaction [13]. The aspects of both methods that are similar will not be discussed in depth, refer to [14].

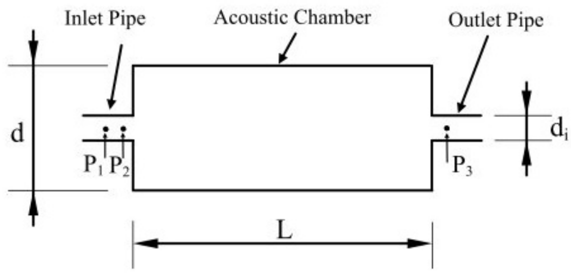

Figure 1: **Single Expansion Chamber Muffler**

2 MUFFLER DEVICE: GOVERNING EQUATION AND FINITE ELEMENT MODEL

The governing equation of steady-state linear acoustic problems in frequency domain, valid inside the muffler acoustic chambers is the Helmholtz equation as shown in [8]. Its possible to simulate exhaust pipe conditions to a certain extent using the Helmholtz equation subjected to some boundary conditions. The necessary set of equations bellow represent the differential problem to be solved.

$$\nabla^2 P_{(x,y)} + \frac{\omega^2}{c^2} P_{(x,y)} = 0 \tag{1}$$

$$\nabla P \cdot \vec{n} = \frac{\partial P}{\partial n} \tag{2}$$

$$V_n = -\frac{1}{j\rho\omega}\frac{\partial P}{\partial n} \tag{3}$$

$$P = \bar{Z} V_n = -\frac{\bar{Z}}{j\rho\omega}\frac{\partial P}{\partial n} = -\frac{1}{j\rho\omega\bar{A}}\frac{\partial P}{\partial n} \tag{4}$$

where eq. (1) is the Helmhotz equation, eq. (2) is used to implement the necessary boundary conditions, eq. (4) is an impedance boundary condition and eq. (3) is a particle velocity boundary condition. ω is the angular frequency in (rad/s), P is the acoustic pressure and ∇^2 is the Laplacian operator. Equation (1) is valid in the acoustic domain shown in Fig. 2 in $(\Omega_d \mathrm{U} \Omega_f)$.

The weighted residual formulation for Eq. (1) can be written as;

$$\frac{1}{\rho}\int_\Omega \Phi \cdot \nabla^2 P d\Omega + \frac{\omega^2}{\rho c^2}\int_\Omega \Phi \cdot P d\Omega = 0 \tag{5}$$

where ρ is the air density, ϕ is the Weight Function and Ω_f is the fluid domain with Ω_d being a partition of it, represented in Fig. 2.

Rearranging the first term of Eq. (5) and using the Divergence Theorem, Eq. (5) can be written as:

$$\frac{1}{\rho}\int_\Gamma \Phi \cdot \nabla P \cdot \vec{n} d\Gamma - \frac{1}{\rho}\int_\Omega \nabla\Phi \cdot \nabla P d\Omega + \frac{\omega^2}{\rho c^2}\int_\Omega \Phi \cdot P d\Omega = 0 \tag{6}$$

Using Eq. (2), Eq. (6) can be rearranged as:

$$\frac{1}{\rho}\int_{\Omega}\nabla\Phi\cdot\nabla P d\Omega-\frac{\omega^2}{\rho c^2}\int_{\Omega}\Phi\cdot P d\Omega=\frac{1}{\rho}\int_{\Gamma}\Phi\cdot\frac{\partial P}{\partial n}d\Gamma \tag{7}$$

where Γ is the boundary of the acoustic domain.

2.1 Boundary and Problem Definition:

For the problem proposed in this paper two main boundary conditions will be implemented, Eqs. (3) and (4). In Fig. 2, Ω_f is the full domain filled with fluid and Ω_d represents part of the domain where partitions will be introduced. The Ω_d region is the design domain for the evolutionary optimization method.

Normal velocity V_n in boundary Γ_i, expressed in Eq. (3), and normal impedance $\bar{Z}$ in boundary Γ_o, expressed in Eq. (4).

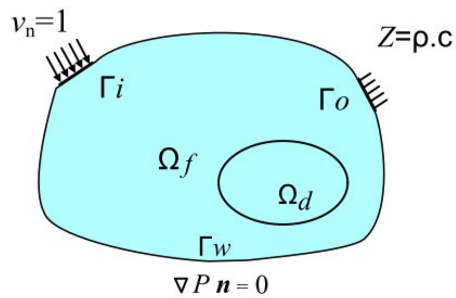

Figure 2: **Acoustic domain and Boundary conditions**

where V_n is a vector of imposed velocities in Γ_i and $\bar{A}$ is acoustic admittance in Γ_o. To completely represent the whole boundary boundary problem rigid wall natural conditions ($\nabla Pn = 0$) are imposed in Γ_w.

Applying Eq. (3) and Eq. (4) in Eq. (7) we have

$$\frac{1}{\rho}\int_{\Omega}\nabla\Phi\cdot\nabla P d\Omega-\frac{\omega^2}{\rho c^2}\int_{\Omega}\Phi\cdot P d\Omega=-\frac{1}{\rho}\left(\int_{\Gamma_i} j\rho\omega\Phi V_n d\Gamma_i+\int_{\Gamma_o} j\rho\omega\Phi\bar{A}P d\Gamma_o\right) \tag{8}$$

Using the finite element method is possible to approximate Eq. (8). Using Galerkin's method the system response equation for the stated problem is:

$$\left([\mathbf{K}]+j\omega\,[\mathbf{C}]-\omega^2\,[\mathbf{M}]\right)\cdot\{\mathbf{P}\}=\{\mathbf{V_{ni}}\} \tag{9}$$

where,

$$[\mathbf{K}]=\int_{\Omega}[\mathbf{B}]^t\,[\mathbf{B}]\,d\Omega \tag{10}$$

$$[\mathbf{C}]=\rho\bar{A}\int_{\Gamma_o}[\mathbf{N}]^t\,[\mathbf{N}]\,d\Gamma_o \tag{11}$$

$$[\mathbf{M}]=\frac{1}{c^2}\int_{\Omega}[\mathbf{N}]^t\,[\mathbf{N}]\,d\Omega \tag{12}$$

$$\{\mathbf{V_{ni}}\}=-j\rho\omega\int_{\Gamma_i}[\mathbf{N}]^t\,V_n d\Gamma_i \tag{13}$$

and $[\mathbf{N}]$ is the vector containing the shape functions for the acoustic element discretization with $[\mathbf{B}]$ being its derivatives [15], $[\mathbf{K}]$ is the acoustic stiffness matrix, $[\mathbf{C}]$ is the equivalent damping matrix relative to the output boundary condition, $[\mathbf{M}]$ is the mass matrix and $[\mathbf{V_{ni}}]$ is the vector relative to inlet conditions.

3 ANALYTICAL AND APPROXIMATE TRANSMISSION LOSS IN A MUFFLER

An automotive exhaust system, two-dimensional muffler Fig. 1, presents a Transmission Loss (TL) function that can be analytically calculated by the following equation [16],

$$TL = 10 \times Log_{10}\left(1 + \frac{1}{4}\left(m - \frac{1}{m}\right)^2 \cdot sin^2\left(k \cdot L\right)\right) \tag{14}$$

where,

$$m = \frac{d}{d_i}, k = \frac{2\pi f}{c} \tag{15}$$

and where d is the acoustic chamber diameter, d_i is the inlet and outlet pipes diameter, k is the wave number, f is the frequency and c is the speed of sound in the medium.

Using Eq. (14) to predict the TL function for a muffler with, $L = 0.5$m, $d = 0.15$m and $d_i = 0.03$m, considering that the domain is filled with air ($c = 343$m/s) for a frequency range, results shown in Fig. 3 are obtained.

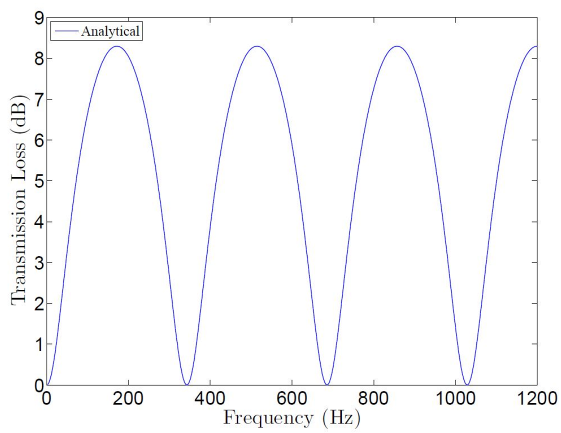

Figure 3: **TL analytical function of a single expansion chamber Eq.** (14)

The analytical model for TL function is no longer valid when rigid wall conditions are included inside the muffler acoustic chamber [5]. In order to obtain an approximated solution the Finite Element Method is used and another equation is stated to find the TL function for an acoustic chamber with rigid barriers, Eq. (16);

$$TL = 20 \times Log_{10}\left(\left|\frac{1}{P_3}\frac{P_1 - P_2 \cdot e^{-jk \cdot l}}{1 - e^{-j2k \cdot l}}\right|\right) \tag{16}$$

where l is the distance between points 1 and 2, P_1 and P_2 are pressures in the inlet pipe and P_3 is the pressure in the outlet pipe as shown in Fig. 1. The $j = \sqrt{-1}$ is the imaginary unit.

3.1 Mesh and Validation:

In this work, linear 4 node elements are used. Figure 4 depicts a mesh used for the results shown in the further sections.

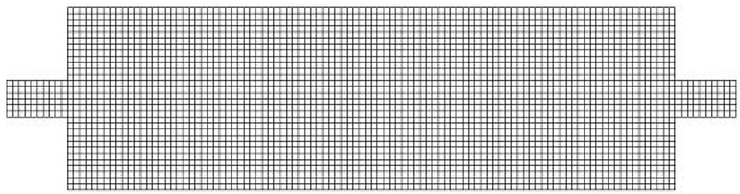

Figure 4: **Muffler Mesh with 12480 regular elements of side measuring 0.0025m.**

Equation (9) can be used to verify the TL behavior for our domain previous to the addition of partitions, using the boundary conditions presented in Fig. 2. Figure 5 shows a comparison of results achieved with Eq. (14)and results from the formulation used in this work.

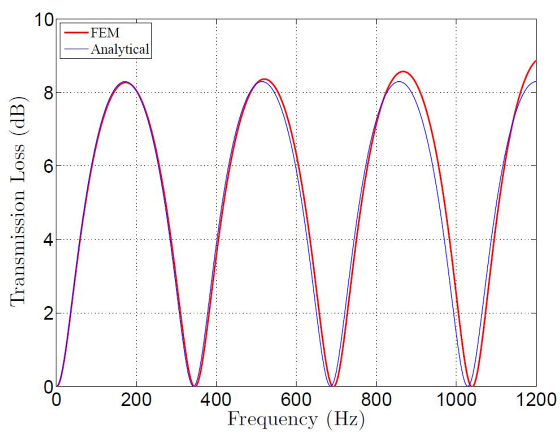

Figure 5: **Comparison between analytical TL and FEM approximated TL.**

4 BI-DIRECTIONAL EVOLUTIONARY ACOUSTIC OPTIMIZATION PROBLEM FOR TL MAXIMIZATION:

In this section the bi-directional evolutionary acoustic optimization problem is stated, the approach is described and the sensitivity number is presented. In this work an Evolutionary Topology optimization strategy is proposed, considering discrete values 1 or 0 which correspond to acoustic and void elements respectively, in a discretized form of the equation system, this approach is called "hard kill" in the literature [2].

The approach used in this paper, avoids intermediate density elements during the optimization procedure as well as preventing the usage of post-processing algorithms, while having a smaller number of iterations than general. In addition to what is done in (ESO) method, in the (BESO) approach used here, a numeric filter, presented in [2], is implemented in order to have a smoother sensitivity number and also, the filter has the function of averaging a sensitivity number to a rigid element that otherwise would have none. It is important to notice that the sensitivity number can be either positive or negative, so the influence of the rigid elements in the optimization process have to be carefully analyzed.

4.1 Problem statement

The goal of the optimization is to maximize the objective function (TL) for a predefined frequency. The design variable x_i indicates the presence ($x_i = 1$) or absence ($x_i = 0$) of our fluid element. When the fluid element is removed of the design domain, a rigid element with a rigid wall boundary condition is naturally placed on the system, the local inclusion of several rigid elements will create the barriers need for noise attenuation in this system.

Considering volume constraints, as measure of barriers inclusion, the evolutionary optimization problem is stated as:

$$\text{Maximize } \mathbf{TL} = 20 \times Log_{10}\left(\left| \frac{1}{P_3} \frac{P_1 - P_2 \cdot e^{-jk\cdot l}}{1 - e^{-j2k\cdot l}} \right| \right)$$

$$\text{Subject to: } \left([\mathbf{K}] + j\omega [\mathbf{C}] - \omega^2 [\mathbf{M}] \right) \cdot \{\mathbf{P}\} = \{\mathbf{V_{ni}}\}$$

$$V_f - \sum_{i=1}^{nel} v_i x_i = 0$$

$$x_i = 0 \text{ or } 1$$

4.2 BESO Approach

The BESO method uses a gradient-based optimizer in order to evaluate the relevance of each element after the model analysis. This optimizer is generally called sensitivity and its calculation is described bellow.

4.2.1 Transmission Loss Sensitivity Analysis

The sensitivity number is the objective function derivative with respect to the design variable, since transmission loss can be written as,

$$TL(\omega, x_i) = 10 \times log_{10}\left(\frac{|\ Pin\ |^2}{|\ Pout\ |^2} \right) \tag{17}$$

the derivative is,

$$\frac{\partial TL(\omega, x_i)}{\partial x_i} = \frac{10}{ln10} \times \left(\frac{\partial \mid P_{in} \mid^2}{\partial x_i} \cdot \frac{1}{\mid P_{in} \mid^2} - \frac{\partial \mid P_{out} \mid^2}{\partial x_i} \cdot \frac{1}{\mid P_{out} \mid^2} \right) \tag{18}$$

where P_{in} is,

$$P_{in} = \mid \left(\frac{P_1 - P_2 \cdot e^{-jk\cdot l}}{1 - e^{-j2k\cdot l}} \right) \mid \tag{19}$$

and P_{out} is,

$$P_{out} = \mid P_3 \mid \tag{20}$$

Since P_{in} and P_{out} in Eq. (19) and Eq. (20) are complex numbers, they can be expanded as follows:

$$P_{in}^2 = \frac{1}{\gamma}\left(P_{1Re} - P_{2Re} \cdot cos(k \cdot l) - P_{2Im} \cdot sin(k \cdot l)\right)^2 + \frac{1}{\gamma}\left(P_{1Im} - P_{2Im} \cdot cos(k \cdot l) + P_{2Re} \cdot sin(k \cdot l)\right)^2 \tag{21}$$

$$P_{out}^2 = P_{3Re}^2 + P_{3Im}^2 \tag{22}$$

with γ defined as,

$$\gamma = \left(1 - cos\left(2k \cdot l\right)\right)^2 + \left(sin\left(2k \cdot l\right)\right)^2 \tag{23}$$

where subscripts (Re) and (Im) means real and imaginary parts respectively.

In [14] a more explicit sensitivity number calculation is presented and in [17, 18] ways of facilitating the calculation of the pressure derivative making the procedure less computational intensive are described.

5 NUMERICAL RESULTS

The objective of the example presented bellow is to implement the methodology developed for TL maximization. In this section the results achieved using that optimization strategy are studied.

The proposed example in Fig. 1, with the configuration presented in section 2 is a bi-dimensional representative acoustic model, for a simple automotive muffler. Table 1 shows BESO parameters used to optimize the system.

The topology optimization strategy proposed in this article can be applied to any wanted frequency. In this section the results presented used frequencies of 520 and 693 Hz, they are relative to peak and valley frequencies in Fig. 5.

Table 1: **BESO Parameters.**

Evolutionary Ratio (ER)	0.166%
Admition Ratio (ARmax)	0.05%
Final Volume (V_f)	97 %

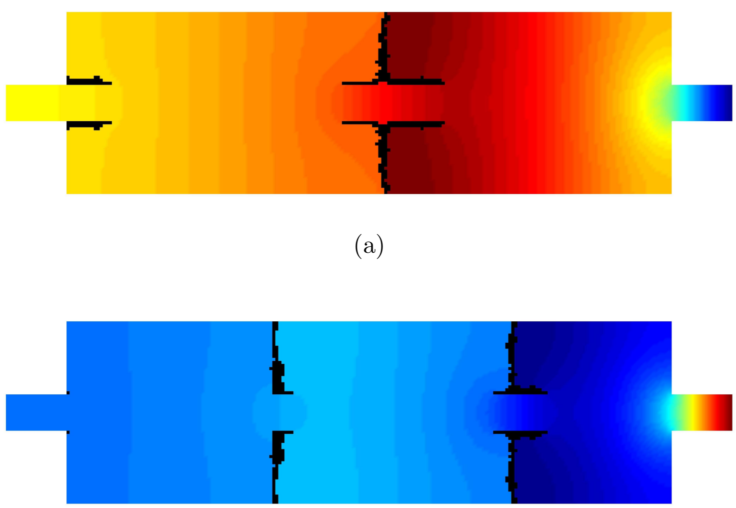

(a)

(b)

Figure 6: **Final topologies using BESO method ; (a): topology for a frequency of 520 Hz; (b): topology for a frequency of 693 Hz;**

It is possible to see that the final topologies produced in this work, shown in Fig. 6, are similar to the ones presented by Lee and Kim[5]. Figure 7 shows the evolution of the Transmission loss function amplitude through the optimization process for ($\omega = 520$ Hz) and ($\omega = 693$ Hz).

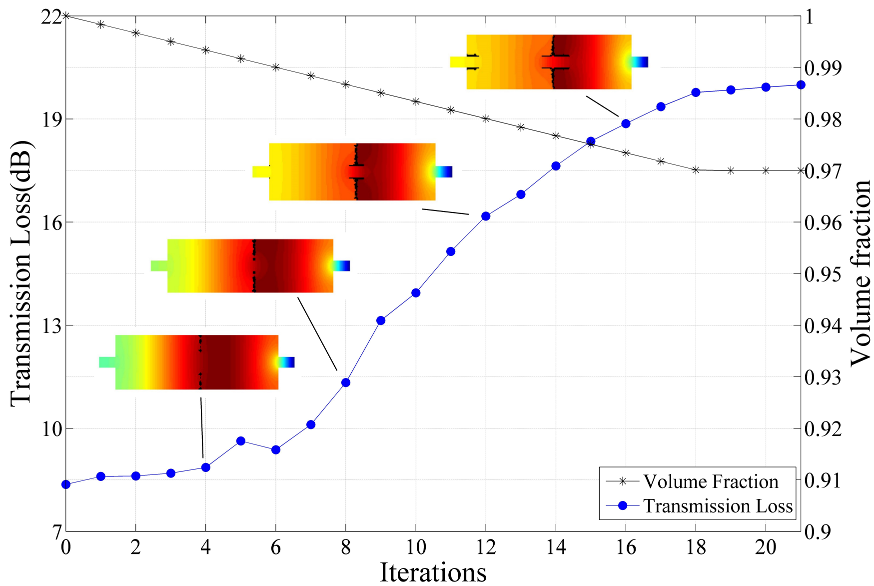

Figure 7: **Fluid volume evolution in the design domain and TL evolution considering a frequency of 520 Hz**

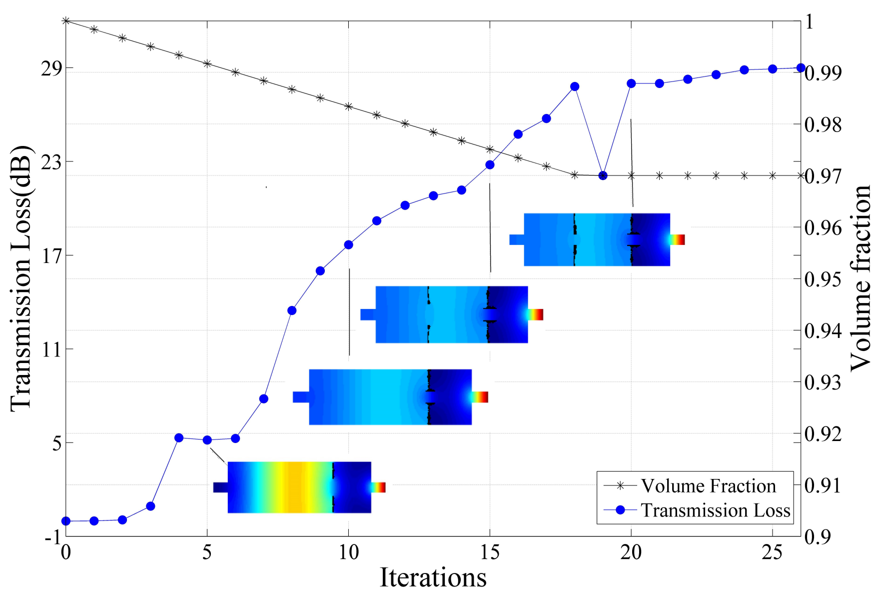

Figure 8: **Fluid volume evolution in the design domain and TL evolution considering a frequency of 693 Hz**

At the end of the optimization the maximum TL obtained for 520 Hz was over 19 dB and for 693

Hz was 29 dB. Figure 9 shows TL response for a range of frequencies for mufflers presented in Fig. 6, characterizing the noise attenuation performance of the mufflers produced in this paper.

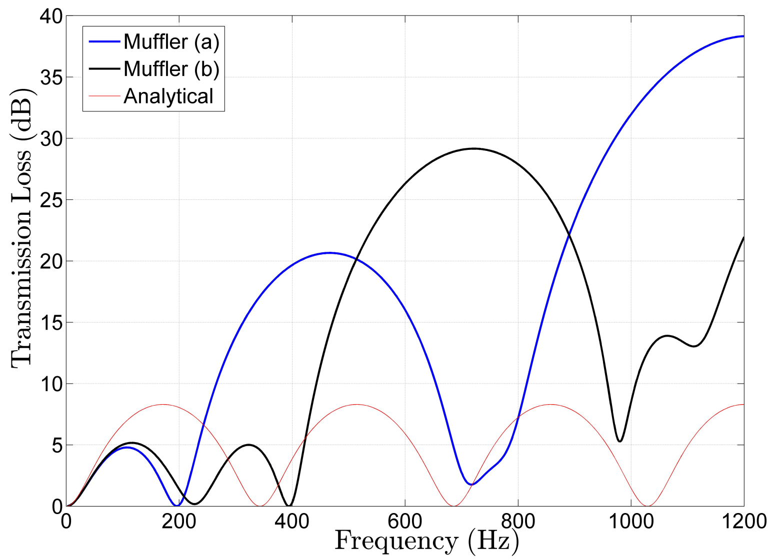

Figure 9: **(a) TL responses for Mufflers (a) and (b)**

According to the results presented here the BESO approach showed itself a viable option of optimization.

6 CONCLUSION

The main objective of this work is to propose a bi-directional evolutionary methodology for acoustic optimization of automotive mufflers, a new approach for this case study, exploiting its advantages. A sensitivity analysis of the optimization problem has been presented considering an evolutionary approach.

In order to minimize sound pressure level at the muffler outlet, the optimiztion process has added attenuation barriers in the expansion chamber interior in order to raise the Transmission Loss function thus reaching the proposed goal. For different frequencies, the results presented show the capability of the proposed methodology to maximize noise attenuation in the studied system. As a further work, new elements can be introduced in the problem in order to make the mufflers more realistic, for example, adding porous materials inside the acoustic chamber.

7 ACKNOWLEDGMENTS

The authors are grateful to FAPESP (So Paulo Research Foundation, grant numbers 2013/08293-7, 2013/00085-6 and 2015/18607-4) and CAPES for the financial support of this work.

References

[1] M P Bendsoe and O Sigmund. *Topology Optimization: Theory Methods and Applications*. Springer, 2004.

[2] X Huang and Y M Xie. *Evolutionary Topology Optimization of Continuum Structures: Methods and Applications*. Wiley, 2010.

[3] M L Munjal. *Acoustic of Duct and Muffler with Application to Exhaust and Ventilation System Design*. Wiley, 1987.

[4] Gil Ho Yoon. Acoustic topology optimization of fibrous material with denaly-bazley empirical material formulation. *Journal of Sound and Vibration*, 332:1172–1187, 2013.

[5] J W Lee and Y Y Kim. Topology optimization of muffler internal partitions for improving acoustical attenuation performance. *International Journal for Numerical Methods in Engineering*, 80:455–477, 2009.

[6] E L Yedeg, E Wadbro, and M Berggren. Interior layout topology optimization of a reactive muffler. *Structural and Multidisciplinary Optimization*, 2015.

[7] J W Lee and G W Jang. Topology design of reactive mufflers for enhancing their acoustic attenuation performance and flow characteristics simultaneously. *International Journal for Numerical Methods in Engineering*, 91:552–570, 2012.

[8] Maria B Dhring, Jakob S Jensen, and Ole Sigmund. Acoustic design by topology optimization. *Journal of Sound and Vibration*, 317:557–575, 2008.

[9] F I Silva. *Sntese Computacional de Absorvedores Acsticos Poroelsticos*. PhD thesis, Universidade Estadual de Campinas, 2007.

[10] F. I. Silva and R Pavanello. Synthesis of porous-acoustic absorving systems by an evolutionary optimization method. *Engineering Optimization*, 42:10:887–905, 2010.

[11] R Barbieri and N Barbieri. Finite element acoustic simulation based shape optimization of a muffler. *Applied Accoustics*, 67:346–357, 2005.

[12] R. Picelli, R. van Dijk, W. M. Vicente, R. Pavanello, M. Langelaar, and F. van Keulen. Topology optimization for submerged buoyant structures. *Engineering Optimization*, 2016.

[13] R. Picelli, W. M. Vicente, R. Pavanello, and Y. M. Xie. Evolutionary topology optimization for natural frequency maximization problems considering acoustic-structure interaction. *Finite Elements in Analysis and Design*, 106:56–64, 2015.

[14] F. Azevedo, R. Picelli, W. M. Vicente, and R. Pavanello. Topology optimization for acoustic muffler. In *Congresso Nacional de Engenharia Mecnica*, 2016.

[15] W Desmet and D Vandepitte. *Finite Element Method for Acoustics*. LMS International, 2005.

[16] A Selamet and P M Radavich. The effect of length on the acoustic attenuation performance of concentric expansion chambers: Analytical, computacional and experimental investigation. *Journal of Sound and Vibration*, 201:407–426, 1997.

[17] W M Vicente, R Picelli, R Pavanello, and Y M Xie. Topology optimization of frequency responses of fluid-structure interaction systems. *Finite Elements in Analysis and Design*, 98:1–13, 2015.

[18] W M Vicente, Z H Zuo, R Pavanello, T K L Calixto, R Picelli, and Y M Xie. Concurrent topology optimization for minimizing frequency responses of two-level hierarchical structures. *Computer Methods in Applied Mechanics and Engineering*, 301:116–136, 2016.